DEVELOPING MULTIFUNCTIONAL FORWARD OSMOSIS (FO)

DRAW SOLUTES FOR SEAWATER DESALINATION

ZHAO DIELING

NATIONAL UNIVERSITY OF SINGAPORE

2015

DEVELOPING MULTIFUNCTIONAL FORWARD OSMOSIS (FO) DRAW SOLUTES FOR SEAWATER DESALINATION

ZHAO DIELING

(*B. Eng, Zhejiang University,*

P. R. China)

A THESIS SUBMITTED FOR THE DEGREE OF DOCTOR OF PHILOSOPHY

DEPARTMENT OF CHEMICAL AND BIOMOLECULAR ENGINEERING
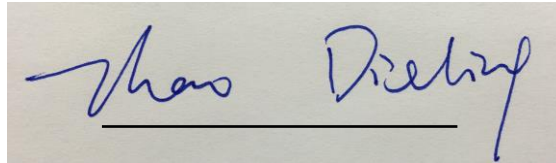
NATIONAL UNIVERSITY OF SINGAPORE

2015

DECLARATION

I hereby declare that this thesis is my original work and it has been written by me in its entirety.

I have duly acknowledged all the sources of information which have been used in the thesis.

This thesis has also not been submitted for any degree in any university previously.

Zhao Dieling

Aug 06, 2015

Acknowledgement

Table of Contents

Summary

To reduce the cost of existing membrane technology for seawater desalination, forward osmosis (FO) as an osmotic-driven membrane process has attracted increasing attention in recent years. The performance and the energy requirement of FO largely depend on the draw solution which is responsible for providing the driving force of FO. The primary objective of this study is to develop novel FO draw solutions with facile regeneration method for seawater desalination.

Firstly, a dendrimer-based FO draw solute, poly(amidoamine) terminated with sodium carboxylate groups (PAMAM-COONa), was investigated for seawater desalination. Compared with existing FO draw solutes, PAMAM-COONa offers unique advantages including: 1) its aqueous solution can generate high osmotic pressure due to the large number of -COONa groups; 2) the low viscosity of PAMAM-COONa solution can reduce concentration polarization, which adversely affects water flux of FO processes; and 3) PAMAM-COONa has a relatively large molecular size, favoring reduced reverse solute flux. Using 2.5-generation (2.5G) PAMAM-COONa draw solution (33.3 wt%) and seawater (from Singapore coast) feed solution, a relatively high FO water flux of 9 L m^{-2} h^{-1} was achieved. After FO testing, the diluted PAMAM-COONa solution was re-concentrated to its original osmotic pressure with membrane distillation (MD) with an average MD water flux of 3.2 L m^{-2} h^{-1}. In addition to seawater desalination, the dendrimer-based FO draw solute may find applications in wastewater treatment and protein enrichment.

Next, we studied Na^+–functionalized carbon quantum dots (Na_CQDs) as FO draw solute. The unique characteristics of Na_CQDs, including an ultra–small size of 3.5 nm, abundant carboxyl groups, and rich ionic species, favor high osmotic pressure and thus high FO water flux. At

concentrations of 0.4 and 0.5 g mL^{-1}, the Na_CQDs provided respective osmotic pressures of 30.9 and 53.6 atm, much higher than that of seawater (~26 atm). In FO tests with DI water as the model feed solution, the Na_CQDs (0.4 g mL^{-1}) solution showed a water flux of 29.8 LMH, exceeding that of 2.0 M NaCl draw solution by 55%. This FO water flux is among the highest reported. When seawater was used as the feed solution, the Na_CQDs provided an FO water flux of 10.4 LMH with only a slight drop after 5 cycles. In addition, the Na_CQDs showed negligible reverse solute permeation. The good biocompatibility of this new class of draw solute also makes it promising for producing clean drinking water *via* FO.

Because of unique response to temperature, thermoresponsive compounds have exhibited distinct advantages in the regeneration process of draw solute. A thermoresponsive copolymer, poly(sodium styrene-4-sulfonate-*co*-n-isopropylacrylamide) (PSSS-PNIPAM), was employed as a draw solute in FO for seawater desalination. When PSSS-PNIPAM was dissolved in water to form a draw solution, PSSS as a strong polyelectrolyte generated a high enough osmotic pressure to extract water from seawater in an FO process. The draw solute was then regenerated with membrane distillation (MD) at a temperature above the lower critical solution temperature (LCST) of PNIPAM, which agglomerated and led to decreased osmotic pressure of the solution and thus higher water vapor pressure. The combined FO-MD process with PSSS-PNIPAM as the draw solute should be promising for many membrane-involved separation processes.

However, the high viscosity of concentrated thermoresponsive copolymer solution makes it difficult to increase FO water flux by increasing the draw solution concentration. Therefore, we investigated a thermoresponsive ionic liquid (IL), tetrabutylphosphonium trifluoroacetate (abbreviated as P$_{4444}$[CF$_3$COO]), as an FO draw solute for seawater and brackish water desalination. Its inherent ionic nature, low viscosity even at high concentration, and ease of

separation from water make thermoresponsive ILs promising FO draw solutes. However, our experimental results revealed that, the water flux provided by $P_{4444}[CF_3COO]$ solution was considerably low despite its high osmolality. With simulated brackish water as the feed solution and IL-rich sediments of $P_{4444}[CF_3COO]$ solution at 60 °C (73 wt%) as the draw solution, FO water fluxes of 4.2 LMH and 4.9 LMH were obtained under 25 °C and 50 °C, respectively. Film-theory was then employed to analyze the results and it was found that external concentration polarization is the dominant role in determining the water flux. At higher temperatures, both increased mass transfer of the draw solute molecules and improved permeability of FO membrane contributed to the increased FO water flux.

List of Tables

List of Figures

Nomenclature

A solvent permeability through the membrane (LMH atm^{-1})

A_m effective membrane surface area (m^2)

d_h hydraulic diameter (m)

Ds solute diffusion coefficient (m^2 s^{-1})

J_s reverse solute flux (gram m^{-2} h^{-1}, abbreviated as gMH)

J_v FO water flux (liter m^{-2} h^{-1}, abbreviated as LMH)

k mass transfer coefficient (m s^{-1})

k_0 Boltzman constant (= 1.38×10^{-23} m^2 kg s^{-2} K^{-1})

L channel length (m)

Δm mass of water permeated across FO membrane (g)

ΔP transmembrane pressure (atm)

r hydrodynamic radius of the particle/molecule (nm)

Re Reynolds number

Sc Schmidt number

Sh Sherwood number

t elution time (s)

Δt operation time interval (h)

T absolute temperature (K)

V bulk crossflow velocity (m s^{-1})

Greek

η_r relative viscosity

ρ density (g ml^{-1})

$\Delta\pi$ osmotic pressure (atm)

π_1 osmotic pressure of feed solution near the membrane

        surface (atm)

π_2 osmotic pressure of draw solution near the membrane

        surface (atm)

μ solution shear viscosity (mPa·s)

CHAPTER 1

INTRODUCTION

1.1 Background

Clean water supply plays a crucial role in multiple aspects of our life, such as public health, human consumption, agricultural and industrial production. However, clean water scarcity has long been a serious concern for many communities. 1.2 billion people lack access to clean drinking water and millions of people died from disease via unsafe water every year.[1] To make things worse, clean water shortage will be aggravated due to the rapid growth of population, industrialization and environmental pollution unless new ways to produce clean water can be found.[2] To solve this worldwide problem, people have been looking for effective and low-cost methods to decontaminate and disinfect water. However, improving the use of existing water sources is not enough. Only searching for other water supply can alleviate the stress of water shortage.[2]

Seawater desalination has been proposed as a solution to the worldwide scarcity of clean water. Since seawater constitutes more than 97% of the total water on earth, capturing even a tiny fraction could have a huge impact on the water supply.[3, 4] Seawater desalination means producing drinking water by removing dissolved solids from seawater. Nowadays, widely employed desalination technologies include thermal distillation, namely multi-effect distillation (MED), multi-stage flash (MSF), and membrane separation via reverse osmosis (RO). However, conventional thermal methods require high temperature and meanwhile they are inefficient in the use of energy. Another problem is that they suffer from corrosion. Therefore, the market share of

these thermal desalination plants is declining. Compared to MED and MSF, RO is currently the state-of-the-art desalination technology as it requires a relatively low rate of energy input.[2, 5] But RO could only utilize electricity which is high grade energy to produce the high hydraulic pressure. Other major challenges of RO include membrane fouling, low recovery for seawater desalination, and relatively low efficiency in removal of low-molecular-weight impurities.[6] Therefore, seawater desalination remains a challenge so far.

The growing awareness of water and energy scarcity has given rise to great efforts to the search for seawater desalination technologies. In recent years, forward osmosis (FO) has attracted increasing attention because of its low energy requirement.[7-10] In a typical FO process, water molecules in solution of low osmotic pressure (feed solution) can spontaneously pass across a semi-permeable membrane to solution of high osmotic pressure (draw solution). After the draw solution draws clean water from the feed solution, it will go through a regeneration process to extract water from the draw solution and be reused in the next FO process. Contrary to RO, FO is a spontaneous process only depending on the osmotic pressure difference between the feed solution and draw solution. Consequently, FO demands much less energy as long as the regeneration of FO draw solution is facile and economical.

1.2 Osmotic Processes

Osmosis is the transport of water across a selectively permeable membrane from the side of higher water chemical potential to the side of lower water chemical potential. There are three osmotic processes, namely forward osmosis (FO), reverse osmosis (RO) and pressure retarded osmosis (PRO) as shown in Figure 1.1.[11] FO utilizes the osmotic pressure difference ($\Delta\pi$) across

the membrane as the driving force, while RO uses the hydraulic pressure difference (ΔP) which is greater than the osmotic pressure difference ($\Delta \pi$). PRO takes place when the applied pressure difference is between zero and the flux reversal point.
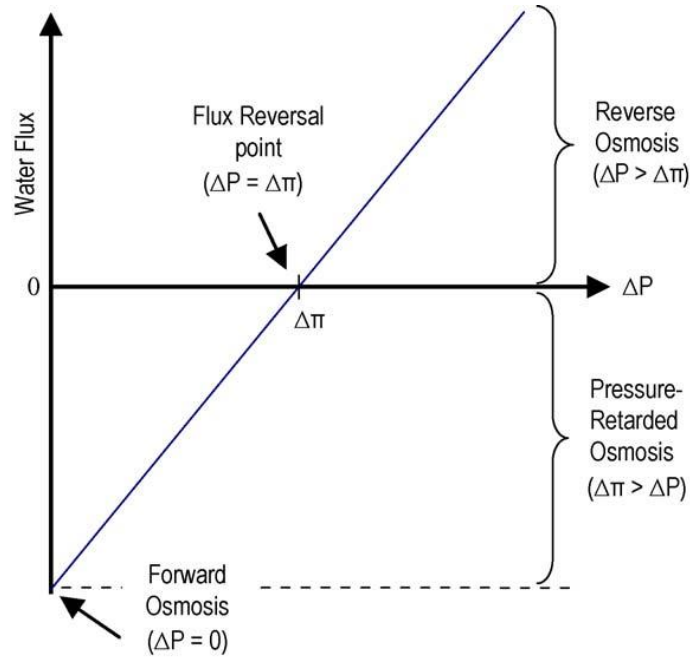
Figure 1.1 Schematic illustration of forward osmosis, reverse osmosis and pressure retarded osmosis.[11]

The general equation describing water flux in osmosis is

$$J_w = A \ (\sigma\Delta\pi - \Delta P) \qquad\qquad (1)$$

where Jw is the water flux, A the water permeability constant of the membrane, and σ the reflection coefficient. For FO, ΔP is zero; for RO, $\Delta P > \Delta \pi$; and for PRO, $\Delta \pi > \Delta P$. [6, 9]

1.3 Forward Osmotic (FO) Process

In a typical FO process, water molecules in solution of low osmotic pressure (feed solution) can spontaneously pass across a semi-permeable membrane to solution of high osmotic pressure (draw solution). Contrary to RO, FO is a spontaneous process only depending on the osmotic pressure difference between the feed solution and draw solution. After the draw solution draws clean water from the feed solution, it will go through a regeneration process to extract water from the draw solution and be reused in the next FO process. For cases of direct applications, regeneration of draw solution may not be necessary. A close-loop FO process with a regeneration unit is shown in Figure 1.2.
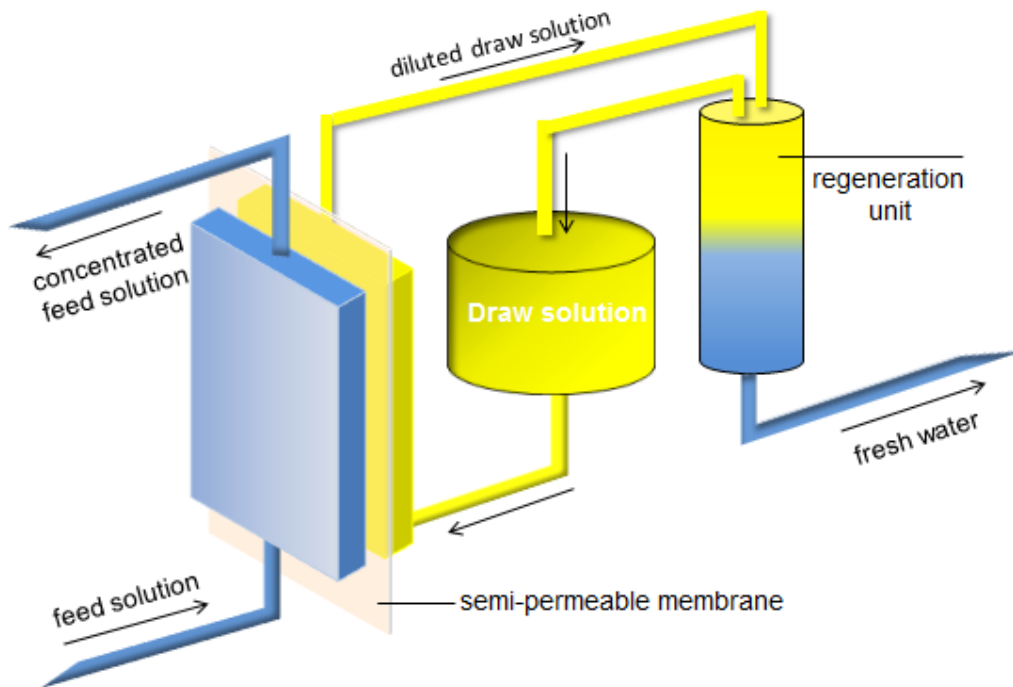
Figure 1.2 Schematic illustration of a forward osmotic process.[12]

4

FO membrane is a semi-permeable membrane with a dense selective layer and also a supporting

layer. Based on the membrane orientation, there are two operational modes in a FO process,

namely pressure retarded osmosis (PRO) mode and forward osmosis (FO) mode. When the draw

solution faces the dense selective layer, it is pressure retarded osmosis (PRO) mode. On the

contrary, when the feed solution faces the selective layer, it is forward osmosis (FO) mode

(Figure 1.3).
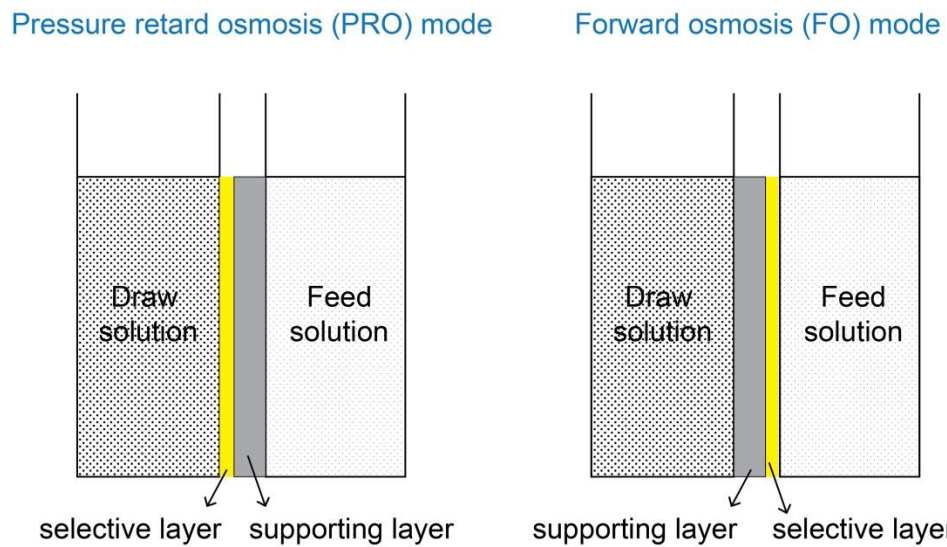
Figure 1.3 Schematic illustration of two operational modes of forward osmosis.

1.4 Concentration Polarization

The water flux of an osmotic-driven membrane process is described by Equation 1. In the

equation, $\Delta\pi$ represents the osmotic pressure difference across the active layer of the membrane.

In real cases, the effective osmotic pressure difference across the active layer is much lower than

the bulk osmotic pressure difference, which leads to a much lower water flux. This is mainly

attributed to membrane-associated transport phenomena. Two types of concentration polarization

phenomena may take place in FO processes, namely external concentration polarization (ECP) and internal concentration polarization (ICP) (Figure 1.4).
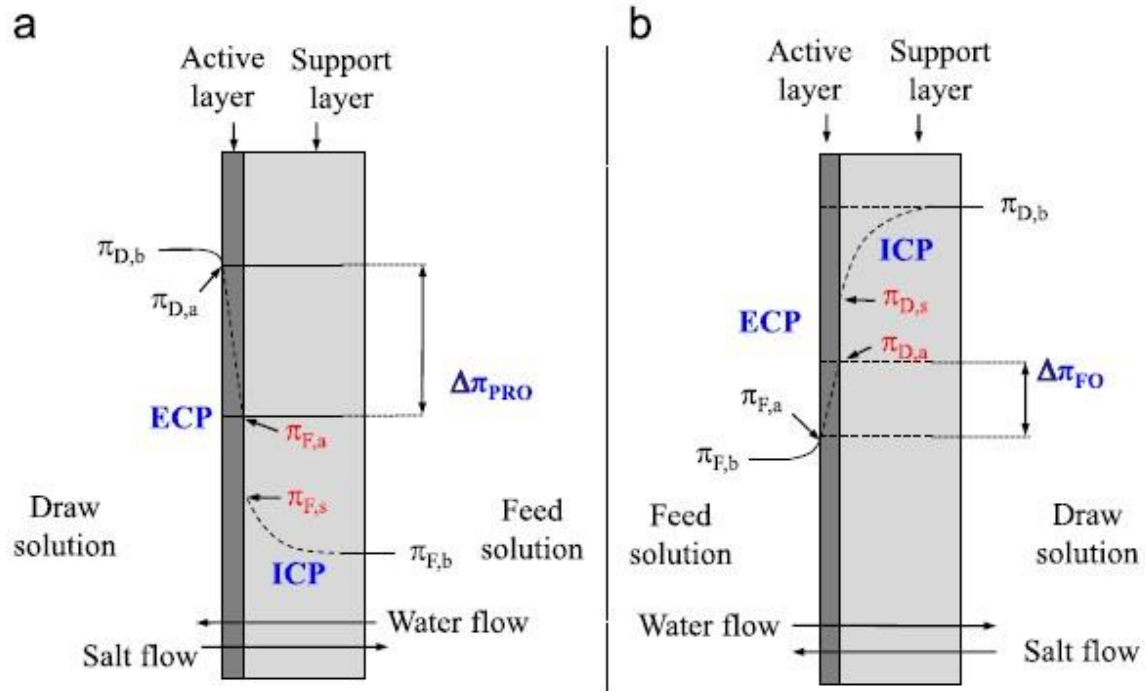
Figure 1.4 Illustration of external and internal concentration polarization in a) PRO mode and b) FO mode.[13]

1.4.1 External Concentration Polarization (ECP)

When the feed solution flows on the active layer of the FO membrane, solutes build up at the active layer which is called as concentrative ECP. Meanwhile, the draw solution in contact with the active layer of membrane is diluted by the permeating water. This is dilutive ECP. Both concentrative and dilutive ECP will reduce the effective osmotic pressure difference. As a result, the water flux will be lower than expectation. ECP can be alleviated by increasing the flow rate and inducing turbulence near the membrane surface. In most cases, ECP may have a minor effect

on the water flux and is not the main reason for the lower FO water flux than the theoretical value.[8]

1.4.2 Internal Concentration Polarization (ICP)

As FO membrane is asymmetric, more complexity is added to CP phenomena. If the porous supporting layer faces the feed solution, namely PRO mode, the solutes in the feed solution may accumulate inside the porous layer and the concentration in the supporting layer is higher than the bulk solution. This is concentrative ICP. In FO mode, the concentration of the draw solution in the supporting layer is lower than the bulk as the water from the feed solution permeates the membrane and dilutes the draw solution in the supporting layer. This is referred to as dilutive ICP. Compared to ECP, ICP is more critical in reducing the water flux when the FO membrane is used with salts on both sides. And it is more difficult to eliminate ICP as it happens inside the membrane. The water flux under FO mode is usually lower than the PRO mode due to the ICP. Research has shown that the severity of ICP is mainly influenced by the structure of the membrane (thickness, tortuosity and porosity) and the diffusion coefficient of the draw solution and feed solution. Once the draw solution and the feed solution are decided, the minimization of ICP may mainly depend on the design of FO membrane.[13]

1.5 Membrane Development

An ideal FO membrane must possess properties like high water flux, high salt rejection, low concentration polarization and high mechanism strength.[14] Before 1960s, most of FO tests employed RO membranes until Loeb-Sourirajan membrane was developed.[11, 15] Only since

2000s, there have been increasing studies on FO membranes. Based on the fabrication methods, FO membranes can be generally classified into inversion-formed membranes, thin film composite (TFC) membranes and chemically modified membranes.[14]

Polybenzimidazole (PBI) and cellulose acetate (CA) are two materials that have been widely used to fabricate FO membrane using phase inversion technique. In 2007, Wang first fabricated PBI nanofiltration (NF) hollow fiber membrane for use in FO.[16] They further modified the membrane by cross-linking using p-xylylene dichloride to achieve a higher permeate flux and salt rejection.[17] However, the water flux and salt rejection were still not satisfying. CA shows favorable properties, such as high hydrophilicity, good mechanical strength, and good resistance to chlorine. The high hydrophilicity allows low fouling tendency and high water flux.[18] Recently, various cellulose ester-based membranes, in both format of flat sheet and hollow fiber, have been developed.[18-21] Among them, double skinned CA membranes with the aim to reduce ICP effects have achieved growing attention.[18, 20] However, hydrolysis will easily happen on CA membranes when the pH is below 3 and above 7, or the temperature is above 30~35 °C.[8, 15]

TFC FO membranes have been fabricated by phase inversion (for preparation of porous substrate) followed by interfacial polymerization (for formation of polyamide active layer).[22-27] It is important to note that the ICP effects of TFC FO membranes are governed by the porous substrate while the active layer determines the salt rejection and reverse solute permeation.[14] Favorable porous substrates should be highly porous and hydrophilic with low tortuosity and high mechanical strength to allow high water flux through reduced ICP.[22] Both the material and structure of the substrate layer can determine its performance.[26, 27] For example, it was observed that the substrate with straight finger-like pore structure functioned better than spongy pore structure to minimize ICP.[27] Compared to inversion-formed membranes, TFC membranes are

8

more promising in FO processes due to their high water flux and salt rejection, and better stability towards pH, hydrolysis and biodegradation.[14]

Besides inversion-formed membranes and TFC membranes, chemical modification methods have been employed recently for fabrication of novel FO membranes. For example, to improve the performance of support layer, effects of incorporation of titanium dioxide nanoparticles,[28] carbon nanotubes[29] or zeolites[30] into the support layer have been studied. Layer-by-layer assembly method has also been used to prepare NF-like FO.[31-34] Also, to confirm the stability of membrane performance for commercialization, study on minimizing membrane fouling has attracted increasing attention recently.[35, 36]

1.6 Forward Osmosis (FO) vs. Reverse Osmosis (RO)

Currently, reverse osmosis (RO) is a widely employed desalination technology and has about 60% share in the total number of world desalination plants.[4] As a new desalination technology, forward osmosis (FO) is frequently compared with RO. Though both are membrane separation processes, many other aspects of these two processes are different, such as solute and water flow direction, the driving force, etc. As mentioned in the previous section, FO is driven by osmotic pressure while RO relies on the external hydraulic pressure. Accordingly, there are different requirements for suitable membranes to each process. Comparison between FO and RO is provided in Table 1.1. In this Chapter, we mainly compare two major aspects of FO and RO, namely membrane fouling and energy consumption.

Table 1.1 Comparison between FO and RO.[6]

	FO	RO
Driving force	Osmotic pressure	External hydraulic pressure
Main application	• Water purification • Desalination • Protein concentration	• Water purification • Desalination
Operation condition	atmosphere	10~70 bar
Desirable membrane property		
1) Physical morphology	Thin membrane with dense selective layer on porous supporting layer	• Dense top layer and porous supporting layer • Good mechanical stability
2) Chemical property	• Very hydrophilic • Good chemical stability to feed and draw solution	• Good chemical stability to chloride solution
3) Other requirement	• High water permeability • High solute rejection	• High water permeation • High solute rejection • Robust for high pressure operation
Challenges	• Concentration polarization • Suitable draw solution • Draw solution regeneration	• Membrane fouling • Energy consumption

1.6.1 Membrane Fouling

Membrane fouling is defined as the process that leads to a decrease in performance of a membrane, caused by the deposition of suspended or dissolved substances on the membrane surface, on the membrane pores, or within the membrane pores. As a result, it causes significant flux decline and affects the quality of the water product. Severe membrane fouling may require frequent membrane cleaning and replacement which results in an increased operating cost. Basing on the cause, membrane fouling can be classified into colloidal fouling, inorganic fouling due to crystallization/scaling, organic fouling and biofouling. It is a complex problem affected by several factors, such as solution chemistry, level of pre-treatment, membrane property and

operational condition. It is a major problem for the application of membrane technology, especially for RO as the applied hydrodynamic force will drag the foulants towards the membrane surface and thus promoting the membrane fouling.[9] Compared to RO, FO works at low or without hydraulic pressure. Consequently, the fouling layer is much less compact. Usually it can be removed easily by backwashing or mild periodic chemical washing. Therefore, many applications of FO can be operated with low quality feed solutions.[6]

1.6.2 Energy Consumption

The energy consumption of an RO process has been extensively studied. However, confusion exists regarding the energy consumption of an FO process. The minimum energy needed for seawater of 3.5 wt% total dissolved solids and a recovery of 50% is approximately 1.5 kWh/m^3.[2] The real energy input for state-of-art RO plants is about 4-7 kWh/m^3 considering the differences in operational condition.[2] The electrical power needed of an FO process alone (without regeneration of the draw solution) for seawater desalination is about 0.25 kWh/m^3.[37] The energy consumption of a close-loop FO process (with regeneration condition) mainly depends on the regeneration method used. Theoretically, the energy requirement of an FO process reaches 2.5 kWh/m^3 (mean osmotic pressure differential of 50 bar, feed solution is 3.5% NaCl solution).[38] For real cases, the energy requirement will be higher due to the energy loss along the process. Therefore, the energy consumption of FO processes should be larger than that of RO processes.

One implication of this analysis is that the research on FO draw solution may increasingly focus on regeneration-free application, such as fertilizers, nutrient containing bags, etc.[39] For other applications, FO can still show advantages over RO regarding the energy consumption. To

provide high external hydraulic pressure, RO can only consume electricity which is high-grade energy and the price of electricity may fluctuate substantially. In contrast, FO can utilize low grade or renewable energy, such as waste industry heat, geothermal or solar thermal energy, etc. NH_4HCO_3 promoted FO seawater desalination process was claimed to save up to 85% energy compared with other desalination technologies.[37] Therefore, searching for draw solutions with regeneration methods that can induce cheap or even free energy is critical for the development of FO.

1.7 Research Objectives and Project Organization

1.7.1 Research Objectives

Despite the rapid progress in the development of FO draw solution recently, existing draw solutions still have disadvantages such as low osmotic pressure, high reverse solute flux, or requirement of complex and energy-intensive regeneration method. Moreover, the application of FO in seawater desalination has yet to be fully investigated with eligible draw solutions. The studies on the fundamental science and engineering of novel FO draw solutions in seawater desalination need to be conducted. Our ultimate goal of this project is to investigate novel FO draw solutions with feasible regeneration method for seawater desalination. The highest FO water flux reported so far is about 5 LMH for seawater desalination.[13] We aimed to achieve higher water flux by improving the hydrophilicity of draw solutes. To reduce energy consumption in the regeneration process, the draw solutes should be re-concentrated via mild heating which can take the advantage of low-grade heat that is abundant from industry or solar thermal energy. The specific objectives of this project are:

1. to design and synthesize multifunctional FO draw solutes with high osmolality and proper stimuli-responsiveness;

2. to apply these draw solutes in FO processes to investigate their effectiveness in seawater desalination;

3. to investigate the effects of different parameters of draw solutions on the performance of FO;

4. to investigate draw solute regeneration methods.

1.7.2 Project Organization

This dissertation is to explore novel FO draw solutions for seawater desalination. It is composed of seven chapters. Chapter 1 provides the general background of forward osmosis (FO). Chapter 2 provides a literature review of current FO draw solutions. In Chapter 3, we introduce a dendrimer-based FO draw solute for seawater desalination. In Chapter 4, we demonstrate that Na^+-functionalized carbon quantum dots are promising FO draw solutes for seawater desalination. Chapter 5 reports thermoresponsive copolymers as FO draw solutes for seawater desalination. In Chapter 6, a thermoresponsive ionic liquid is studied as an FO draw solute for brackish water and seawater desalination. Chapter 7 summaries the major findings of this project and recommendations for future work.

1.8 References

1. Montgomery, M. A.; Elimelech, M. Water and sanitation in developing countries: including health in the equation. *Environ. Sci. Technol*. **2007**, 41, 17-24.

2. Elimelech, M.; Phillip, W. A. The future of seawater desalination: energy, technology, and the environment. Science **2011**, 333, 712-717.

3. Shannon, M. A.; Bohn, P. W.; Elimelech, M.; Georgiadis, J. G.; Marinas, B. J.; Mayes, A. M. Science and technology for water purification in the coming decades. *Nature* **2008**, 452, 301-310.-

4. Ghaffour, N.; Missimer, T. M.; Amy, G. L. Technical review and evaluation of the economics of water desalination: Current and future challenges for better water supply sustainability. *Desalination* **2013**, 309, 197-207.

5. Greenlee, L. F.; Lawler, D.F.; Freeman, B. D.; Marrot, B.; Moulin, P. Reverse osmosis desalination: water sources, technology, and today's challenges. *Water Res.* **2009**, 43, 2317–2348.

6. Klaysom, C.; Cath, T. Y.; Depuydt, T.; Vankelecom, F. J. Forward and pressure retarded osmosis: potential solutions for global challenges in energy and water supply. *Chem. Soc. Rev.* **2013**, 42, 6959- 6989.

7. Chung, T.-S.; Zhang, S.; Wang, K. Y.; Su, J.; Ling, M. M. Forward osmosis processes: yesterday, today and tomorrow. *Desalination* **2012**, 287, 78–81.

8. Zhao, S.; Zou, L.; Tang, C. Y.; Mulcahy, D. Recent developments in forward osmosis: opportunities and challenges. *J. Membr. Sci.* **2012**, 396, 1–21.

9. Wilf, M. Future of the osmotic processes. *Desali. Water Treat*. **2010**, 15, 292–298.

10. Qin, J. J.; Lay, W. C. L.; Kekre, K. A. Recent developments and future challenges of forward osmosis for desalination: A review. *Desalination* **2012**, 39, 123-136.

11. Cath, T. Y.; Childress, A. E.; Elimelech, M. Forward osmosis: principles, applications, and recent developments. *J. Membr. Sci*. **2006**, 281, 70-87.

12. Zhao, D.; Chen, S.; Guo, C.; Zhao, Q.; Lu, X. Multi-functional forward osmosis draw solutes for seawater desalination. *Chinese J. Chem. Eng.* **2015**, Accepted.

13. Ge, Q.; Ling, M.; Chung, T.-S. Draw solutions for forward osmosis processes: Developments, challenges, and prospects for the future. *J. Membr. Sci.* **2013**, 442, 225-237.

14. Qasim, M.; Darwish, N. A.; Sarp, S.; Hilal, N. Water desalination by forward (direct) osmosis phenomenon. *Desalination* **2015**, 374, 47-69.

15. Baker, R. W. Membrane technology and applications. 2nd ed., John Wiley & Sons, Ltd., New York, **2004**.

16. Wang, K. Y.; Chung, T.-S.; Qin, J. J. Polybenzimidazole (PBI) nanofiltration hollow fiber membranes applied in forward osmosis process. *J. Membr. Sci*. **2007**, 300, 6-12.

17. Wang, K. Y.; Yang, Q.; Chung, T.-S.; Rajagopalan, R. Enhanced forward osmosis from chemically modified polybenzimidazole (PBI) nanofiltration hollow fiber membranes with a thin wall. *Chem. Eng. Sci*. **2009**, 61, 1577-1584.

18. Zhang, S.; Wang, K. Y.; Chung, T.-S.; Chen, H.; Jean, Y. C.; Amy, G. Well-constructed cellulose acetate membranes for forward osmosis: minimized internal concentration polarization with an ultra-thin selective layer. *J. Membr. Sci*. **2010**, 360, 522-535.

19. Su, J.; Yang, Q.; Teo, J. F.; Chung, T.-S. Cellulose acetate nanofiltration hollow fiber membranes for forward osmsis processes. *J. Membr. Sci*. **2010**, 355, 36-44.

20. Wang, K. Y.; Ong, R. C.; Chung, T.-S. Double-skinned forward osmosis membranes for reducing internal concentration polarization within the porous sublayer. *Ind. Eng. Chem. Res.* **2010**, 49, 4824-4831.

21. Sairam, M.; Sereewatthanawut, E.; Li, K.; Bismarck, A.; Livingston, A. G. Method for the preparation of cellulose acetate flat sheet composite membranes for forward osmosis – desalination using MgSO4 draw solution. *Desalination* **2011**, 273, 299-307.

22. Akther, N.; Sodiq, A.; Giwa, A.; Daer, S.; Arafat, H. A.; Hasan, S. W. Recent advancement in forward osmosis desalination: A review. *Chem. Eng. J.* **2015**, 281, 502–522.

23. Wang, K. Y.; Chung, T.-S.; Amy, G. Developing thin-film-composite forward osmosis membranes on the PES/SPSf substarte through interfacial polymerization. *AICHe J.* **2012**, 58, 770-781.

24. Wei, J.; Liu, X.; Qiu, C.; Wang, R.; Tang, C. Y. Influence of monomer concentrations on the performance of polyamide-base thin film composite forward osmosis membranes. *J. Membr. Sci.* **2011**, 381, 110-117.

25. Tiraferri, A.; Yip, N. Y.; Phillip, W. A.; Schiffman, J. D.; Elimelech, M. Relating performance of thin-film composite forward osmosis membranes to support layer formation ans structure. *J. Membr. Sci.* **2011**, 367, 340-352.

26. Widjojo, N.; Chung, T.-S.; Weber, M.; Maletzko, C.; Warzelhan, V. The role of sulfonated polymer and macrovoid-free structure in the support layer for thin-film composite (TFC) forward osmosis (FO) membranes. *J. Membr. Sci.* **2011**, 383, 214-223.

27. Wei, J.; Qiu, C.; Tang, C. Y.; Wang, R.; Fane, A. G. Synthesis and characterization of flat-sheet thin film composite forward osmosis membranes. *J. Membr. Sci.* **2011**, 372, 292-302.

28. Emadzadeh, D.; Lau, W. J.; Matsuura, T.; Rahbari-Sisakht, M.; Ismail, A. F. A novel thin film composite forward osmosis membrane prepared from PSf-TiO2 nanocomposite substarte for water desalination. *Chem. Eng. J.* **2014**, 237, 70–80.

29. Amini, M.; Jahanshahi, M.; Rahimpour, A. Synthesis of novel thin film nanocomposite (TFN) forward osmosis membranes using functionalized multi-walled carbon nanotubes. *J. Membr. Sci.* **2013**, 435, 233-241.

30. Ma, N.; Wei, J.; Qi, S.; Zhao, Y.; Gao, Y.; Tang, C. Y. Nanocomposite substrates fro controlling internal concentration polarization in forward osmosis membranes. *J. Membr. Sci.* **2013**, 441, 54-62.

31. Saren, Q.; Qiu, C. Q.; Tang, C. Y. Synthesis and characterization of novel forward osmosis membranes based on layer-by-layer assembly. *Environ. Sci. Technol*. **2011**, 45, 5201-5208.

32. Qiu, C.; Qi, S.; Tang, C. Y. Synthesis of high flux forwasrd osmosis membranes by chemically crosslinked layer-by-layer polyelectrolytes. *J. Membr. Sci*. **2011**, 381, 74-80.

33. Cui, Y.; Wang, H.; Chung, T.-S. Micro-morphology and formation of layer-by-layer membranes and their performance in osmotically driven processes. *Chem. Eng. Sci.* **2013**, 101, 13-26.

34. Qi, S.; Qiu, C. Q.; Zhao, Y.; Tang, C. Y. Double-skinned forward osmosis membranes based on layer-by-layer assembly-FO performance and fouling behavior. *J. Membr. Sci*. **2012**, 405-406, 20-29.

35. Cai, T.; Li, X.; Wan, C.; Chung, T.-S. Zwitterionic polymers grafted poly(ether sulfone) hollow fiber membranes and their antifouling behaviors for osmotic power generation. *J. Membr. Sci*. **2016**, 497, 142-152.

36. Li, X.; Cai, T.; Chung, T.-S. Anyi-fouling behavior of hyperbranched polyglycerol-grafted poly(ether sulfone) hollow fiber membranes for osmotic power generation. *Environ. Sci. Technol.* **2014**, 48, 9898-9907.

37. McGinnis, R. L.; Elimelech, M. Energy requirements of ammonia-carbon dioxide forward osmosis desalination. *Desalination* **2007**, 207, 370-382.

38. McGovern, R. K.; Lienhard, J. H. On the potential of forward osmosis to energetically outperform reverse osmosis desalination. *J. Membr. Sci*. **2014**, 469, 245-250.

39. Shaffer, D. L.; Werber, J. R.; Jaramillo, H.; Lin, S.; Elimelech, M. Forward osmosis: Where are we now? *Desalination* **2015**, 356, 271-284.

CHAPTER 2

LITERATURE REVIEW

2.1 Draw Solution

Two major components of FO, the semi-permeable membrane and the draw solution, would determine the outcome of an FO process. Many researchers have put extensive effort in the fabrication of FO membrane with high water flux and low salt leakage.[1-5] Recently, the focus has been averted to looking for ideal draw solutions. In FO, draw solution is responsible for providing the driving force for the transport of water molecule from the feed solution. The criteria for selecting a suitable draw solution include:

(1) the draw solution should be able to provide high osmotic pressure, especially for the application of seawater desalination;

(2) the reverse solute flux should be low, otherwise the replenishment cost will be higher;

(3) the draw solution can be easily and economically regenerated;

(4) the draw solution should not cause damage, scaling or fouling to the FO membrane;

(5) the draw solution should be nontoxic and cheap. [6]

Some parameters of the draw solution will significantly affect the performance of FO processes, especially in the terms of water flux. Table 2.1 summarizes such characteristics of draw solution and their possible impact on FO performance. Nowadays, FO process is not only employed in seawater desalination,[7-10] but also many other areas, such as wastewater treatment,[11, 12] protein concentration,[13-15] fertigation,[16-19] power generation.[20, 21] Draw solutes coupled with different regeneration methods have been proposed according to different applications. Basically, these

draw solutes can be classified into inorganic and organic-based draw solutes which are naturally or commercially available and other synthetic draw solutes.

Table 2.1 Characteristics of draw solutes that affect FO performance and their impact on FO performance.[7]

Characteristics	Impact on FO performance
Osmotic pressure difference	A high osmotic pressure difference between draw solution and feed solution induces a high FO water flux.
Molecular weight (Mw)	Draw solutes with small MW usually produce higher osmotic pressure but a larger reverse flux than draw solutes with larger MW. In addition, draw solutes with larger MW usually have a higher viscosity when dissolve in water, which has an adverse impact on FO water flux.
Viscosity	A low viscosity leads to a high water flux as internal concentration polarization (ICP) is less serious.
Particle size	The size of nanostructured draw solutes will usually affect their FO performance. It not only determines the hydrophilicity/osmotic pressure of the draw solutes, but also the severity of agglomeration when MNPs are the draw solutes.
Temperature	Higher operational temperature can decrease the solution viscosity, thus enhancing the water flux. But the reverse flux will be more significant due to higher diffusivity rate and membrane scaling and fouling can be adversely affected as well.

2.1.1 Inorganic Draw Solutes

Conventional draw solutes are mainly water soluble inorganic salts, such as NaCl, $MgCl_2$, $MgSO_4$ and KCl.[22] These draw solutes usually have high water flux due to their high water

solubility, high dissociation rate and low viscosity. However, the significant reverse flux resulted from their small molecular size increases the replenishment cost. More importantly, there are no suitable regeneration methods for such draw solutions.

In 1970s, a series of salts with water solubility controlled were developed as FO draw solutes for seawater desalination. Aluminum sulfate ($Al_2(SO_4)_3$) solution has adequate osmotic pressure and can generate high water flux in FO process. Afterwards, the product water was produced by a precipitation reaction between $Al_2(SO_4)_3$ and calcium hydroxide ($Ca(OH)_2$). As the resultant salts, namely calcium sulfate ($CaSO_4$) and aluminum hydroxide ($Al(OH)_3$) are both water insoluble, no ion was left in water. [23] Subsequently, the excess $Ca(OH)_2$ left in water was neutralized by H_2SO_4 and CO_2. Similarly, copper sulfate ($CuSO_4$) and magnesium sulfate ($MgSO_4$) were investigated as draw solutes and regenerated by precipitation reactions with barium hydroxide ($Ba(OH)_2$).[24, 25] This regeneration method requires accurate addition of counter ions and involves addition of chemicals which may contaminate the product water. Therefore, this approach might not be practical. Another type of inorganic-based draw solute is thermal reversible salts such as ammonia-carbon dioxide (NH_4HCO_3).[26-29] Since early 2000s, MsCutcheon, Elimelech and co-workers studied NH_4HCO_3 in FO seawater desalination process coupled with its thermal regeneration method. NH_4HCO_3 solution was used as draw solution in FO, after which it was decomposed to NH_3 and CO_2 gases around 60 °C and separated from water. By dissolving CO_2 and NH_3 back into water, the draw solution could be regenerated for use. However, its serious reverse flux remains a problem. Meanwhile, it is difficult to remove ammonia in product water and reduce its concentration to less than 2.0 mg/L which is a standard for drinking water set by World Health Organization (WHO). Moreover, the system needs to induce waste heat from other

industry to enhance its energy-efficiency advantages.[28] It is worth noting that in 2011, Oasys Water commercialized this draw solution in FO process to treat wastewater in pilot tests.

In 2009, Tan [30] and Zhao [31] investigated the feasibility of nanofiltration (NF) to regenerate inorganic salts ($MgCl_2$, $MgSO_4$, and Na_2SO_4). A hydraulic driving force of ~3 MPa was needed in the NF cell and a relatively high salt rejection (> 90 %) could be achieved. However, the FO-NF hybrid process was also energy-intensive and only limited to multivalent ions-based salts.

Shon and co-workers investigated inorganic salts which are also fertilizers as draw solutes.[16, 17, 19] Figure 2.1 briefly illustrates their approach. The diluted draw solution would be directly used in fertigation system rather than going through the regeneration process. As the regeneration process usually consumes most of the energy in the whole system, their work apparently reduces much of the energy cost. However, drawbacks and limitation of this kind of draw solute still exist. First, this kind of draw solute can only be used in agriculture, but is not suitable for other applications. Secondly, the minimum nutrient concentration in the in the product might exceed the required concentration limit for direct fertigation caused by the osmotic equilibrium between the feed solution and draw solution. Thus, it remains a challenge to achieve desired fertilizer concentration before direct fertigation.[32]
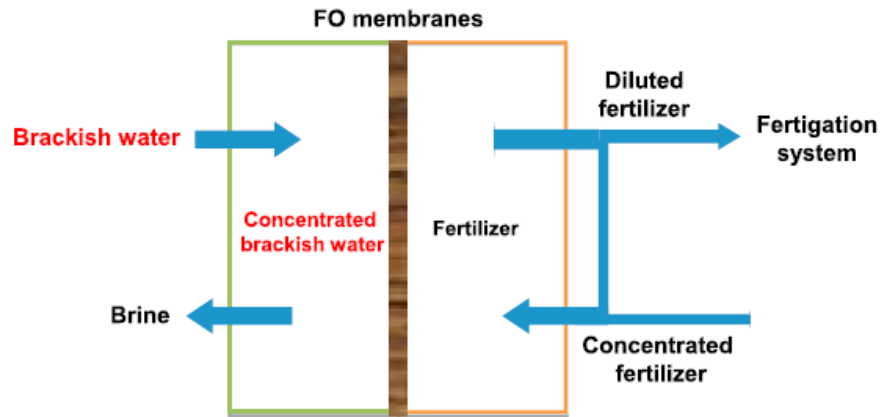
Figure 2.1 Schematic illustration of the fertilizer drawn FO process for irrigation.[32]

Recently, Mondal *et al.* employed sea bittern, which is the mother liquor that remains after recovery of common salt from seawater, as the draw solution to efficiently dewater clarified sugarcane juice.[33] Up to 4-fold concentration of sucrose was achieved while much less energy was needed compared to multiple effect evaporation.

2.1.2 Organic Molecules Based Draw Solutes

Another type of conventional draw solutes is organic nutrient compounds. Although they are not electrolytes, these compounds still have the potential to generate FO water flux due to their high water solubility.[34, 35] It was originally proposed for water supply in emergency lifeboats and the final product was intended for drinking and supply of energy (Figure 2.2).[36] Thus, there is no need for regeneration process for this purpose. Kravath *et al*. first explored the feasibility of using glucose as a draw solute for seawater desalination in 1975.[35] Later, Stache replaced glucose with fructose to avoid the thirst induced after drinking glucose solution.[34] Furthermore, fructose shows an advantage of higher osmosis efficiency than glucose.
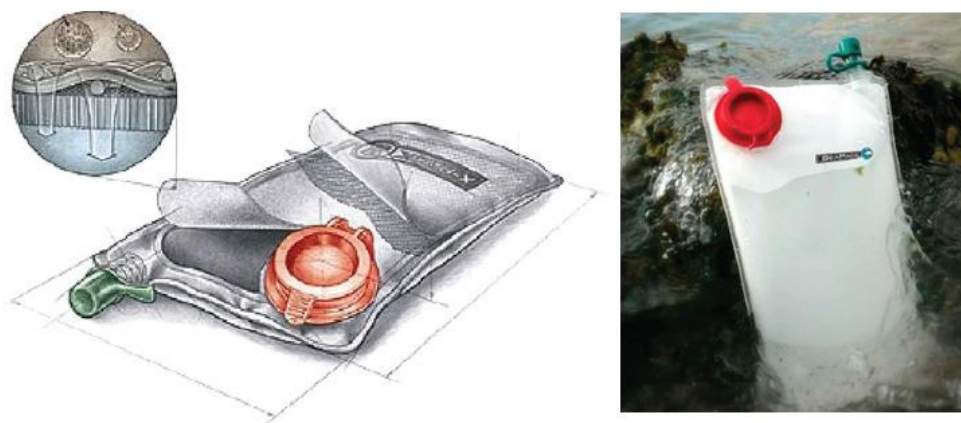
Figure 2.2 Schematic drawing of a hydration bag.[36]

2.1.3 Larger-Molecular-Sized Electrolytes

To minimize the high reverse flux, a variety of electrolytes with larger molecular sizes than inorganic salts were developed. Ge and co-workers synthesized a poly-electrolyte of polyacrylic acid sodium (PAA-Na) salt and applied it as a FO draw solute.[11, 37] FO tests showed its capability to generate high water flux with an insignificant reverse flux for several cycles. The large molecular size also allowed the regeneration of PAA-Na by an ultrafiltration (UF) at a low solution concentration.[37] However, the high viscosity of concentrated solution prevents this polyelectrolyte from being practically used as FO draw solute. Therefore, the authors conducted FO process at a higher temperature to reduce the viscosity and integrated membrane distillation (MD) as the regeneration method.[11] MD is a mass transfer process driven by a partial vapor pressure difference because of a temperature gradient across a hydrophobic porous membrane. During MD, volatile compounds in the hot feed solution evaporate at the hot side, diffuse through the membrane pore and then condense into a liquid flow at the cold side. In the FO-MD

24

hybrid system, PAA-Na solution (50-70 °C) would circulate in the FO part first to attract water from seawater or wastewater, after which the diluted draw solution with the same temperature circulated towards the shell side of the MD membrane, while cold water (20 °C) flowed in the lumen side. The regenerated draw solution flows back to the FO part. This FO-MD hybrid system was employed to recycle water from acid dye contaminated wastewater. Yen *et al*. also employed this system to recycle a series of 2-methylimidazole-based draw solutes for seawater desalination.[38] The FO-MD process was demonstrated to be a highly stable and continuous process for long time. However, it is necessary to find low quality waste heat to reduce the energy cost.[11]

Recently, Ge and coworkers explored hydroacid and oxalic acid complexes as a new class of draw solutes.[12, 39-41] Their abundant hydrophilic groups and expanded configurations make them appropriate candidates to be FO draw solutes. Superior FO performance was achieved in terms of high water flux and negligible reverse flux. When at the same molar concentration, these complexes showed even higher water fluxes than NaCl solution while a much lower reverse flux was also obtained. A pressure driven nanofiltration (NF) was used to regenerate the draw solution at a low concentration. The salt rejection in NF was relatively low which would cause loss of draw solute. Thus, it is necessary to explore more efficient regeneration methods for this kind of draw solutes.

In 2014, Duan demonstrated that sodium lignin sulfonate (NaLS) is a potential draw solute candidate and can be utilized in desert restoration.[42] NaLS is an abundant waste product in paper manufacturing industry and is nontoxic to plants and animals. After the NaLS solution is sprayed on desert, the water of the solution permeates into sand while NaLS is left on the surface and forms a relatively firm 'sand crust' with a thickness of 0.5~1 cm. This crust is able to stabilize

the sand against wind and retain water for plant growth. Therefore, similarly as the concept of fertilizers, the authors used concentrated NaLS solution to attract water from wastewater or brackish water for dilution and then directly used the diluted draw solution on desert. However, people need to induce wastewater or brackish water from near cities first and the feasibility of this concept requires further investigation.

2.1.4 Magnetic Nanoparticle (MNPs)

Functional MNPs are considered as promising draw solutes and have attracted considerable interest in last few years.[13, 15, 43-49] Warne *et al*. first demonstrated this concept that hydrophilic MNPs could be employed as FO draw solutes and removed from water with an external magnetic field.[49] MNPs coated with 2-pyrrolidone (2-Pyrol-MNPs), triethylene glycol (TREG-MNPs) and polyacrylic acid (PAA-MNPs) were synthesized by one-pot reaction and evaluated as FO draw solutes by Ling and co-workers.[47] Among these MNPs, PAA-MNPs exhibited the highest driving force and subsequently the highest FO water flux. The driving force could be enhanced by increasing the hydrophilicity of capping ligand and/or reducing nanoparticle size. Bai and co-workers synthesized MNPs coated with dextran and utilized them in FO for brackish water desalination.[43] These MNPs can generate osmotic pressure as high as those inorganic salts. Additionally, they can be easily recovered from draw solution by an external magnet and recycled back into draw solution stream. It should be noted that the reverse flux of MNPs was negligible due to their relatively large size.[47]

However, during recyclability test, researchers found that agglomeration happened under a high-strength magnetic field.[44] This leads to a drop in FO water flux after every cycle. In response to

this problem, Ling *et al*. redispersed agglomerated MNPs with ultrasonication after every cycle.[44] While the size of MNPs was maintained to their original value, the magnetic core of the MNPs was gradually oxidized and lost their magnetic force to some extent. Other regeneration method was also employed to overcome the problem of MNPs agglomeration. Ling *et al*. recycled MNPs with ultrafiltration (UF) instead of high-strength magnetic field.[44] The agglomeration of MNPs was avoided, while MNPs smaller than the pore size of UF membrane might leak through the membrane.

To avoid using high-strength magnetic field, thermoresponsive MNPs were proposed.[45, 46] MNPs coated with thermoresponsive polymer/copolymer would agglomerate spontaneously to lager particles when heated above the low critical solution temperature (LCST). [45] These much larger particles could be easily trapped by either a low-strength magnetic field or UF membrane. PNIPAM-modified MNPs developed by Ling *et al*. successfully showed thermal responsiveness and good recyclability.[45] However, the FO water flux obtained with water as the feed solution was too low for any practical FO process. Thus, Zhao *et al*. modified the MNPs with copolymer poly(sodium styrene-4-sulfonate)-co-poly(N-isopropylacrylamide) (PSSS-PNIPAM).[46] This draw solute shows high osmotic pressure for seawater desalination. The proposed FO process together with regeneration process was illustrated in Figure 2.3. Magnetic separation of the MNPs was assisted by mild heating and followed by an ultrafiltration step.
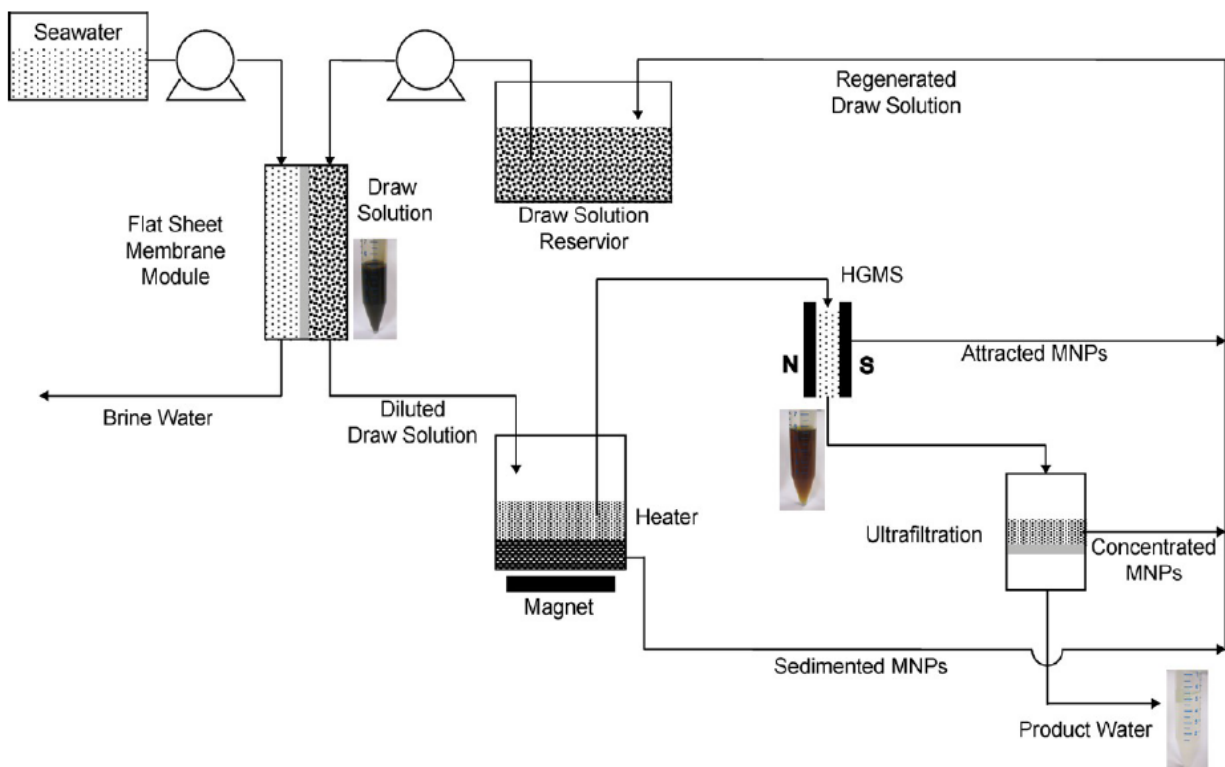
Figure 2.3 Scheme of FO process (using PSSS-PNIPAM capped MNP as the draw solute) together with the regeneration process.[46]

2.1.5 Stimuli Responsive Hydrogels

In recent years, various hydrogels with intelligent response to temperature, solar energy, electric field or pressure stimuli were proposed for use in FO.[50-54] These hydrogels can change their structures reversibly in response to external stimuli, thus facilitating the regeneration of the diluted draw solutions. For example, poly(*N*-isopropylacrylamine) (PNIPAM) hydrogel is thermoresponsive. It absorbs water at the volume phase transition temperature (VPTT, ~32 °C) and expels water in its network when the temperature is above the VPTT.[55] However, the driving force of this hydrogel is poor. Researchers induced additional ionic groups to thermoresponsive hydrogels. Therefore, poly(*N*-isopropylacrylamide-*co*-acrylic acid sodium) (P(NIPAM-*co*-SA))

was developed and showed better FO performance in terms of higher water flux.[51] However, addition of ionic groups resulted in decreased thermoresponsive property. Dewatering experiments were carried out at 50 °C and a constant pressure of 3 MPa was applied for 2 min. This significantly increases the energy cost and conflicts with the merit of FO process. It should be noted that the hydrogel size would affect the water flux and also the water recovery.[50, 52]

In recent years, Wang and co-workers utilized solar energy in the regeneration process by incorporating light-absorbing carbon particles or graphene in hydrogels (PNIPAM-C).[53, 54] The carbon particles or graphene can enhance the sunlight absorption and thus increase the temperature of the composite hydrogels when being exposed to sunlight. A water recovery fraction of > 85% from the PNIPAM-C was achieved, which was higher than that obtained with pure PNIPAM hydrogel (water recovery rate of >50%) under sunlight at an irradiation intensity of 1.0 kW/m for 20 min.[54] The use of natural solar energy can greatly reduce the energy cost of the dewatering step. However, reliance on solar energy may raise problems in implementation.

Generally, the development of these intelligent hydrogels inspires more and more novel regeneration methods of draw solutes. However, the FO performance of these hydrogels is usually poor, and most likely, the whole process is still energy intensive. Hence, their practicability is still in doubt and requires further investigation.

2.1.6 Stimuli Responsive Liquids

In 2012, thermoresponsive draw solutes of N,N',N"-triacylated tris(2-aminoethyl)amine (acyl-TAEA) derivatives were designed by Noh and co-workers.[56] Such thermoresponsive solutions can draw water from seawater at temperature lower than the LCST, and the water flows reversely

at temperature higher than the LCST. Similar to hydrogels aforementioned, the water flux of these draw solutions are too low for any FO application.

Recently, switchable polarity solvents (SPS) which are mixtures of carbon dioxide, water and tertiary, were proposed as a novel draws solute by Stone and co-workers.[57] This draw solute exhibits competitive FO water fluxes as inorganic salts at high concentrations. Afterwards, by polar to nonpolar phase shift induced by 1 atm of nitrogen or air with mild heating (60 °C), the SPS could be spontaneously separated from water (Figure 2.4). To obtain drinking water, RO is still necessary as the final step. In addition, the high pH of the concentrated SPS requires more robust FO membranes with a wider pH tolerance range. The proposed SPS FO system was illustrated in Figure 2.5.

$$NR_3 + CO_2 + H_2O \rightleftharpoons HNR_3^+ + HCO_3^-$$

water immiscible   water miscible
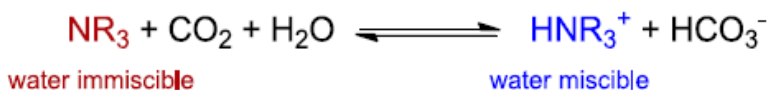
Figure 2.4 Nonpolar to polar shift of a switchable polarity solvent.[57]
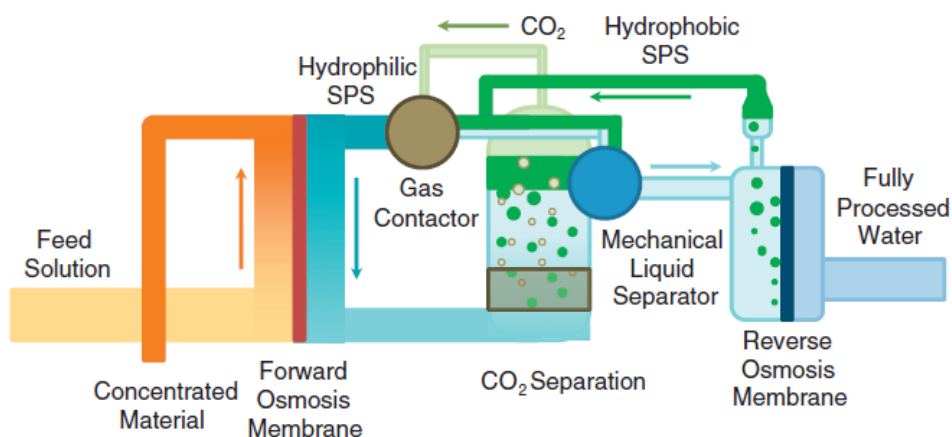
Figure 2.5 Proposed FO together with regeneration process using switchable polarity solvents as the draw solution.[57]

Very recently, Cai *et al.* employed thermoresponsive ionic liquids (ILs), tetrabutylphosphonium 2,4-dimethylbenzenesulfonate (P$_{4444}$DMBS) and tetrabutylphosphonium mesitylenesulfonate (P$_{4444}$TMBS), as draw solutes for FO seawater desalination (Figure 2.6).[58] However, similarly to the case of DEH solution, 60 wt% P$_{4444}$DMBS solution with an osmolality of 4000 mOsm kg^{-1} gave only 2.7 LMH for seawater desalination (Cai and Shen, 2015). These water fluxes are much lower than the ones obtained by other draw solutions that have similar osmolality.
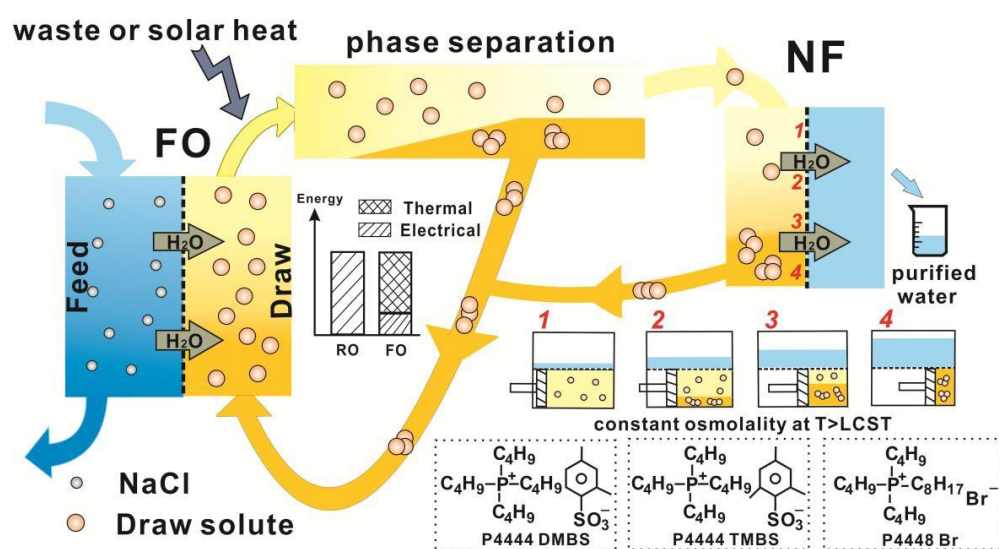
Figure 2.6 FO processes with thermoresponsive ionic liquids as draw solutes.[58]

2.2 Regeneration Methods of Draw Solution

The energy input of a close-loop FO process mainly depends on the recovery method of draw solution. In recent years, a number of novel draw solutions have been reported together with a variety of regeneration methods have been reported, including thermal separation, precipitation, membrane separation, stimuli-response separation, and direct application without regeneration. Luo *et al.* conduct a review on the regeneration methods of draw solution.[59] An overview of the

existing recovery methods of draw solution and their advantages and disadvantages are present in Table 2.2. However, existing regeneration methods still face many challenges, such as low energy-efficiency and environmental friendliness, low water recovery rate, low water quality, complicated procedures, *etc*. Among these challenges, reducing energy input in regeneration process is most essential. Therefore, future work on draw solution should focus on utilizing low-cost energy sources, like industrial waste heat or renewable energy source such as solar energy. In this way, FO process can show its advantages over other desalination technologies and increase its sustainability as mature membrane-based technologies for clean water production.

Table 2.2 An overview of existing regeneration approaches of draw solution in FO.[59]

Category	Draw solution (DS)	Method	Advantages & disadvantages	Ref.
Thermal separation	SO_2	Heating or air stripping	Easy, but energy intensive and toxic	[60]
	NH_3/CO_2	Heating (~60 °C)	Energy-efficient, but poor water quality	[26-29]
	SPS	Heating (~60 °C) with bubbling N_2	Energy-efficient, but poor water quality	[56]
	Thermoresponsive ionic liquid	Heating (~60 °C)	Energy efficient and facile, poor water quality	[58]
Precipitation	$Al_2(SO_4)_3$	Precipitation by adding $Ca(OH)_2$	Energy–efficient, but costly consumables, toxic by-products	[23]
	$MgSO_4$, $CuSO_4$	Precipitation by adding $Ba(OH)_2$	Energy –efficient, but costly consumables, toxic by-products	[24, 25]
Membrane separation	Seawater	Reverse osmosis (RO)	High water quality, but high operating cost	[61]
	Inorganic salts, hydroacid complexes	Nanofiltration (NF)	Relatively high water quality, but relatively high operating cost	[30, 31, 39]
	PAA-Na	Ultrafiltration (UF)	Relatively poor water quality and operating cost	[37]
	PAA-Na	Membrane distillation (MD)	High water quality and recovery rate, low capital cost, high energy cost unless using low-grade heat	[11]
Stimuli-response separation	Functionalized MNPs	Magnetic separation	Easy, energy-efficient, but poor reusability due to agglomeration, poor water quality	[13, 15, 43-49]
	Thermoresponsive MNPs	Magnetic heating	Energy-efficient, poor water quality	[45, 46]
	Hydrogel	Heating combined with hydraulic pressure	Relative energy-efficient, but low recovery rate, unsuitability for continuous FO process	[55]
	Composite hydrogel	Response to sunlight	Low recovery rate, unsuitability for continuous FO process	[53, 54]
Direct use	Sugars	None	No energy input, but limited to special applications, possible requirement of post treatment	[36]
	Fertilizers			[16]
	NaLS			[42]

2.3 Challenges

The requirements of selecting a suitable draw solution highly depend on the purpose of the FO process. Given the advantages and limitations of draw solutions reported, none of them is perfect for FO seawater desalination processes. Developing ideal FO draw solutions for the application of seawater desalination to obtain clean water or even drinkable water still needs a great deal of effort.

Firstly, unlike other FO applications, the draw solution employed in seawater desalination must have osmotic pressure higher that of seawater which is about 27 atm. This requires that the draw solute is highly hydrophilic which is contributed by high percentage of dissociable species. In addition, the reverse solute flux should be minimal in order to reduce replenishment cost and also to meet the standard of clean water or drinkable water. This means that the size of draw solute molecule should be optimized. Finally, easy separation of draw solute and product water is critical so that the cost on energy is affordable. Therefore, this study emphasizes on the development of eligible draw solutions that meet the above requirements.

2.4 References

1. Ong, R. C.; Chung, T.-S. Novel cellulose ester substrates for high performance flat-sheet thin-film composite (TFC) forward osmosis (FO) membranes. *J. Membr. Sci*. **2015**, 473, 63-71.

2. Duong, P. H.; Chung, T.-S. Application of thin film composite membranes with forward osmosis technology for the separation of emulsified oil-water. *J. Membr. Sci*. **2014**, 452, 117-126.

3. Gai, J. G.; Gong, X. L. Zero internal concentration polarization FO membrane: functionalized graphene. *J. Mater. Chem. A*. **2014**, 2, 425-429.

4. Pardeshi, P.; Mungray, A. A. Synthesis, characterization and application of novel high flux FO membrane by layer-by-layer self-assembled polyelectrolyte. *J. Membr. Sci*. **2014**, 453, 202-211.

5. Wang, R.; Shi, L.; Tang, C. Y. Characterization of novel forward osmosis hollow fiber membranes. *Desalination*, **2009**, 239, 1-3.

6. Klaysom, C.; Cath, T. Y.; Depuydt, T.; Vankelecom, F. J. Forward and pressure retarded osmosis: potential solutions for global challenges in energy and water supply. *Chem. Soc. Rev*. **2013**, 42, 6959- 6989.

7. Chekli, L.; Phuntsho, S.; Shon, H. K.; Vigneswaran, S.; Kandasamy, J.; Chanan, A. A review of draw solutes in forward osmosis process and their use in modern applications. *Desali. Water Treat.* **2012**, 43, 167-184.

8. Ghaffour, N.; Missimer, T. M.; Amy, G. L. Technical review and evaluation of the economics of water desalination: Current and future challenges for better water supply sustainability. *Desalination* **2013**, 309, 197-207.

9. Elimelech, M.; Phillip, W. A. The future of seawater desalination: energy, technology, and the environment. Science 2011, 333, 712-717.

10. Shannon, M. A.; Bohn, P. W.; Elimelech, M.; Georgiadis, J. G.; Marinas, B. J.; Mayes, A. M. Science and technology for water purification in the coming decades. *Nature* **2008**, 452, 301-310.

11. Ge, Q.; Chung, T.-S. Polyelectrolyte-promoted forward osmosis-membrane distillation (FO-MD) hybrid process for dye wastewater treatment. *Environ. Sci. Technol*. **2012**, 46, 6236-6243.

12. Cui, Y.; Ge, Q.; Liu, X. Y.; Chung, T.-S. Novel forward osmosis process to effectively remove heavy metal ions. *J. Membr. Sci*. **2014**, 467, 188-194.

13. Ling, M. M.; Chung, T.-S. Novel dual-stage FO system for sustainable protein enrichment using nanoparticles as intermediate draw solutes. *J. Membr. Sci*. **2011**, 372, 201-209.

14. Wang, K. Y.; Teoh, M. M.; Nugroho, A.; Chung, T.-S. Integrated forward osmosis–membrane distillation (FO–MD) hybrid system for the concentration of protein solutions. *Chem. Eng. Sci*. **2011**, 66, 2421-2430.

15. Guo, C. X.; Huang, S.; Lu, X. A solventless thermolysis route to large-scale production of ultra-small hydrophilic and biocompatible magnetic ferrite nanocrystals and their application for efficient protein enrichment. *Green Chem*. **2014**, 16. 2571-2579.

16. Phuntsho, S.; Shon, H. K.; Hong, S.; Lee, S.; Vigneswaran, S. A novel low energy fertilizer driven forward osmosis desalination for direct fertigation: Evaluating the performance of fertilizer draw solutions. *J. Membr. Sci*. **2011**, 375, 172-181.

17. Phuntsho, S.; Shon, H. K.; Hong, S.; Lee, S.; Vigneswaran, S; Kandasamy, J. Fertiliser drawn forward osmosis desalination: the concept, performance and limitations for fertigation. *Rev. Environ. Sci. Biotechnol* **2011**, 11, 147-168.

18. Phuntsho, S.; Lotfi, F.; Hong, S.; Shaffer, D. L.; Elimelech, M. Membrane scaling and flux decline during fertilizer-drawn forward osmosis desalination of brackish groundwater. *Water Res*. **2014**, 57, 172-182.

19. Sahebi, S.; Phuntsho, S.; Kim, J. E.; Hong, S.; Shon, H. K. Pressure assisted fertilizer drawn osmosis process to enhance final dilution of the fertilizer draw solution beyond osmotic equilibrium. 2015, 481, 63-72.

20. Lee, K. L.; Baker, R. W.; Lonsdale, H. K. Membrane for power generation by pressure-retarded osmosis. *J. Membr. Sci*. **1981**, 8, 141-171.

21. Achilli, A.; Cath, T. Y.; Childress, A. E. Power generation with pressure retarded osmosis: An experimental and theoretical investigation. *J. Membr. Sci*. **2009**, 343, 42-52.

22. Achilli, A.; Cath, T.Y.; Childress, A.E. Selection of inorganic-based draw solutions for forward osmosis applications. *J. Membr. Sci.* **2010**, 364, 233-241.

23. Frank, B.S. Desalination of sea water. US Patent **1972**.

24. Alnaizy, R.; Aidan A.; Qasim, M. Copper sulfate as draw solute in forward osmosis desalination. *J. Environ. Chem. Engin.* **2013**, 1, 424-430.

25. Alnaizy, R.; Aidan, A.; Qasim,M. Draw solute recovery by metathesis precipitation in forward osmosis desalination. *Desali. Water Treat*. **2013**, 51, 5516-5525.

26. McCutcheon, J. R.; McGinnis, R. L.; Elimelech, M. A novel ammonia--carbon dioxide forward (direct) osmosis. *Desalination* **2005**, 174, 1-11.

27. McCutcheon, J.R.; McGinnis, R. L.; Elimelech, M. Desalination by ammonia–carbon dioxide forward osmosis: Influence of draw and feed solution concentrations on process performance. *J. Membr. Sci*. **2006**, 278, 114-123.

28. McGinnis, R.L.; Elimelech, M. Energy requirements of ammonia–carbon dioxide forward osmosis desalination. *Desalination* **2007**, 207, 370-382.

29. Boo, C.; Khalil, Y. F.; Elimelech, M. Performance evaluation of trimethylamine-carbon dioxide thermolytic draw solution for engineered osmosis. *J. Membr. Sci.* **2015**, 473, 302-309.

30. Tan, C.H.; Ng, H. Y. A novel hybrid forward osmosis - nanofiltration (FO-NF) process for seawater desalination: Draw solution selection and system configuration. *Desali. Water Treat.* **2010**, 13, 356-361.

31. Zhao, S.; Zou, L.; Mulcahy, D. Brackish water desalination by a hybrid forward osmosis–nanofiltration system using divalent draw solute. *Desalination* **2012**, 284, 175-181.

32. Ge, Q.; Ling, M.; Chung, T.-S. Draw solutions for forward osmosis processes: Developments, challenges, and prospects for the future. *J. Membr. Sci.* **2013**, 442, 225-237.

33. Mondal, D.; Nataraj, S. K.; Reddy, A. V. R.; Ghara, K. K.; Maiti, P.; Upadhyay, S. C.; Ghosh, P. K. Four-fold concentration of sucrose in sugarcane juice through energy efficient forward osmosis using sea bittern as draw solution. *RSC Adv*. **2015**, 5, 17872-17878.

34. Stache, K. Apparatus for transforming sea water, brackish water, polluted water or the like into a nutrious drink by means of osmosis. US Patent **1989**.

35. Kravath, R.E.; Davis, J. A. Desalination of sea water by direct osmosis. *Desalination* **1975**, 16, 151-155.

36. Retrieved from http://www.hydrationtech.com.

37. Ge, Q.; Su, J.; Amy, G. L.; Chung, T.-S. Exploration of polyelectrolytes as draw solutes in forward osmosis processes. *Water Res*. **2012**, 46, 1318-1326.

38. Yen, S.K.; Su, M.; Wang, K. Y.; Chung, T.-S. Study of draw solutes using 2-methylimidazole-based compounds in forward osmosis. *J. Membr. Sci*. **2010**, 364, 242-252.

39. Ge, Q.; Chung, T.-S. Hydroacid complexes: a new class of draw solutes to promote forward osmosis (FO) processes. *Chem. Commun*. **2013**, 49, 8471-8473.

40. Ge, Q.; Fu, F.; Chung, T.-S. Ferric and cobaltous hydroacid complexes for forward osmosis (FO) processes. *Water Res*. **2014**, 58, 230-238.

41. Ge, Q.; Chung, T.-S. Oxalic acid complexes: promising draw solutes for forward osmosis (FO) in protein enrichment. *Chem. Commun*. **2015**, 51, 4854-4857.

42. Duan, J.; Litwiller, E.; Choi, S. H.; Pinnau, I. Evaluation of sodium lignin sulfonate as draw solute in forward osmosis for desert restoration. *J. Membr. Sci*. **2014**, 453, 463-470.

43. Bai, H.; Liu, Z.; Sun, D. D. Highly water soluble and recovered dextran coated Fe3O4 magnetic nanoparticles for brackish water desalination. *Sep. Purif. Technol*. **2011**, 81, 392-399.

44. Ling, M. M.; Chung, T.-S. Desalination process using super hydrophilic nanoparticles via forward osmosis integrated with ultrafiltration regeneration. *Desalination* **2011**, 278, 194-202.

45. Ling, M. M.; Chung, T.-S.; Lu, X. M. Facile synthesis of thermosensitive magnetic nanoparticles as "smart" draw solutes in forward osmosis. *Chem. Commun*. **2011**, 47, 10788-10790.

46. Zhao, Q.; Chen, N.; Zhao. D.; Lu, X. Thermoresponsive magnetic nanoparticles for seawater desalination. *ACS Appl. Mater*. *Interfaces* **2013**, 5, 11453-11461.

47. Ling, M. M.; Wang, K. Y.; Chung, T.-S. Highly water-soluble magnetic nanoparticles as novel draw solutes in forward osmosis for water reuse. *Ind. Eng. Chem. Res*. **2010**, 49, 5869-5876.

48. Ge, Q.; Su, J.; Chung, T.-S. Hydrophilic superparamagnetic nanoparticles: Synthesis, characterization, and performance in forward osmosis processes. *Ind. Eng. Chem. Res*. **2011**, 50, 382-388.

49. Warne, B. Water purification method. GB Patent **2008**.

50. Li, D.; Zhang, X.; Simon, G. P.; Wang, H. Forward osmosis desalination using polymer hydrogels as a draw agent: influence of draw agent, feed solution and membrane on process performance. *Water Res*. **2013**, 47, 209-15.

51. Li, D.; Zhang, X.; Yao, J.; Simon, G. P.; Wang, H. Stimuli-responsive polymer hydrogels as a new class of draw agent for forward osmosis desalination. *Chem. Commun*. **2011**, 47, 1710-1712.

52. Razmjou, A.; Simon, G. P.; Wang, H. Effect of particle size on the performance of forward osmosis desalination by stimuli-responsive polymer hydrogels as a draw agent. *Chem. Engin. J.* **2013**, 215-216, 913-920.

53. Zeng, Y.; Qiu, L.; Wang, K.; Yao, J.; Li, D.; Simon, G. P. Significantly enhanced water flux in forward osmosis desalination with polymer-graphene composite hydrogels as a draw agent. *RSC Advances* **2013**, 3, 887-894.

54. Li, D.; Zhang, X.; Yao, J.; Zeng, Y.; Simon, G. P.; Wang, H. Composite polymer hydrogels as draw agents in forward osmosis and solar dewatering. *Soft Matter*. **2011**, 7, 10048-10056.

55. Fei, R.; George, J. T. Ultra-strong thermoresponsive double network hydrogels. *Soft Matter*. **2013**, 9, 2912-2919.

56. Noh, M.; Mok, Y.; Lee, S.; Kim, H.; Lee, S. H.; Jin, G. Novel lower critical solution temperature phase transition materials effectively control osmosis by mild temperature changes. *Chem. Commun*. **2012**, 48, 3845-3847.

57. Stone, M. L.; Rae, C.; Stewart, F. F.; Wilson, A. D. Switchable polarity solvents as draw solutes for forward osmosis. *Desalination* **2013**, 312, 124-129.

58. Cai, Y.; Shen, W.; Wei, J.; Chong, T. H.; Wang, R. Energy-efficient desalination by forward osmosis using responsive ionic liquid draw solutes. *Eviron. Sci.: Water Res. Technol*. **2015**, 1, 341-347.

59. Luo, H.; Wang, Q.; Zhang, T. C.; Tao, T.; Zhou, A.; Chen, L.; Bie, X. A review on the recovery methods of draw solutes in forward osmosis. *J. Water Process Engin.* **2014**, 4, 212-223.

60. McGinnis, R. L. Osmotic desalination process. US Patent, **2002**.

61. Yangali-Quintanilla, V.; Li, Z.; Valladares, R.; Li, Q; Amy, G. Indirect desalination of Red Sea water with forward osmosis and low pressure reverse osmosis for water reuse. *Desalination* **2011**, 280, 160-166.

CHAPTER 3

A DENDRIMER-BASED FORWARD OSMOSIS DRAW SOLUTE FOR SEAWATER DESALINATION

3.1 Introduction

Clean water supply plays a crucial role in our life. Seawater, which constitutes about 97% of total water on earth, has been a potential fresh water source.[1-4] However, seawater desalination has always been a challenge due to the high energy cost, though great efforts have been devoted by many researchers. Forward osmosis (FO), as one of emerging desalination technologies, can produce clean water based on the osmotic pressure gradient across a semi-permeable membrane.[5-12] Unlike pressure-driven membrane separation processes such as reverse osmosis (RO), FO is a spontaneous process as long as: (1) there is a semi-permeable membrane between a solution with lower osmotic pressure (feed solution) and a solution with higher osmotic pressure (draw solution); and (2) there is an osmotic pressure gradient across the membrane. After drawing water from the feed solution, the diluted draw solution needs to be re-concentrated to regain its original osmotic pressure. Combining FO with a draw solution regeneration process, fresh water can be continuously produced. Therefore, if the regeneration of draw solution is easy and energy-saving, FO may require less energy than RO for seawater desalination.[11, 13]

Semi-permeable membrane and draw solute are two key factors influencing FO performance. While many researchers have focused on the development of FO membranes,[14-16] draw solutes have just attracted increasing attention in recent years.[17, 18] An ideal draw solute not only should provide high osmotic pressure, but also needs to minimize reverse solute flux for lower

replenishment cost. Moreover, facile regeneration method is essential for low energy cost. A wide range of novel draw solutes have been proposed, mainly aiming to reduce reverse flux and lower regeneration cost. These draw solutes can usually be classified into inorganic-based draw solutes, organic-based draw solutes, and other novel draw solutes such as stimuli responsive compounds and hydrophilic magnetic nanoparticles. Draw solutes based on inorganic salts, such as ammonium bicarbonate[19] and sulfur dioxide,[20] have been investigated and show promise for energy-saving desalination, although issues such as reverse flux and damage to membranes remain to be solved. Organic molecule-based draw solutes, such as sodium polyacrylate (PAA-Na) developed by Ge *et al*., may exhibit both high osmotic pressure and low reverse flux.[21] For the regeneration of such draw solutions, both ultrafiltration and membrane distillation (MD) have been demonstrated.[21-23] Draw solutes based on stimuli-responsive compounds and nanostructures have become a new research focus recently, mainly because of their promising new regeneration strategies, such as temperature or CO_2-indcued phase separation or capturing via magnetic field. In recent years, Wang and co-workers utilized solar energy in the regeneration process by incorporating light-absorbing carbon particles or graphene in hydrogels (PNIPAM-C).[24, 25] These hydrogels absorb water at the volume phase transition temperature (VPTT) and expels water in its network when the temperature is above the VPTT.[26] The carbon particles or graphene can enhance the sunlight absorption and thus increase the temperature of the composite hydrogels when being exposed to sunlight. Recently, switchable polarity solvents (SPS) mixed with carbon dioxide, water and tertiary amines were proposed as novel draw solutes by Stone and co-worker.[27] Through polar to nonpolar phase shift induced by nitrogen or air with mild heating (60 °C), the SPS could be spontaneously separated from water. Functional MNPs are also considered as promising draw solutes and have attracted considerable interest in the past few

years because the regeneration can be achieved with magnetic field.[28-33] To avoid using high-strength magnetic field and reduce the agglomeration of MNPs, Zhao *et al*. modified the MNPs with thermoresponsive copolymer poly(sodium styrene-4-sulfonate)-co-poly(N-isopropylacrylamide) (PSSS-PNIPAM).[31,34] MNPs coated with this copolymer agglomerate spontaneously to larger sizes when heated above its low critical solution temperature (LCST), making possible effective separation with low-strength magnetic field or ultrafiltration.

Despite the rapid progress, it is still a challenging task to develop an FO draw solute that offers high osmotic pressure, low viscosity, minimal reverse solute flux, and good compatibility with FO membranes. In this work, we investigated a dendrimer, poly(amidoamine) (PAMAM), as FO draw solute. PAMAM has a highly branched tree-like structure.[35] With tailored core structure and surface groups, PAMAM has found applications in diverse areas such as drug delivery,[36, 37] nanoparticle synthesis,[38, 39] and catalysis.[40] If PAMAM is functionalized with hydrophilic terminal groups such as -COONa or -SO$_3$Na, these groups can be highly dissociated in solution to provide high osmotic pressure. In addition, PAMAM has a relatively large molecular size, which allows minimal reverse solute flux. Compared to linear polyelectrolytes, the hyperbranched structure of PAMAM would allow lower solution viscosity,[41] causing reduced adverse effect of internal concentration polarization (ICP) on water flux of FO processes. Finally, PAMAM also shows advantages of non-toxicity and biocompatibility. Adham *et al*.[42] measured the osmotic pressures of dendrimer solutions. However, the use of dendrimers in FO progress to desalinate seawater has not been reported. In this work, we systematically evaluated PAMAM terminated with –COONa as draw solute for seawater desalination in a process combined with forward osmosis and membrane distillation (FO-MD). PAMAM with different generation numbers were synthesized and their FO performances were evaluated in terms of water flux,

reverse solute flux, as well as regeneration with MD. When 2.5-generation (2.5G) PAMAM-COONa was used as the draw solute in FO processes under PRO mode, relatively high water fluxes of 29.7 and 9 liter/(m^2·hr) were achieved using DI water and seawater as the feed solutions, respectively. A low reverse solute flux of about 10 gMH was attained. The draw solution was successfully re-generated using MD.

3.2 Materials and Methods

3.2.1 Materials

Ethylenediamine (EDA, >99%), methyl acrylate (MA, 99%), methanol (anhydrous, 99.8%), sodium hydroxide (>98.0%), sodium chloride (>99.5%) were purchased from Sigma-Aldrich and used as received. Deionized (DI) water with a resistivity of 18MΩ·cm used in all experiments was purified by a Milli-Q unit (Millipore, USA). Thin film composite embedded support membrane (batch number: 842121) in all FO tests was provided by Hydration Technologies Inc. (HTI, Albany, OR). Seawater (osmolality: 842 mOsm kg^{-1}) as the feed solution in the FO tests was collected from Sentosa coast, Singapore.

3.2.2 Synthesis of PAMAM of Different Generations

PAMAM of different generations were prepared by an iterative process involving two reactions: (a) Michael addition of the amino-terminated surface onto methyl acrylate, resulting in an ester-terminated outer layer; and (b) coupling with ethylene diamine to achieve a new amino-terminated surface (Figure 1).[43, 44] Typically, to synthesize 0.072 mol of 0.5G PAMAM, 50 mL

46

of anhydrous methanol and 4.8 ml of ethylenediamine (EDA) (0.072 mol) were added to a flask under an ice bath and N_2 protection. The mixture was stirred for 15 mins followed by the addition of 51.8 mL of methyl acrylate (MA) (0.576 mol). After 30 mins, the ice bath and N_2 were removed and the mixture was then stirred continuously at room temperature for 24 hrs. Before the reaction for 1.0G PAMAM, methanol and excess MA were evaporated completely under vacuum at room temperature. Afterwards, 50 mL of anhydrous methanol was added to 0.5G PAMAM in an ice bath with N_2 protection. After stirring for 15 mins, 38.5 mL EDA (0.576 mol) was added and the ice bath and N_2 protection were removed 30 mins later. The mixture was left for 24 hrs at room temperature before the methanol and excess EDA were removed by vacuum evaporation. These two reactions were carried out alternatively for the synthesis of PAMAM of different generations. Each cycle of the two reactions forms a new generation, with subsequent reaction (a) giving rise to a "half" generation (Figure 3.2). In this work, 1.5G, 2.5G, 3.5G and 4.5G PAMAM were prepared.
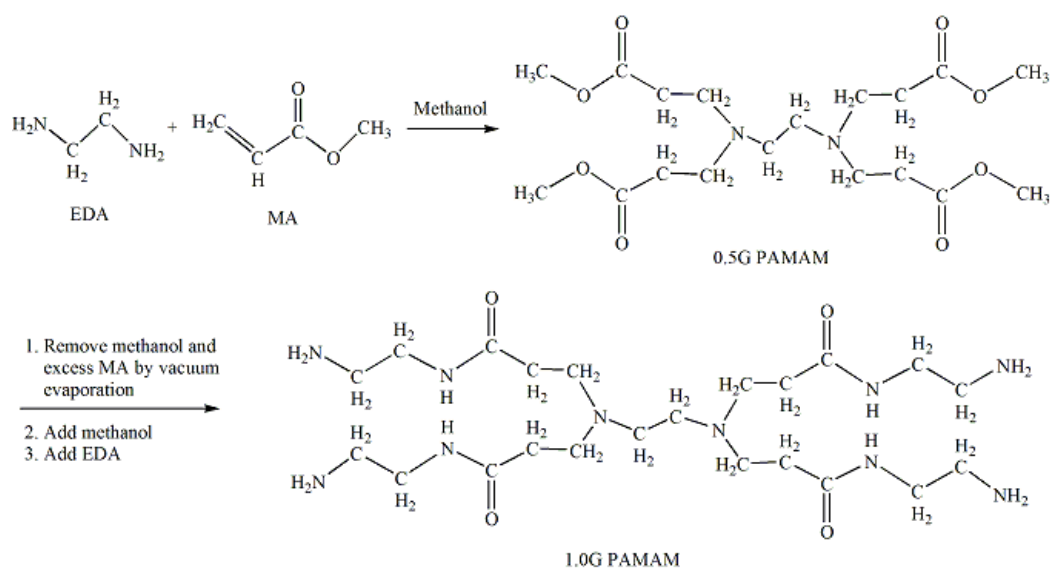
Figure 3.1 Schematic illustration of the synthesis of PAMAM.
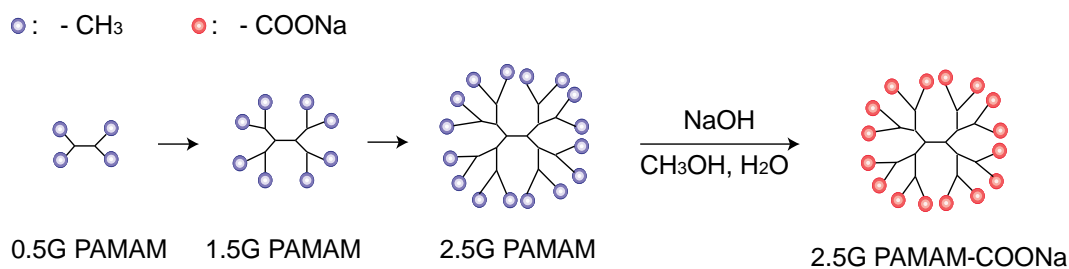
Figure 3.2 Synthesis of 2.5G PAMAM-COONa.

3.2.3 Modification of Terminal Groups

The as-synthesized PAMAM terminated with ester groups is hydrophobic. Hydrolysis of the ester group was employed to terminate PMAMA with hydrophilic -COONa groups. Using 2.5G PAMAM as an example (Figure 3.2),[45] 11.52 g NaOH (0.288 mol) was added to a stirred and cooled (ice/water bath) solution of 2.5G PAMAM (50.5 g, 0.018 mol) in a mixed solvent containing 200 ml methanol and 120 ml water. After 30 mins the ice/water bath was removed, then the reaction mixture was stirred overnight. The solvent was evaporated under vacuum to give PAMAM-COONa.

Osmolalities of 1.5G, 2.5G, 3.5G and 4.5G PAMAM-COONa aqueous solutions (33.3 wt%) were measured with an osmometer (Wescor, Vapro vapor pressure osmometer). The relative viscosities (η_r, compared to DI water) of the solutions were calculated with the following equation:

$$\eta_r = \eta/\eta_0 = (t\,\rho)/(t_0\,\rho_0)$$

where t and t_0 (s) are the respective elution times of PAMAM-COONa solution and DI water measured by an AVS 360 inherent viscosity meter; ρ and ρ_0 (g mL^{-1}) are the densities of PAMAM-COONa solution and DI water, respectively.

3.2.4 FO Tests

A lab-scale FO setup as shown in Figure 3.3 (left part) was employed for all FO tests with a membrane area of 1cm×2cm. HTI thin film composite (TFC) embedded support membrane was chosen for the FO tests. Water fluxes using pure DI water, seawater from Singapore coast (osmolality: 842 mOsm kg^{-1}), and simulated seawater (3.5 wt% NaCl solution, osmolality: 1200 mOsm kg^{-1}) as feed solutions were measured respectively. Draw solutions were prepared from 1.5G, 2.5G, 3.5G, 4.5G PAMAM-COONa and saturated salt water. During the FO process, the feed solutions and draw solutions flowed concurrently through the two sides of the cell channel at a velocity of 20 cm s^{-1} and each process was run for 30 mins to determine the average water flux. Both FO and pressure retarded osmosis (PRO) modes were applied in this process at room temperature (about 25 °C). PRO mode indicates that the water flux is measured with the selective layer of the FO membrane facing the draw solution, while FO mode means the selective layer facing the feed solution. Water fluxes (J_v, L m^{-2} h^{-1}, abbreviated as LMH) were calculated from the weight increment of the draw solution during certain time using the following equation:

$$J_v = \Delta m/(A_m \cdot \Delta t \times 1000)$$

where Δm (g) is the mass of water permeated across the effective FO membrane area A_m (m^2) over a time period of Δt (h), assuming the density of water is 1000 g L^{-1}.

Reverse fluxes were measured with a conductivity meter (Schott Instrument, Lab 960) by using DI water as the feed solution. Calibration lines of the conductivity *vs*. the concentration of PAMAM-COONa were first obtained. Once the conductivity of the feed solution were measured upon the completion of FO, the amount of draw solute leaked into the feed solution was calculated. Reverse solute fluxes (J_s, g m^{-2} h^{-1}, abbreviated as gMH) were obtained according to the following equation:

$$J_s = c \cdot V / (A_m \cdot \Delta t)$$

where c (g/L) is the concentration of the PMAMA-COONa leaked into the feed solution with a volume of V (L) over a time period of Δt (h).

3.2.5 Regeneration of Draw Solution by Membrane Distillation

MD was employed to regenerate the draw solution as shown in Figure 3.3 (right part). The spinning conditions and characterizations of the MD membrane are given in the Table 3.1 with an effective MD membrane area of 28 cm^2. The diluted draw solutions after FO process were circulated through the shell side of the MD module after being heated up to 50 °C, while cold water (10 °C) was circulated through the lumen side. MD water fluxes were also calculated using eq. (2) with Δm (g) as the mass of water permeated across the effective MD membrane area A_m (cm^2).
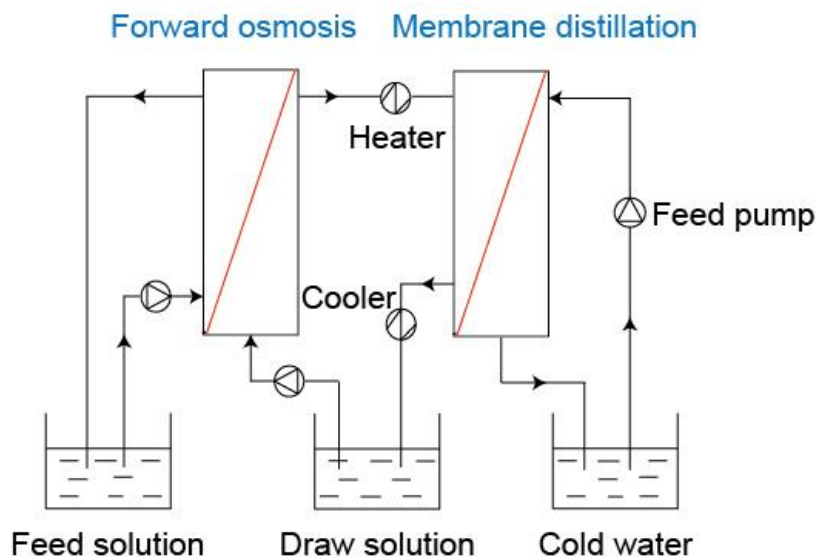
Figure 3.3 Lab-scale FO-MD process.

Table 3.1 Parameters for MD hollow fiber fabrication.

Dope Composition (wt%)	PVDF/NMP/EG 15/70/15
POSS loading in total solid (wt%)	30
Bore flow rate (ml/min)	NMP/water: 85/15
Dope flow rate (ml/min)	5
Bore flow rate (ml/min)	3
External coagulant (wt%)	IPA/water: 60/40
Air gap (cm)	5
Post-treatment	3 days store in tap water, freeze drying

3.3 Results and Discussion

3.3.1 Characterizations of PAMAM-COONa of Different Generations

PAMAM-COONa of various generations were evaluated as FO draw solutes. For FO draw solutes based on large molecules, the solution viscosity can affect FO performance significantly.

51

A high viscosity of the draw solution not only leads to high energy consumption for fluid pumping, but also results in severe internal polarization concentration. As mentioned earlier, dendrimers should exhibit lower viscosity than linear polymers of similar molecular weight.[41] As shown in Figure 3.4a, the relative viscosity (η_r) of 1.5G PAMAM-COONa solution (33.3 wt.%) is about 7, and it increases with the generation number due to the increased molecular weight. For 4.5G PAMAM-COONa solution, the relative viscosity is 11. But this viscosity is still lower than other linear polymer draw solutions such as PAA-Na.[21]

The dendrimer generation number not only affects its solution viscosity, but the osmolality and water flux of FO processes as well. The osmolality of a dendrimer solution is mainly determined by the number of dissociated terminal groups. Although the number of terminal groups increases progressively with the generation number, the ratio between the number of terminal groups and the dendrimer molecular weight decreases (the ratios for 1.5G, 2.5G, 3.5G and 4.5G PAMAM-COONa are 0.0063, 0.005, 0.0047 and 0.0046, respectively). In addition, because the charges of terminal groups are too close to each other due to compacter structure at higher generation, the dissociation rate of Na^+ ions from the terminal groups decreases with the generation number.[42] Consequently, the solution (fixed mass fraction) of a higher generation dendrimer gives a lower osmotic pressure. As shown in Figure 3.4b, the osmolalities of 33.3 wt.% 1.5G, 2.5G, 3.5G and 4.5G PAMAM-COONa solutions are 3846, 3603, 3417, and 2990 mOsm/kg, respectively. We also measured the water fluxes of the dendrimer solutions using DI water as the feed solution under PRO mode. For 1.5G, 2.5G, 3.5G, and 4.5G PAMAM-COONa, the water fluxes were 31.8, 29.7, 29.4, and 19.8 LMH, respectively.
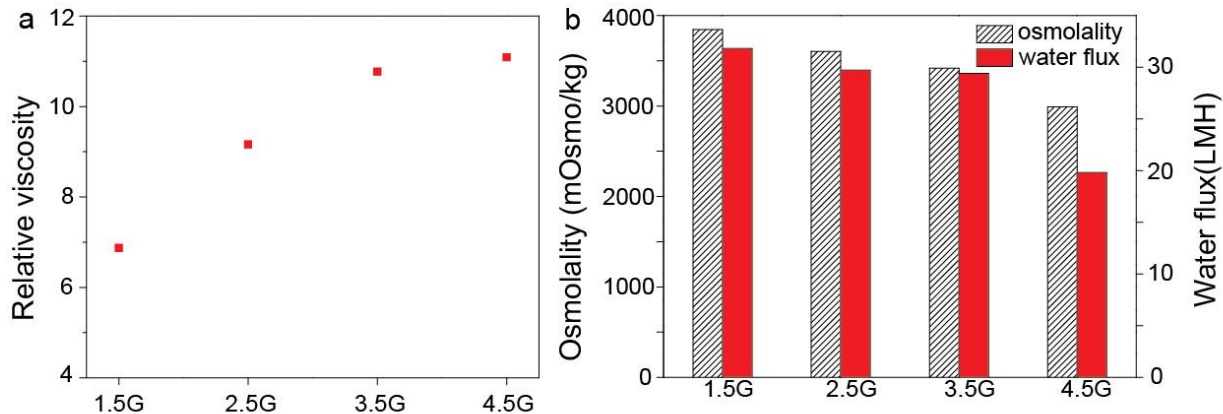
Figure 3.4 (a) Relative viscosities and (b) osmolalities and water fluxes of 1.5G, 2.5G, 3.5G, and 4.5G PAMAM-COONa aqueous solutions (33.3 wt%) in FO processes. The water fluxes of FO processes were obtained under PRO mode using DI water as the feed solution.

The reverse fluxes of PAMAM-COONa of various generations were measured and compared with saturated and 1.8 M NaCl solutions under the same FO process. As shown in Figure 3.6, PAMAM-COONa solutions of all generations have significantly lower reverse fluxes than NaCl solutions. In addition, the reverse fluxes of PAMAM-COONa decreased with increasing generation number -- for 1.5G, 2.5G, 3.5G and 4.5G PAMAM-COONa, the reverse solute fluxes were 10.42, 8.86, 5.64, and 4.68 gMH, respectively. When 1.8 M NaCl solution (osmolality ~ 3600 mOsmo/kg) was used as the draw solution, its reverse solute flux (42 gMH) was more than four times higher than that of the dendrimer solutions. The much lower reverse fluxes of PAMAM-COONa solutions can be attributed to the larger molecular sizes of PAMAM-COONa. Also, when the generation number of PAMAM-COONa increases, the molecular size increases, resulting in larger barrier for the diffusion of draw solute across the FO membrane.
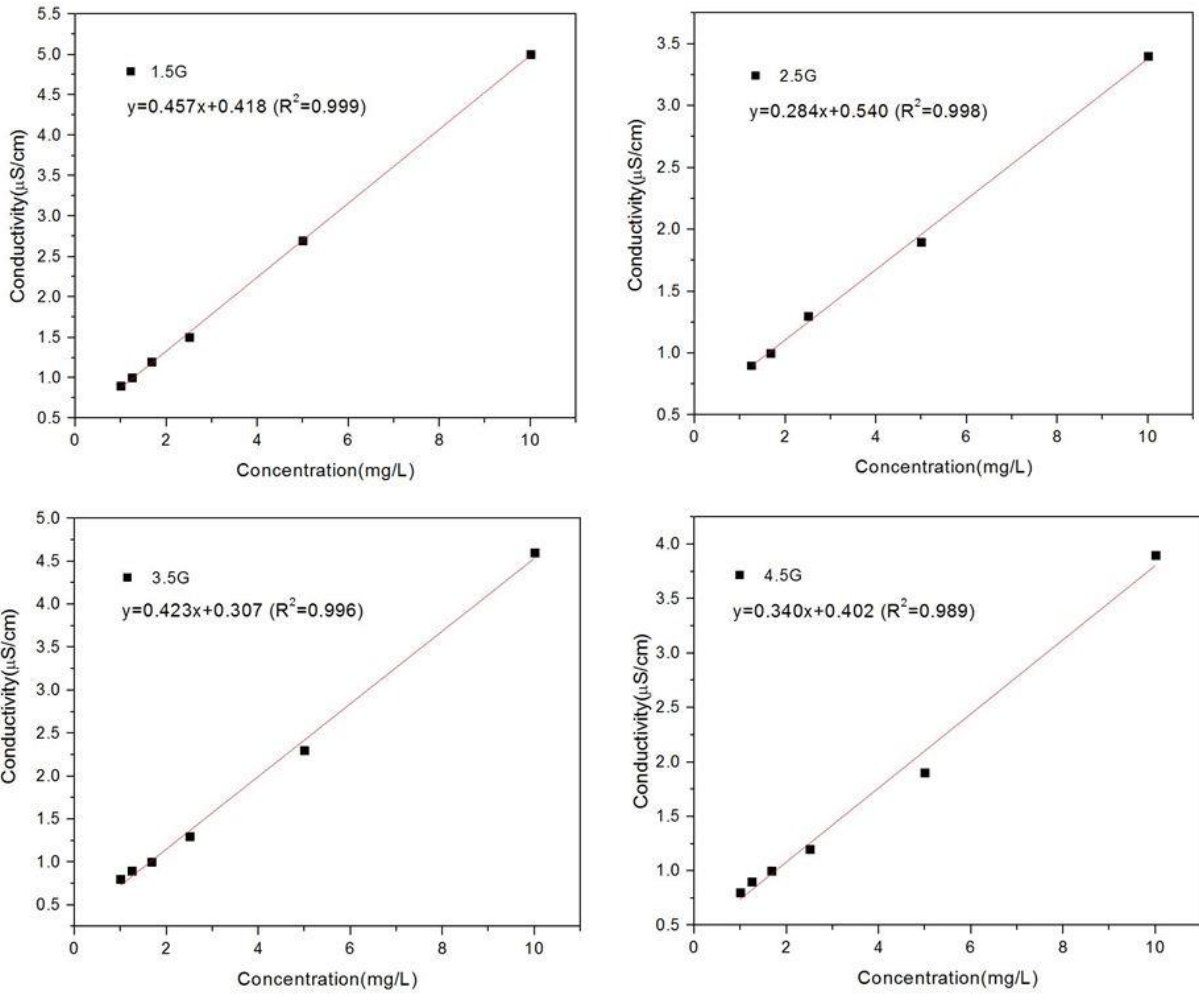
Figure 3.5 Calibration line of conductivity vs. different concentrations of dendrimer-based draw solution.
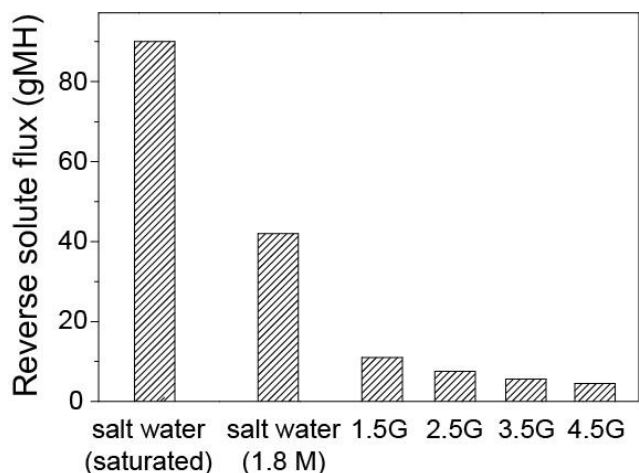
Figure 3.6 Reverse solute fluxes of 1.5G, 2.5G, 3.5G, 4.5G PAMAM-COONa, and NaCl solutions.

Based on the above results, we summarized the key properties of PAMAM-COONa solutions of different generations. As shown in Table 3.2, 1.5G PAMAM-COONa exhibits the lowest relative viscosity, highest osmolality, and water flux of FO processes. But it also shows highest reverse solute flux. Considering that the reverse solute flux of 2.5G PAMAM-COONa is below 10 gMH, and higher generation number causes high cost of synthesis and lower water flux of FO processes, we chose 2.5G PAMAM-COONa as the model FO draw solute for further tests.

Table 3.2 Summary of molecular weighht, relative viscosity, osmolality, water flux of FO processes and reverse solute fluxes of 1.5G, 2.5G, 3.5G, and 4.5G PAMAM-COONa aqueous solutions (33.3 wt%).

	Molecular weight	Relative viscosity	Osmolality (mOsmo/kg)	Water flux of FO processes (LMH)	Reverse solute flux (gMH)
1.5 G	1268	6.87	3846	31.8	11
2.5 G	3200	9.16	3603	29.7	7.5
3.5 G	6808	10.77	3417	29.4	5.5
4.5 G	13913	11.09	2990	19.8	4.54

3.3.2 2.5G PAMAM-COONa as FO Draw Solute for Desalination

Alternating FO and MD processes were conducted for multiple cycles to investigate 2.5G PAMAM-COONa as the draw solute for desalination. In the FO tests, three feed solutions, namely DI water, seawater from Singapore coast, and 3.5 wt% NaCl solution as simulated seawater, were employed. When DI water was used as the feed solution, the water flux of FO processes slightly dropped from 26 LMH (1st cycle) to 21.3 LMH (4th cycle). With seawater from Singapore coast and simulated seawater as the feed solutions, the water fluxes almost retained their original values after 4 cycles. The average water fluxes of FO processes over 4 cycles were 24.0, 8.0, and 7.2 LMH with DI water, seawater from Singapore coast, and simulated seawater as the feed solutions, respectively.

After each FO test, the draw solution was regenerated using MD process so its concentration was restored to 33.3 wt.% by producing fresh water. The average MD water flux for 4 cycles was 3.2 LMH (Figure 3.7b). To evaluate the solute leakage in the MD process, the conductivities of the permeate water before and after MD test were obtained. With 2.5G PAMAM-COONa draw solution as the feed to the MD process, the conductivity of the circulating DI water barely increased (from 0.7 to 0.8 μS cm^{-1}). This result indicates a low solute leakage of 2.5G PAMAM-COONa in MD due to its large molecular size. Although MD may be applied for seawater desalination directly, NaCl and water can penetrate into the membrane pores and cause serious membrane fouling and pore wetting problems.[46] The combination of FO and MD systems may allow high quality water product as well as prolonged lifetime of MD membranes.
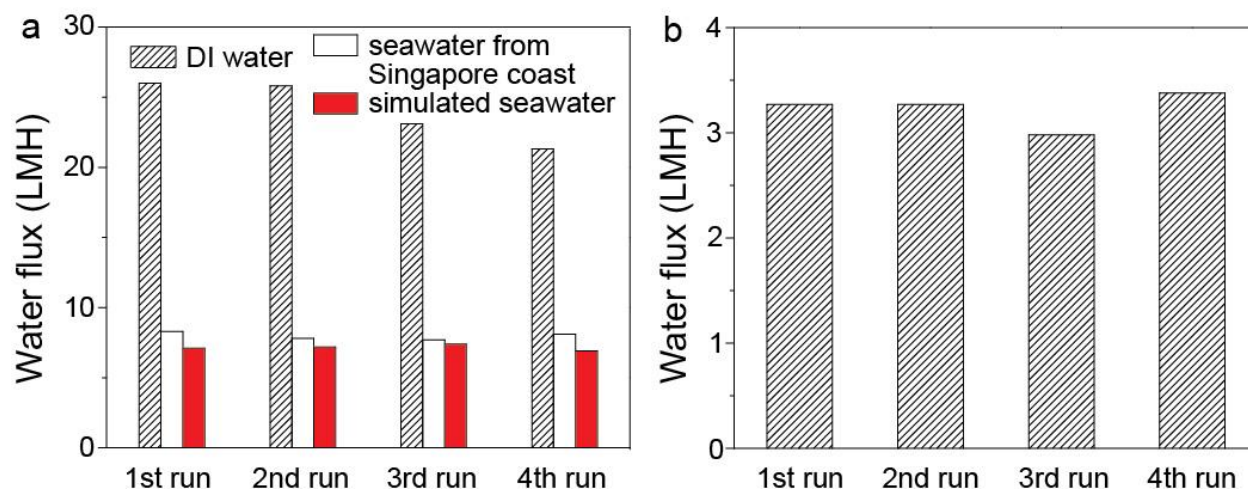
Figure 3.7 (a) Water fluxes of FO processes under PRO mode with 2.5G PAMAM-COONa as the draw solution and DI water, seawater from Singapore coast (osmolality: 842 mOsm kg^{-1}), and simulated water (0.6 M NaCl, osmolality: 1200 mOsm kg^{-1}) as the feed solutions, respectively; (b) MD water fluxes.

We also compared the water fluxes of FO processes with different membrane orientations. As seen in Figure 3.8, the orientation of the FO membrane affects the water flux of FO processes considerably – this can be attributed to the different concentration polarizations. In FO mode (feed solution facing the selective layer of FO membrane), water permeates through the membrane and dilutes the draw solution in the porous supporting layer. This is known as internal concentration polarization (ICP), which leads to a small water flux in FO mode than that of in PRO mode (draw solution facing the selective layer). For example, when using 33.3 wt% 2.5G PAMAM-COONa as the draw solution, the water flux under PRO mode was 26 LMH; while under FO mode, the flux dropped to 12 LMH. The severity of the ICP is affected both by the membrane (porosity, tortuosity and thickness) and draw solution (viscosity and molecular size). In our work, the water flux ratio of FO to PRO mode is about 45%. This ratio can be used to

57

predict water flux of FO processes under PRO mode if water flux under FO mode is known or in the opposite situation. For the HTI FO membrane employed in this work, this ratio is 41% with 1M NaCl solution as draw solute,[47] a value close to our measurement using PAMAM-COONa as the draw solute. This result indicates that the ICP of PAMAM-COONa draw solution may be less severe than other draw solutions with higher viscosities or molecular sizes. It is worth noting that the concentration of the 2.5G PAMAM-COONa can be further increased to generate higher water flux of FO processes – for 40 wt% of 2.5G PAMAM-COONa draw solution, we obtained water fluxes of 30, 9, and 7.5 LMH using DI water, seawater from Singapore coast, and simulated seawater as the feed solutions under PRO mode, respectively (Figure 3.8).
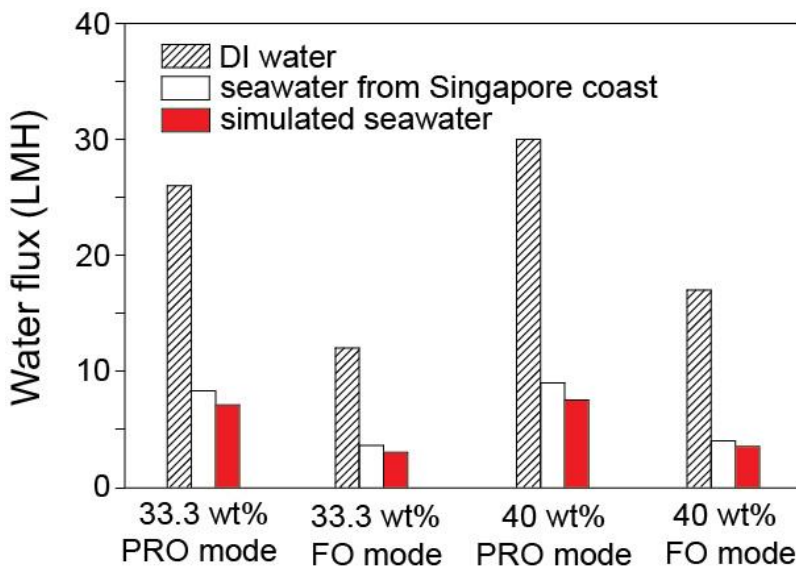
Figure 3.8 Water fluxes under PRO and FO modes using 2.5G PAMAM-COONa (40.0 wt% and 33.3 wt%) as the draw solution and DI water, seawater from Singapore coast and simulated seawater as the feed solutions.

3.4 Conclusions

In this work, 1.5G, 2.5G, 3.5G and 4.5G PAMAM-COONa were synthesized and evaluated as FO draw solutes. At the same solution concentration, PAMAM-COONa of higher generation exhibits lower osmotic pressure and water flux of FO processes, but smaller reverse solute flux. As the synthesis of higher generation of PAMAM-COONa takes longer time and requires higher cost, PAMAM-COONa with lower generation is more suitable for practical applicability. Taking into consideration of water flux, solute leakage and synthesis cost, 2.5G PAMAM-COONa was selected as the optimal FO draw solute among all four generations of dendrimers. With DI water, seawater from Singapore coast, and simulated seawater as the feed solutions, water flux of 26, 8.3 and 7.1 LMH was achieved respectively using 33.3 wt% 2.5G PAMAM as the draw solution in FO processes. After FO testing, the diluted draw solution was re-concentrated *via* MD. At a mild temperature of 50 °C, an average MD water flux of 3.2 LMH was attained.

3.5 References

1. Elimelech, M.; Phillip, W. A. The future of seawater desalination: energy, technology, and the environment. *Science* **2011**, 333, 712-717.

2. Ghaffour, N.; Missimer, T. M.; Amy, G. L. Technical review and evaluation of the economics of water desalination: Current and future challenges for better water supply sustainability. *Desalination* **2013**, 309, 197-207.

3. Likhachev, D. S.; Li, F.-C. Large-scale water desalination methods: a review and new perspectives. *Desali. Water Treat*. **2013**, 51, 2836-2849.

4. Shannon, M. A.; Bohn, P. W.; Elimelech, M.; Georgiadis, J. G.; Marinas, B. J.; Mayes, A. M. Science and technology for water purification in the coming decades. *Nature* **2008**, 452, 301-310.

5. Lee, K. L.; Baker, R. W. Membranes for power generation by pressure-retarded osmosis. *J. Membr. Sci*. **1981**, 8, 141-171.

6. Cath, T.; Childress, A.; Elimelech, M. Forward osmosis: Principles, applications, and recent developments. *J. Membr. Sci*. **2006**, 281, 70-87.

7. Chung, T.-S.; Li, X.; Ong, R. C.; Ge, Q.; Wang, H.; Han, G. Emerging forward osmosis (FO) technologies and challenges ahead for clean water and clean energy applications. *Current Opinion Chem. Engin*. **2012**, 1, 246-257.

8. Chung, T.-S.; Zhang, S.; Wang, K. Y.; Su, J.; Ling, M. M. Forward osmosis processes: Yesterday, today and tomorrow. *Desalination* **2012**, 287, 78-81.

9. Klaysom, C.; Cath, T. Y.; Depuydt, T.; Vankelecom, I. F. Forward and pressure retarded osmosis: potential solutions for global challenges in energy and water supply. *Chem. Soc. Rev.* **2013**, 42, 6959-6989.

10. Phuntsho, S.; Hong, S.; Elimelech, M.; Shon, H. K. Forward osmosis desalination of brackish groundwater: Meeting water quality requirements for fertigation by integrating nanofiltration. *J. Membr. Sci*. **2013**, 436, 1-15.

11. Wilf, M. Future of the osmotic processes. *Desali. Water Treat*. **2010**, 15, 292-298.

12. Zhao, S.; Zou, L.; Tang, C. Y.; Mulcahy, D. Recent developments in forward osmosis: Opportunities and challenges. *J. Membr. Sci*. **2012**, 396, 1-21.

13. Greenlee, L. F.; Lawler, D. F.; Freeman, B. D.; Marrot, B.; Moulin, P. Reverse osmosis desalination: water sources, technology, and today's challenges. *Water Res*. **2009**, 43, 2317-2348.

14. Duong, P. H. H.; Zuo, J.; Chung, T.-S. Highly crosslinked layer-by-layer polyelectrolyte FO membranes: Understanding effects of salt concentration and deposition time on FO performance. *J. Membr. Sci*. **2013**, 427, 411-421.

15. Fu, F. J.; Zhang, S.; Sun, S. P.; Wang, K. Y.; Chung, T.-S. POSS-containing delamination-free dual-layer hollow fiber membranes for forward osmosis and osmotic power generation. J. Membr. Sci. 2013, 443, 144-155.

16. Zhong, P.; Fu, X.; Chung, T.-S.; Weber, M.; Maletzko, C. Development of thin-film composite forward osmosis hollow fiber membranes using direct sulfonated polyphenylenesulfone (sPPSU) as membrane substrates. *Environ. Sci. Technol*. **2013**, 47, 7430-7436.

17. Chekli, L.; Phuntsho, S.; Shon, H. K.; Vigneswaran, S.; Kandasamy, J.; Chanan, A. A review of draw solutes in forward osmosis process and their use in modern applications. *Desali. Water Treat.* **2012**, 43, 167-184.

18. Ge, Q.; Ling, M.; Chung, T.-S. Draw solutions for forward osmosis processes: Developments, challenges, and prospects for the future. *J. Membr. Sci.* **2013**, 442, 225-237.

19. McCutcheon, J. R.; McGinnis, R. L.; Elimelech, M. A novel ammonia-carbon dioxide forward (direct) osmosis desalination process. *Desalination* **2005**, 174, 1-11.

20. Achilli, A.; Cath, T. Y.; Childress, A. E. Selection of inorganic-based draw solutions for forward osmosis applications. *J. Membr. Sci*. **2010**, 364, 233-241.

21. Ge, Q.; Su, J.; Amy, G. L.; Chung, T.-S. Exploration of polyelectrolytes as draw solutes in forward osmosis processes. *Water Res*. **2012**, 46, 1318-1326.

22. Ge, Q.; Wang, P.; Wan, C.; Chung, T.-S. Polyelectrolyte-promoted forward osmosis-membrane distillation (FO-MD) hybrid process for dye wastewater treatment. *Environ. Sci. Technol*. **2012**, 46, 6236-6243.

23. Ge, Q.; Chung, T.-S. Hydroacid complexes: a new class of draw solutes to promote forward osmosis (FO) processes. *Chem. Ccommun*. **2013**, 49, 8471-8473.

24. Li, D.; Zhang, X.; Yao, J.; Zeng, Y.; Simon, G.; Wang, H. Composite polymer hydrogels as draw agents in forward osmosis and solar dewatering. *Soft Matter* **2011**, 7, 10048-10056.

25. Zeng, Y.; Qiu, L.; Wang, K.; Yao, J.; Li, D.; Simon, G. P.; Wang, R.; Wang, H. Significantly enhanced water flux in forward osmosis desalination with polymer-graphene composite hydrogels as a draw agent. *RSC Advances* **2013**, 3, 887-894.

26. Ou, R.; Wang, Y.; Wang, H.; Xu, T. Thermo-sensitive polyelectrolytes as draw solutions in forward osmosis process. *Desalination* **2013**, 318, 48-55.

27. Stone, M. L.; Rae, C.; Stewart, F. F.; Wilson, A. D. Switchable polarity solvents as draw solutes for forward osmosis. *Desalination* **2013**, 312, 124-129.

28. Ling, M. M.; Chung, T.-S. Desalination process using super hydrophilic nanoparticles via forward osmosis integrated with ultrafiltration regeneration. *Desalination* **2011**, 278, 194-202.

29. Han, H.; Lee, J. Y.; Lu, X. Thermoresponsive nanoparticles + plasmonic nanoparticles = photoresponsive heterodimers: facile synthesis and sunlight-induced reversible clustering. *Chem. Commun*. **2013**, 49, 6122-6124.

30. Ling, M. M.; Chung, T.-S.; Lu, X. Facile synthesis of thermosensitive magnetic nanoparticles as "smart" draw solutes in forward osmosis. *Chem. Commun*. **2011**, 47, 10788-10790.

31. Zhao, Q.; Chen, N.; Zhao, D.; Lu, X. Thermoresponsive magnetic nanoparticles for seawater desalination. *ACS Appl. Mater. Interfaces* **2013**, 5, 11453-11461.

32. Ge, Q.; Su, J.; Chung, T.-S. Hydrophilic superparamagnetic nanoparticles: Synthesis, characterization, and performance in forward osmosis processes. *Ind. Eng. Chem. Res*. **2011**, 50, 382-388.

33. Bai, H.; Liu, Z.; Sun, D. D. Highly water soluble and recovered dextran coated Fe3O4 magnetic nanoparticles for brackish water desalination. *Sep. Purif. Technol*. **2011**, 81, 392-399.

34. Zhao, D.; Wang, P.; Zhao, Q.; Chen, N.; Lu, X. Thermoresponsive copolymer-based draw solution for seawater desalination in a combined process of forward osmosis and membrane distillation. *Desalination* **2014**, 348, 26-32.

35. Tomalia, D. A. Birth of a new macromolecular architecture: dendrimers as quantized building blocks for nanoscale synthetic polymer chemistry. Prog. Polym. Sci. 2005, 30, 294-324.

36. Lee, C. C.; MacKay, J. A.; Frechet, J. M.; Szoka, F. C. Designing dendrimers for biological applications. *Nature Biotech*. **2005**, 23, 1517-1526.

37. Svenson, S.; Tomalia, D. A. Dendrimers in biomedical applications--reflections on the field. *Adv. Drug Deliv Rev*. **2005**, 57, 2106-2129.

38. Crooks, R. M.; Zhao, M.; Sun, L.; Checchik, V.; Yeung, L. K. Dendrimer-Encapsulated Metal nanoparticles: synthesis, characterization, and applications to catalysis. *Acc. Chem. Res*. **2001**, 34, 181-190.

39. Zhao, P.; Li, N.; Astruc, D. State of the art in gold nanoparticle synthesis. *Coord. Chem. Rev.* **2013**, 257, 638-655.

40. Wang, D.; Astruc, D. Dendritic catalysis—Basic concepts and recent trends. *Coord. Chem. Rev.* **2013**, 257, 2317-2334.

41. Hobson, L. J.; Feast, W. J. Poly(amidoamine) hyperbranched systems: Synthesis, structure and characterization. *Polym*. **1999**, 40, 1279-1297.

42. Adham, S. Dewatering reverse osmosis concentrate from water reuse applications using forward osmosis. retrieved from http://www.watereuse.org/product/dewatering-reverse-osmosis-concentrate-water-reuse-applications-using-forward-osmosis-0.

43. Tomalia, D. A.; Hall, M. Starbursts dendrimers.3. The importance of branch junction symmetry in the development of topological shell molecules. *J. Am. Chem. Soc*. **1987**, 109, 1601-1603.

44. Tomalia, D. A.; Baker, H.; Dewald, J. Dendritic macromolecules: synthesis of starburst dendrimers. *Macromolecules* **1986**, 19, 2466-2468.

45. van Duijvenbode, R. C.; Rajanayagam, A.; Koper, G. J. M. Synthesis and protonation behavior of carboxylate-functionalized poly(propyleneimine) dendrimers. *Macromolecules* **2000**, 33, 46-52.

46. Wang, P.; Chung, T.-S. Design and fabrication of lotus-root-like multi-bore hollow fiber membrane for direct contact membrane distillation. *J. Membr. Sci*. **2012**, 421-422, 361-374.

47. Retrieved from

http://www.businesswire.com/news/home/20120426006968/en/HTI%E2%80%99S-Thin-Film-Osmosis-Membrane-Production#.U2SCQXmQeQI.

CHAPTER 4

Na$^+$-FUNCTIONALIZED CARBON QUANTUM DOTS: A NEW DRAW SOLUTE IN FORWARD OSMOSIS FOR SEAWATER DESALINATION

4.1 Introduction

Surface-passivated carbonaceous quantum dots (CQDs) with size less than 10 nm are a fascinating class of nanostructured carbons discovered recently.[1-3] CQDs not only inherit the merits of traditional semiconductor-based quantum dots (QDs) such as size-dependent optical properties, but also show advantages of high chemical inertness, biocompatibility and hydrophilicity.[4-6] They can be produced inexpensively on large scale based on synthetic approaches such as hydrothermal treatment of biomass, oxidation of graphite, and candle burning.[7-10] To date, CQDs have been explored in a wide range of applications including bioimaging, drug delivery, diagnostics, sensing and energy conversion/storage.[11-15] Considering their ultra-small size and rich surface chemistry, broader applications are expected for CQDs with further functionalization.

Forward osmosis (FO) is an emerging technology for seawater desalination, wastewater treatment, and green energy.[16-19] An FO process takes the advantage of the difference in osmotic pressure of two solutions separated by a semi-permeable membrane. Spontaneously, water molecules of the less concentrated solution (feed solution, low osmotic pressure) can be drawn to the solution with higher concentration (draw solution, high osmotic pressure).[20] After drawing

water, the diluted draw solution can be regenerated for reuse *via* a separation step that concentrates the solution and produces clean water. Compared to pressure-driven membrane processes such as reverse osmosis (RO) and other water production techniques, FO shows advantages of high rejection to contaminants, low membrane fouling, and potentially less energy consumption.[21,22] For a high-performance FO system, the selection of a suitable draw solute is critical.[23] In general, an ideal FO draw solute should have high hydrophilicity to generate high osmotic pressure and hence high water flux, low solute leakage to reduce replenish cost, facile and low-cost regeneration mechanism, and capability for large scale production.[24] Two main types of draw solutes, namely inorganic compounds including sodium chloride, magnesium chloride and ammonium bicarbonate, and organic molecules such as sugars, ethanol and polyelectrolytes, have been tested in FO.[23-25] These draw solutes offer high FO water fluxes, although some challenges, such as high reverse draw solute permeation, energy-consuming regeneration, or damage of FO membrane, remain unsolved.[26] In the past few years, novel draw solutes such as hydrogels, stimuli-responsive materials, and magnetic nanoparticles have also been developed with demonstrated promise.[16,24] To achieve high water fluxes, the osmotic pressures produced by these draw solutes in aqueous solutions should be improved.

Here we report a new type of FO draw solutes based on Na^+–functionalized carbon quantum dots (Na_CQDs). The fabrication of Na_CQDs is simple and straightforward (Figure 4.1). Firstly, citric acid powder is heated in air at a moderate temperature to give CQDs passivated with carboxyl groups. The CQDs are then dispersed in water, followed by adjusting the pH to 7.0 with NaOH. As a result, the carboxylic acid groups in CQDs are neutralized to give Na^+–functionalized CQDs (referred to as Na_CQDs). Due to the rich ionic species present in Na_CQDs, their aqueous dispersion (0.5 g mL^{-1}) shows osmotic pressure up to 97.4 atm, much

higher than that of seawater (~26 atm). When employed as draw solutes in FO for seawater desalination, Na_CQDs demonstrate high water flux with negligible reverse draw solute permeation.

4.2 Materials and Methods

4.2.1 Fabrication of Na$^+$-Functionalized Carbon Quantum Dots (Na_CQDs)

The Na_CQDs were prepared as follows.[27] In a typical reaction, 100 g citric acid solid powder was put into a glass beaker covered with a glass slide and was heated at 180 ^{o}C for 150 min under air. After the reaction, yellow powder containing carbon quantum dots (CQDs) was produced. The CQDs were then dispersed in water by stirring for 10 min, followed by neutralization with 5.0 M NaOH solution to pH = 7. The resultant Na_CQDs solution was dialyzed using Slide-A-Lyzer G2 Dialysis Cassettes (2K MWCO) for 12 hours and the dialysis process was repeated until there was no significant change of conductivity of the surrounding distilled water.
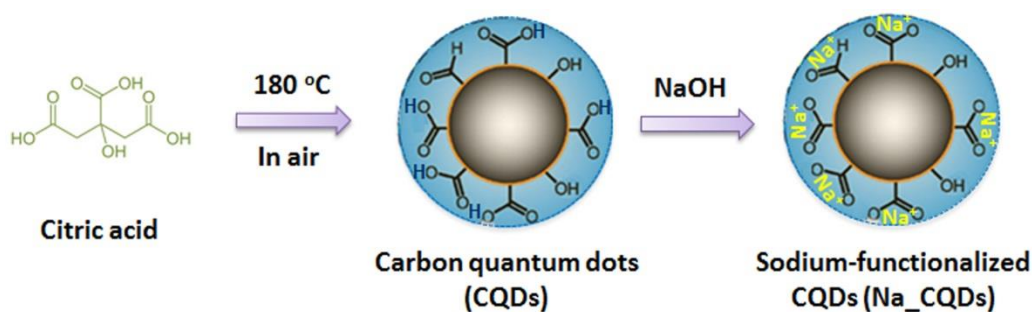
Figure 4.1 Schematic illustration for the fabrication of Na$^+$–functionalized carbon quantum dots (Na_CQDs).

4.2.2 Material Characterizations

Transmission electron microscopy (TEM) images were recorded on a JEM-2100F electron microscope operating at an accelerating voltage of 200 kV. Corresponding particle size distribution histograms were plotted by counting 200 nanoparticles. Energy Dispersive X-ray (EDX) Spectroscopy spectra were recorded using JEOL JSM 6700F scanning electron microscope with Oxford Instruments INCA detector. Fourier transform infrared spectroscopy (FT-IR) spectra were obtained using Bruker FT-IR Research Spectrometers. X-ray photoelectron spectroscopy (XPS) characterizations were performed on a PHI Quantera x-ray photoelectron spectrometer with a chamber pressure of 5×10^{-9} torr, a spatial resolution of 30 μm and an Al cathode as the X-ray source to determine composition of the nanoparticles. The osmolalities of Na_CQDs solutions were measured with an osmometer (Wescor, Vapro vapor pressure osmometer). The effect of $MgCl_2$, NaCl and KCl on Na_CQDs was checked by measuring the osmolality of the Na_CQDs after mixing with 0.1 wt% solution of each salt for 48 h. Negligible osmolality changes (<1%) were observed, indicating minimum poisoning effect of these salts to Na_CQDs.

4.2.3 FO and MD Tests

FO test were conducted on a lab-scale setup using a thin film composite embedded support membrane (batch number 842121) provided by Hydration Technologies Inc. (Albany, OR). The dimensions of the membrane are 1 cm×2 cm. The feed solution was either distilled (DI) water or seawater. The seawater was taken from the sea near Singapore Sentosa beach. Before FO tests, the seawater was filtrated using 220 nm filter membrane to remove large particulate impurities. The draw solution was Na_CQDs solutions with different concentrations. The feed solution and

69

draw solution flowed concurrently through the two sides of the cell channel at a flow velocity of 25 cm s^{-1}. Water fluxes were measured with the selective layer of the membrane in contact with the draw solution at room temperature (25 °C). For the regeneration of draw solution via MD, a multi-bore PVDF hollow fiber (MBF) membrane with lotus root-like geometry was used as the MD membrane. The effective MD membrane surface area is 22.4 cm^2. The diluted draw solution after FO process was circulated through the shell-side of the MD module after heated up to 45 °C. DI water as the permeate solution was concurrently circulated through the lumen side of the MD module after cooled to 10 °C.

4.3 Results and Discussion

4.3.1 Material Characterization

TEM images in Figure 4.2a, b show that the Na_CQDs have an average size of 3.5 nm. Energy dispersive X-ray (EDX) spectrum of the Na_CQDs reveals peaks from C, O and Na, with atomic percentages of 40.7%, 45.3%, and 14.0%, respectively (Figure 4.3). On the other hand, CQDs only show signal of C and O (Figure 4.3). The TEM and EDX results indicate that the Na_CQDs were successful functionalized with Na$^+$ with retained morphology. The presence of Na in Na_CQDs was further confirmed with X-ray photoelectron spectroscopy (XPS). As shown in Figure 4.2c, a peak at 1071 eV corresponding to Na 1s presents in the spectrum of Na_CQDs;[28] while for CQDs the signal of Na is absent.
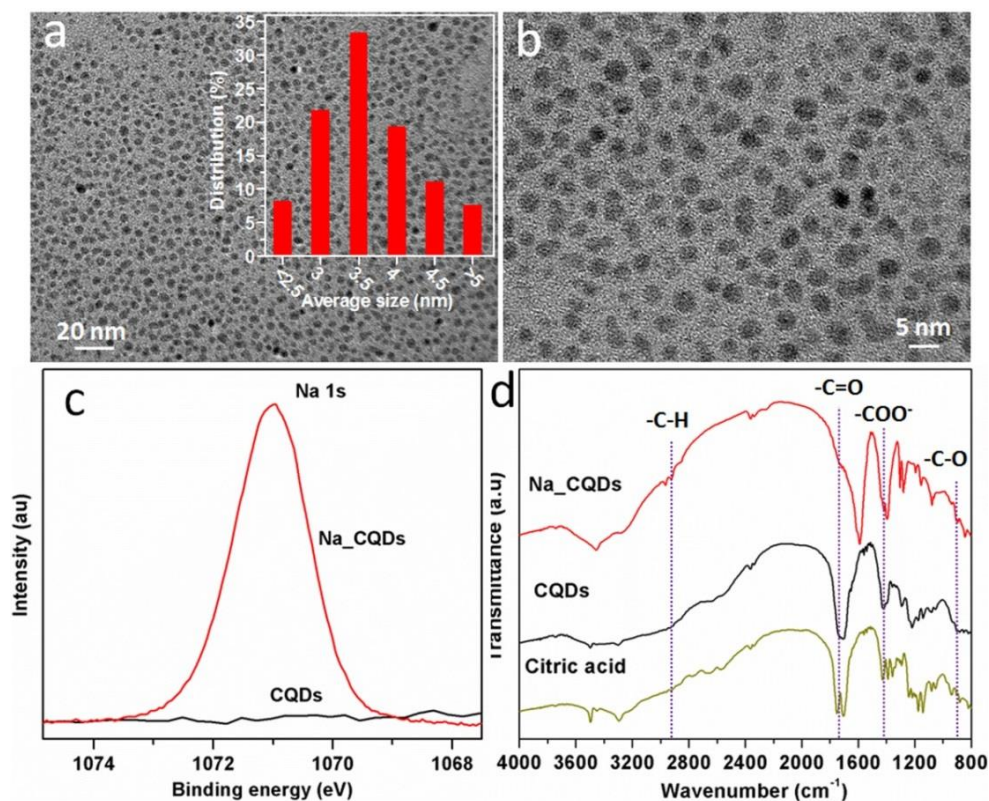
Figure 4.2 (a, b) TEM images of Na_CQDs. The size distribution is given in the inset of (a). (c) XPS high-resolution Na 1*s* spectra of CQDs and Na_CQDs. (d) FT-IR spectra of Na_CQDs, CQDs, and citric acid.

FT-IR spectra of CQDs and Na_CQDs show –C=O and –C–O groups[13,29] that are inherited from citric acid molecules. In addition, the CQDs exhibit characteristic stretching vibration of C–H at 2950 and below 1350 cm^{-1}, indicating that the CQDs contain incompletely carbonized citric acid. EDX spectra in Figure 4.3 demonstrate that the atomic ratio of O/C of citric acid is 52.5/47.5, approximately 1.11. In contrast, CQDs show a lower O/C atomic ratio of 1.02, suggesting that a small portion of oxygen groups were lost during the heating process. It is known that citric acid molecule contains abundant –OH groups, which can cause polymerization (carbonization) during the heat treatment at 180 $^{\circ}$C, similar to that of glucose to form carbonaceous spheres under hydrothermal treatment.[30] Based on FT–IR and TGA analyses, the formation process of

71

Na_CQDs from citric acid can be summarized as follows. During the moderate heat treatment at 180 $^{\circ}$C, citric acid molecules undergo incomplete carbonization by losing some –OH groups, resulting in CQDs with carboxyl groups and an average size of 3.3 nm. Due to the existence of abundant carboxyl groups, CQDs have a relatively acidic nature (pH of around 2.6 at a concentration of 0.4 g mL^{-1}). After adding NaOH, the acidic CQDs were neutralized by converting –COOH groups into –COONa, producing Na_CQDs.
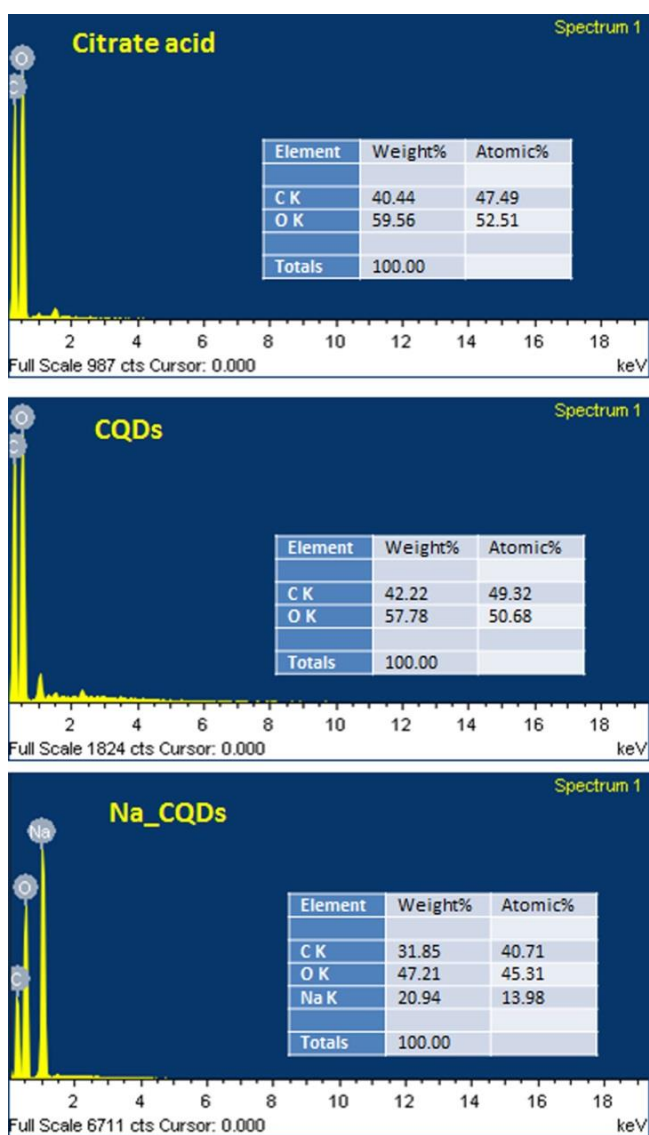
Figure 4.3 EDX spectra of citrate acid, CQDs, and Na_CQDs.

4.3.2 Biocompatibility of Na_CQDs Solution

Biocompatibility of the Na_CQDs was investigated *in vitro* using MCF7 human breast adenocarcinoma cells. Cell viability was monitored by 3-(4,5-dimethylthiazol-2-yl)-2,5-diphenyltetrazolium bromide (MTT) assay, which is a colorimetric assay used to monitor cell viability by measuring the cleavage of MTT *via* the activity of cellular enzymes in living cells. The cell viability value was expressed as the percentage of absorbance observed relative to the control cells cultured with only culture media. Cell viability of 99.8% was observed for Na_CQDs at a concentration of 0.5 mg mL^{-1} (Figure 4.4). Even at a higher concentration of 1.0 mg mL^{-1}, cell viability still retains 92.5%. In contrast, for CQDs at the same concentration (1.0 mg mL^{-1}), a slightly lower viability of 85.6% was observed. This might be due to the acidic nature of CQDs. The cell viability result demonstrates that the Na_CQDs are biocompatible. The good biocompatibility of this new class of draw solute makes it promising for producing clean drinking water *via* FO.
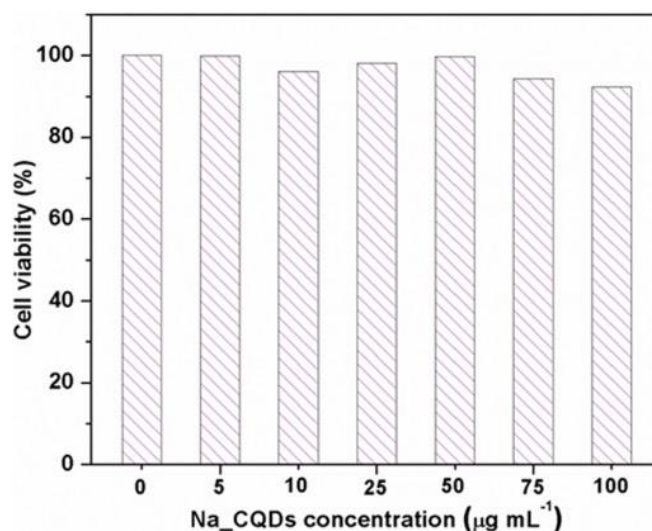
Figure 4.4 MTT cytotoxicity assay using MCF7 cells following 24 hour exposure to various concentrations of Na_CQDs. Cell viability value was expressed as percentage of absorbance observed relative to the control wells receiving only culture media.

4.3.3 Osmolality of Na_CQDs Solution

For FO seawater desalination, high osmolality is critical for the draw solution to offer high osmotic pressure and thus high water flux. The osmolalities of Na_CQDs were measured at various concentrations ranging from 0.2 to 0.5 g mL^{-1}. As shown in Figure 4.5a, at 0.2 g mL^{-1}, the osmolality of Na_CQDs is 1410 mOsm kg^{-1}. However, for CDQs at the same concentration, the osmolality is only 360 mOsm kg^{-1}, much lower than that of Na_CQDs. The osmolality of Na_CQDs increases with concentration. At concentrations of 0.4 and 0.5 g mL^{-1}, the osmolalities reach as high as 3140 and 4350 mOsm kg^{-1}, corresponding to osmotic pressures of 70.3 and 97.4 atm, respectively. These osmotic pressures are much higher than seawater (~26 atm).[24] The high osmotic pressure is clearly attributed to the favorable characteristics of Na_CQDs, namely ultra-small size and rich ions. Compared with CQDs, Na_CQDs are Na$^+$–functionalized and should be able to dissociate in solution to produce abundant ions. The slope of the osmolality vs. concentration curve in Figure 4.5a slightly decreases at higher concentrations. This is possibly caused by reduced degree of dissociation of the Na_CQDs at higher concentrations. It is worth noting that the Na_CQDs exhibited excellent dispersibility in water.

74
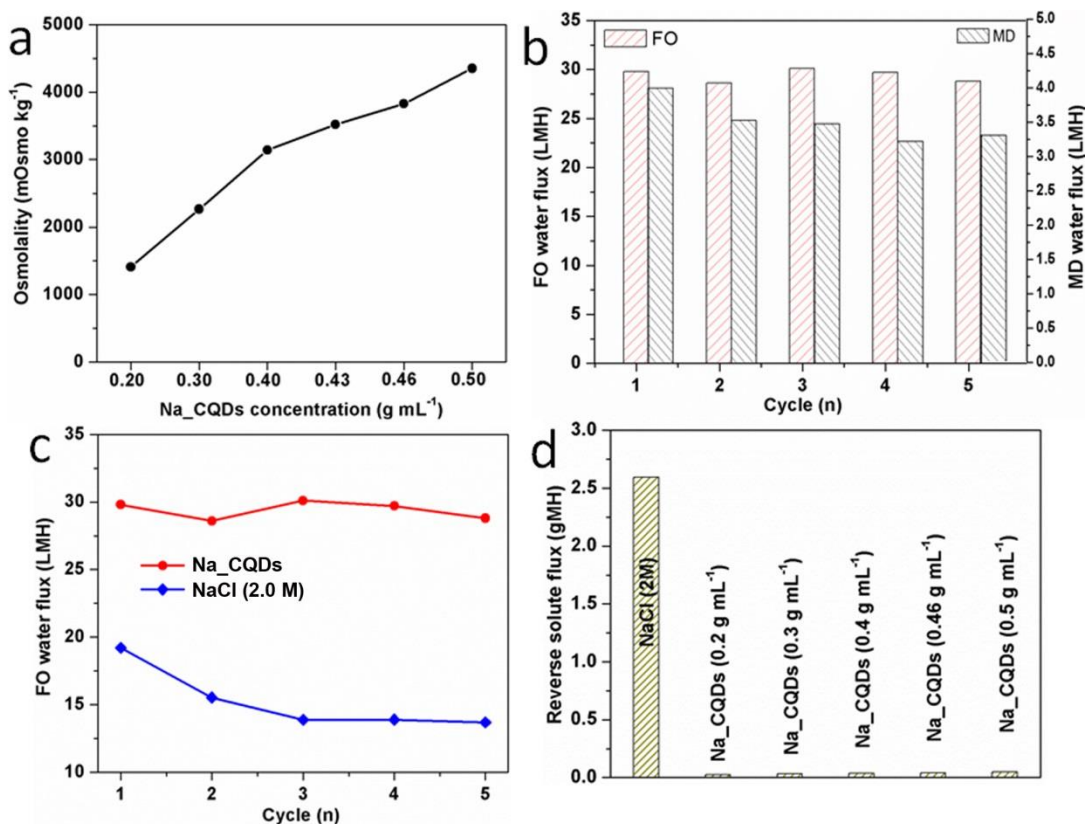
Figure 4.5 (a) Osmolalities of Na_CQDs at various concentrations. (b) FO water fluxes with 0.4 g mL^{-1} Na_CQDs as the draw solution and DI water as the feed solution and MD water fluxes with the diluted Na_CQDs solution as the feed solution. LMH refers to liter/(m^2 membrane·hr). (c) Comparison of FO water fluxes between 2.0 M NaCl and 0.4 g mL^{-1} Na_CQDs draw solutions. (d) Reverse draw solute permeation of 2.0 M NaCl and Na_CQDs at different concentrations. gMH refers to gram solute/(m^2 membrane·hr).

4.3.4 FO and MD Tests

Na_CQDs solution at 0.4 g mL^{-1} was evaluated as FO draw solution using DI water as model feed solution. After each FO test, the diluted Na_CQDs solution was re-concentrated using membrane distillation (MD). For the FO and MD processes, the membranes are commercial HTI thin film composite (TFC) embedded support membrane (2 cm^2) and multi-bore PVDF hollow fiber membrane (28 cm^2), respectively. The FO and MD were repeated for five times and the water fluxes are summarized in Figure 4.5b. A high FO water flux of 29.8 LMH was achieved

for the first cycle with little change in the following cycles. At the 5th cycle, the FO water flux still maintained at 28.8 LMH. This FO water flux exceeds that of existing draw solutes with typical concentrations such as sugars,[31] ethanol,[32] dendrimers,[33] hydroacid complexes,[26] polymer hydrogels,[34] polyelectrolytes,[35] polyelectrolyte-functionalized magnetic nanoparticles,[25,36,37] and it is among the highest water fluxes reported using the same commercial FO membrane.[23] When simulated seawater (0.6 M NaCl) was employed as the feed solution, the FO water flux still reached as high as 7.3 LMH. The reconcentration of Na_CQDs *via* MD was performed at 45 $^{\circ}$C. For the 1st cycle, the MD water flux was 4.0 LMH. It slightly drops in the next few cycles, but still retained at 3.4 LMH in the 5th cycle.

The FO water flux of the Na_CQDs solution (0.4 g mL^{-1}) was compared with that of 2.0 M NaCl, which is widely used as model draw solution in FO. As displayed in Figure 4.5c, for the 1st cycle, the FO water flux of 2.0 M NaCl is 19.2 LMH, much lower than that of of Na_CQDs. After 5 cycles, the water flux dropped 29% for 2.0 M NaCl, but only 3% for Na_CQDs. We also compared the reverse draw solute permeation of 2.0 M NaCl and Na_CQDs at various concentrations (Figure 4.5d). For 2.0 M NaCl solution, a reverse draw solute flux of 2.5 gram per (m^2 membrane·hr) (gMH) was observed. In comparison, negligible reverse solute fluxes (<0.05 gMH) were found for Na_CQDs. The commercial HTI TFC membrane used in this work has an average pore size of 0.5 nm in the active layer. The Na_CQDs have a size range of 2.5 to 5 nm, much larger than the pore size of the membrane. Therefore, the diffusion of Na_CQDs across the membrane is effectively suppressed, resulting in negligible reverse solute flux.

Combined with MD process, the Na_CQDs solution (0.4 g mL^{-1}) was further used in FO for seawater desalination. The seawater was taken from the sea near Singapore coast with a

measured osmolality of 880 mOsm kg^{-1}. With a total salt concentration of 27.5 g L^{-1}, the seawater mainly contains Na$^+$, Mg^{2+}, K$^+$, Cl$^-$ and SO$_4^{2-}$ ions (Figure 4.6). Minimum poisoning effect of MgCl$_2$, NaCl and KCl on the Na_CQDs was observed based on osmolality measurements. Before FO tests, the seawater was filtrated using 220 nm filter membrane to remove impurities. As shown in Figure 4.7, relatively high FO water fluxes of 10.4 and 9.6 LMH were achieved for the 1st and 5th cycles, respectively.

Element	Intensity	Weight%	Atomic%
O K	0.5135	26.11	39.30
Na K	0.9494	18.52	19.40
Mg K	0.6434	11.82	11.71
S K	0.9432	3.20	2.40
Cl K	0.8056	37.09	25.19
K K	0.8736	2.11	1.30
Ca K	0.8648	1.14	0.68
Totals		100.00	
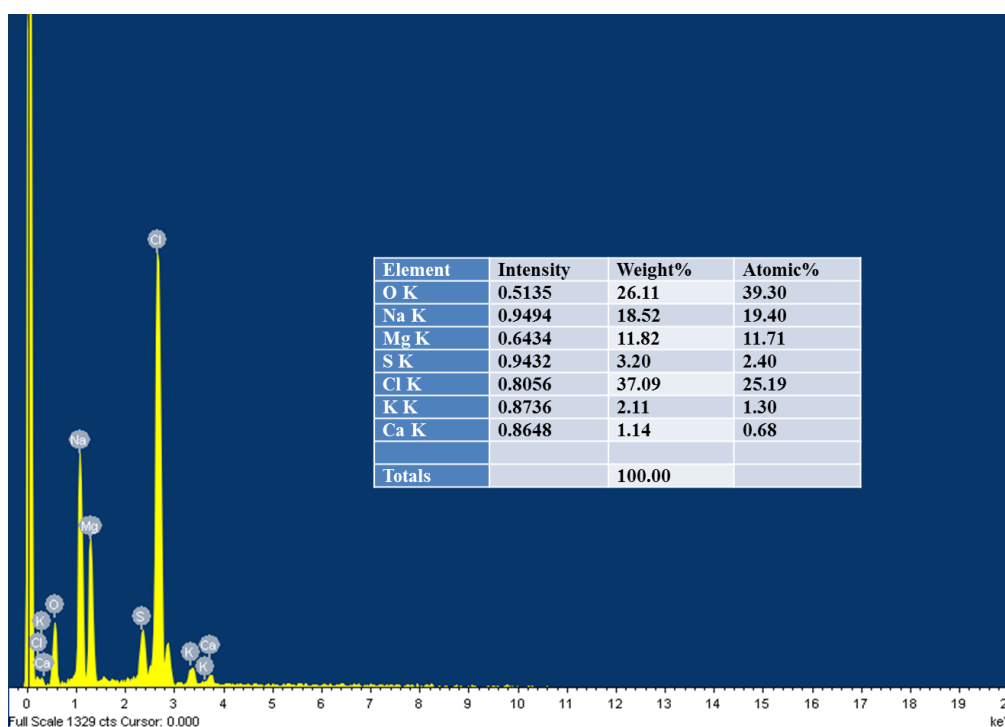
Figure 4.6 Composition of the seawater sample taken from the sea near Singapore coast upon evaporation of water measured by Energy-dispersive X-ray spectroscopy (EDS).
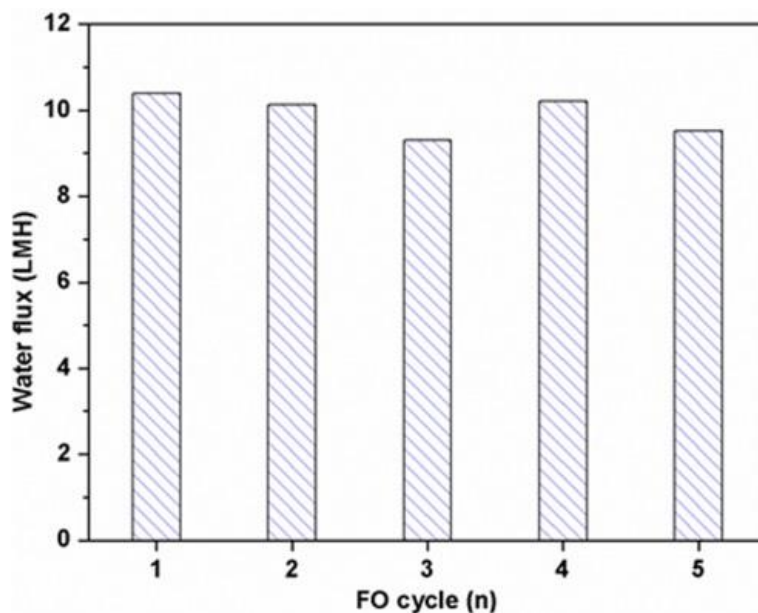
Figure 4.7 FO water fluxes with 0.4 g mL^{-1} Na_CQDs aqueous solution as the draw solution and seawater taken from the sea near Singapore coast as the feed solution. The seawater has an osmolality of 880 mOsm kg^{-1}.

4.4 Conclusions

In conclusion, we report a new draw solute, Na$^+$–functionalized carbon quantum dots, in forward osmosis for seawater desalination. The unique characteristics of Na_CQDs, including an ultra–small size of 3.5 nm, abundant carboxyl groups, and rich ionic species, favor high osmotic pressure and thus FO water flux. At concentrations of 0.4 and 0.5 g mL^{-1}, the Na_CQDs provide respective osmotic pressures of 70.3 and 97.4 atm, much higher than that of seawater (~26 atm). In FO tests with DI water as the model feed solution, the Na_CQDs (0.4 g mL^{-1}) showed a water flux of 29.8 LMH, exceeding that of 2.0 M NaCl draw solution by 55%. This FO water flux is among the highest reported. When seawater was used as feed solution, the Na_CQDs provide an FO water flux of 10.4 LMH with only a slight drop after 5 cycles. In addition, the Na_CQDs showed negligible reverse draw solute permeation. It is worth noting that for practical

78

applications, further investigation is necessary to understand the energy consumption in the FO desalination process using Na_CQDs as draw solutes.

4.5 References

1. Baker, S. N.; Baker, G. A. Luminescent carbon nanodots: Emergent nanolights. *Angew. Chem. Int. Ed.* **2010**, 49, 6726-6744.

2. Zhou, L.; Lin, Y.; Huang, Z.; Ren, J.; Qu, X. Carbon nanodots as fluorescence probes for rapid, sensitive, and lable-free detection of Hg^{2+} and biothiols in coplex matrices. *Chem. Commun.* **2012**, 48, 1147-1149.

3. Fowley, C.; Nomikou, N. A.; McHale, P.; McCaughan, B.; Callan, J. F. Extending the issue penetration capability of conventional photosensitisers: a carbon quantum dot-protoporphyrin IX conjugate for use in two-photon excited photodynamic therapy. *Chem. Commun.* **2013**, 49, 8934-8936.

4. Qu, S.; Wang, X.; Lu, Q.; Liu, X.; Wang, L. A biocompatible fluorescent ink based on water-soluble luminescent carbon nanodots. *Angew. Chem. Int. Ed.* **2012**, 51, 12215-12218.

5. Fowley, C.; McCaughan, B.; Devlin, A.; Yildiz, I.; Raymo, F. M.; Callan, J. F. Highly luminescent biocompatible carbon quantum dots by encapsulation with an amphiphilic polymer. *Chem. Commun.* **2012**, 48, 9361-9363.

6. Guo, C. X.; Xie, J.; Wang, B.; Zheng, X.; Yang, H. B.; Li, C. M. *Sci. Rep.*, 2013, **3**, 2957.

7. Lin, L.; Zhang, S. Creating high yiel water soluble luminescent graphene quantum dots via exfoliating and disintegrating carbon nanotubes and graphite flakes. *Chem. Commun.* **2012**, 48, 10177-10179.

8. Gao, M. X.; Liu, C. F.; Wu, Z. L.; Zeng, Q. L.; Yang, X. X.; Wu, W. B.; Li, Y. F.; Huang, C. Z. A surfactant-assited redox hydrothermal route to prepare highly photoluminescent carbon quantum dots with aggregation-induced emission enhancement properties. *Chem. Commun.* **2013**, 49, 8015-8017.

9. Li, X.; Wang, H.; Shimizu, Y.; Pyatenko, A.; Kawaguchi, K.; Koshizaki, N. Preparation of carbon quantum dots with tunable photoluminescence by rapid laser passivation in ordinary organic solvents. *Chem. Commun.* **2011**, 47, 932-934.

10. Kwon, W.; Rhee, S.-W. Facile synthesis of graphitic carbon quantum dots with size tunability and uniformity using reverse micelles. *Chem. Commun.* **2012**, 48, 5256-5258.

11. Zhang, L.; Zhang, R.; Cui, P.; Cao, W.; Gao, F. Anefficient phosphorescence energy transfer between quantum dots and carbon nanotubes for ultrasensitive turn-on detection of DNA. *Chem. Commun.* **2013**, 49, 8102-8104.

12. Qu, Q.; Zhu, A.; Shao, X.; Shi, G.; Tian, Y. Development of a carbon quantum dots-based fluorescent Cu^{2+} probe suitable for living cell imaging. *Chem. Commun.* **2012**, 48, 5473-5475.

13. Dong, Y.; Chen, C.; Zheng, X.; Gao, L.; Cui, Z.; Yang, H.; Guo, C.; Chi, Y.; Li, C. M. One-step and high yield simultaneous preparation of single- and multi-layer graphene quantum dots from CX-72 carbon black. *J. Mater. Chem.* **2012**, 22, 8764-8766.

14. Dong, Y.; Pang, H.; Yang, H. B.; Guo, C.; Shao, J.; Chi, Y.; Li, C. M.; Yu, T. Carbon-based dots co-doped with nitrogen and sufur for high quantum yield and excitation-independent emission. *Angew. Chem. Int. Ed.* **2013**, 52, 7800-7804.

15. Guo, C. X.; Dong, Y.; Yang, H. B.; Li, C. M. Graphene quantum dots as a green sensitizer to functionalize ZnO nanowire arrays on f-doped SnO2 glass for enhanced photoelectrochemical water splitting. *Adv. Energy Mater.* **2013**, 3, 997-1003.

16. Su, J.; Zhang, S.; Ling, M. M.; Chung, T.-S. Forward osmosis: an emerging technology for sustainable supply of clean water. *Clean Techn. Environ. Policy*, **2012**, 14, 507-511.

17. Liu, Y.; Mi, B. Combined fouling of forward osmosis membranes: Synergistic foulnt interaction and direct observation of fouling layer formation. *J. Membr. Sci.* **2012**, 407, 136-144.

18. Cai, Y.; Shen, W.; Wang, R.; Krantz, W. B.; Fane, A. G.; Hu, X. CO_2 switchable dual responsive polymers as draw solutes for forward osmosis desalination. *Chem. Commun.* **2013**, 49, 8377-8379.

19. Lee, Y. G.; Lee, Y. S.; Kim, D. Y.; Park, M.; Yang, D. R.; Kim, J. H. A fouling model for simulating long-term performance of SWRO desaliantion process. *J. Membr. Sci.* **2012**, 401, 282-291.

20. Zhao, S.; Zou, L.; Tang, C. Y.; Mulcahy, D.Recent development in forward osmosis: Opprtunities and challenges. *J. Membr. Sci.* **2012**, 396, 1-21.

21. Qin, J. J.; Oo, M. H.; Kekre, K. A.; Liberman, B. Development of novel backwash cleaning technique for reverse osmosis in reclamation of secondary effluent. *J. Membr. Sci.* **2010**, 346, 8-14

22. Yangali-Quintanilla, V.; Li, Z.; Valladares, R.; Li, Q.; Amy, G. Indirect desalination of Red Sea water with forward osmosis and low pressure reverse osmosis for water reuse. *Desalination* **2011**, 280, 160-166.

23. Chon, K.; Cho, J.; Shon, H. Fouling characteristics of a membrane bioreactor and nanofiltration bybrid system for municipal wastewater reclamation. *Bioresource Technol.*, **2013**, 130, 239-247.

24. Ge, Q.; Ling, M. M.; Chung, T.-S. Draw solutions for forward osmosis processes: developments, challenges, and prospects for the future. *J. Membr. Sci*. **2013**, 442, 225–237.

25. Ling, M. M.; Wang, K. Y.; Chung, T.-S. Highly water-soluble magnetic nanoparticles as novel draw solutes in forward osmosis for water reuse, *Ind. Eng. Chem. Res*. **2010**, 49, 5869–5876.

26. Ge, Q.; Chung, T.-S. Hydroacid complexes: a new class of draw solutes to promote forward osmosis (FO) processes. *Chem. Commun.* **2013**, 49, 8471-8473.

27. Paikaray, S.; Moharana, P. A simple hydrothermal synthesis of lumnescent carbon quantum dots from different molecular precursors. Master dissertation, **2013**.

28. Desimoni, E.; Casella, G. I.; Morone, A.; Salvi, A. M. XPS determination of oxygen-containing functional groups on carbon-fibre surfaces and the cleaning of these surfaces. *Surf. Interface Anal.* **1990**, 15, 627-634.

29. Guo, C. X.; Ng, S. R.; Khoo, S. Y.; Zheng, X.; Chen, P.; Li, C. M. RGD- peptide functionalized graphene biomimetic live cell sensor for real-time detection of nitric oxidde molecules. *ACS Nano*, **2012**, 6, 6944-6951.

30. Sun, X.; Li, Y. Colloidal carbon spheres and their core/shell structures with noble-metal nanopaticles. *Angew. Chem. Int. Ed.* **2004**, 43, 597-601.

31. Su, J.; Chung, T.-S.; Helmer, B. J.; de Wit, J. S. Enhanced double-skinned FO membranes with inner dense layer for wastewater treatment and macromolecule recycle using Sucrose as draw solute. *J. Membr. Sci.* **2012**, 396, 92-100.

32. McCormick, P.; Pellegrino, J.; Mantovani, F.; Sarti, G. Water, salt, and ethanol diffusion through membranes for water recovery by forward (direct) osmosis processes. *J. Membr. Sci.* **2008**, 325, 467-478.

33. Adham, S.; Oppenheimer, J.; Liu, L.; Kumar, M. Dewatering reverse osmosis concentrate from water reuse applications using forward osmosis. Water Use Foundation Reserch Report, **2007**.

34. Li, D.; Zhang, X.; Yao, J.; Simon, G. P.; Wang, H. Stimuli-responsive polymer hydrogels as a new class of draw agent for forward osmosis desalination. *Chem. Commun.*, **2011**, 47, 1710-1712.

35. Ge, Q.; Su, J.; Amy, G. L.; Chung, T.-S. Exploration of polyelectrolytes as draw solutes in forward osmosis processes. *Water Res*. **2012**, 46, 1318–1326.

36. Ling, M. M.; Chung, T.-S.; Lu, X. Facile synthesis of thermosensitive magnetic nanoparticles as "smart" draw solutes in forward osmosis. *Chem. Commun.*, **2011**, 47, 10788-10790.

37. Zhao, Q.; Chen, N.; Zhao, D.; Lu, X. Thermoresponsive magnetic nanoparticles for seawater desalination. *ACS Appl. Mater. Interfaces* **2013**, 5, 11453-11461.

CHAPTER 5

THERMORESPONSIVE COPOLYMER-BASED DRAW SOLUTION FOR SEAWATER DESALINATION IN A COMBINED PROCESS OF FORWARD OSMOSIS AND MEMBRANE DISTILLATION

5.1 Introduction

Clean water scarcity has long been a serious concern for many communities, and it will be aggravated due to the rapid growth of population. Desalination of seawater has been proposed as a solution to this worldwide problem since seawater accounts more than 97% of the total water resource on earth. For decades, researchers have been looking for low-energy and highly efficient desalination techniques.[1-8] Among existing desalination methods, forward osmosis (FO, also known as direct osmosis) is an attractive and promising one.[1-7, 9, 10] In an FO process, water in the feed solution at a lower osmotic pressure can pass spontaneously through a semipermeable membrane to the draw solution at a higher osmotic pressure. A subsequent regeneration process extracts water from the draw solution and re-concentrates the draw solution for reuse. Unlike reverse osmosis (RO) which requires a high hydraulic pressure to desalinate seawater, FO is driven by the difference in osmotic pressure between the feed and draw solutions and eliminates the need for high hydraulic pressure. As an emerging membrane technology with low energy consumption, FO is promising for wastewater treatment,[11,12] desalination,[13-18] protein concentration,[19-21] power regeneration,[22-24] and many other applications.[25-29]

Research in FO has been mainly focused on both the fabrication of high-performance FO membranes[23, 30-39] and the development of efficient draw solutions.[40, 41] An ideal FO draw solution should meet three general requirements, namely high osmotic pressure for high water flux, facile regeneration method for low energy consumption, and minimum reverse solute flux for low replenishment cost.[40, 41] Conventional draw solutions based on inorganic salts such as NaCl, MgCl$_2$ and NH$_4$HCO$_3$ can generate high water flux, but the corresponding reserve flux of solute is also high, thus affecting the product quality and increasing the replenishment cost.[17, 42] In addition, there is a lack of an efficient method to produce clean water from these draw solutions. Most recently, a number of novel draw solutions have been proposed.[12-15, 43-51] Polyelectrolytes such as sodium polyacrylate (PAA-Na) have been investigated as FO draw solutes by Ge and coworkers.[43] This type of draw solute with relatively high molecular weight can reduce reverse flux. Ultrafiltration (UF) and membrane distillation (MD) are promising for the regeneration of polyelectrolyte-based draw solutions.[11, 43] Draw solutes based on thermoresponsive compounds have also attracted increasing attention because of their unique response to temperature.[45, 46, 52] For instance, n-acylated polyethylenimine derivatives are soluble in water below their lower critical solution temperature (LCST), but phase separation occurs when the temperature is increased above the LCST.[46] Using this type of thermoresponsive draw solute, Lee *et al*. demonstrated temperature-induced reversible water flux between the draw and feed solutions. Ling *et al*. employed thermoresponsive poly(n-isopropylacrylamide) (PNIPAM) to functionalize magnetic nanoparticles (MNPs).[45] The resultant PNIPAM-capped MNPs may agglomerate to larger sizes when heated up to the LCST of PNIPAM. Therefore, when the thermoresponsive MNPs are used as draw solute, the regeneration of draw solution can be achieved efficiently by applying a magnetic field. As another example, Wang *et al.* also

86

evaluated stimuli-responsive polymer hydrogels as FO draw solutes and investigated the effects of hydrogel size on the performance of FO and dewatering process.[15, 53]

Despite the recent progress, it remains a challenging task to employ thermoresponsive materials as draw solutes to desalinate seawater. This is because the osmotic pressure of a thermoresponsive polymer solution is generally not high enough to counteract that of seawater. Here, we present a study on a thermoresponsive copolymer, poly(sodium styrene-4-sulfonate-*co*-n-isopropylacrylamide) (PSSS-PNIPAM), as FO draw solute for seawater desalination in a process combined with forward osmosis and membrane distillation (FO-MD). The purpose of using PSSS-PNIPAM as the draw solute is two-fold: i) PSSS is a strong polyelectrolyte which can provide a large number of ions in aqueous solution and thus a high osmotic pressure; and ii) PNIPAM may facilitate the regeneration of the draw solution based on its thermoresponsive property. In our study, FO desalination is performed at room temperature, which is below the LCST of the polymer. Therefore, the polymer chains are fully expanded in the FO draw solution to provide maximum osmotic pressure. After drawing water from seawater, the polymer solution is re-concentrated by MD to produce clean water and to regenerate the draw solution. Because MD is performed at a temperature (50 $^{\circ}$C) above the LCST of the copolymer, the osmotic pressure of the draw solution drops due to the agglomeration of the polymer chains. Lower osmotic pressure leads to a higher effective water vapor pressure, which facilitates the separation of water from the solution.[54] Although MD may be applied for desalination of seawater directly, NaCl crystals and liquid water can penetrate into the membrane pores and cause serious membrane fouling and pore wetting problems. Therefore, the FO-MD hybrid seawater desalination process with thermoresponsive PSSS-PNIPAM as the draw solute has the potential to achieve high product quality, long operational time and low cost.

5.2 Materials and Methods

5.2.1 Materials

N-isopropylacrylamide (NIPAM, >97%), sodium-4-styrenesulfonate (SSS, >90%), 4,4-azobis(4-cyanovaleric acid) (ACVA, >98%), dimethyl sulfonate (DMSO) and sodium chloride (>99.5%) were purchased from Sigma-Aldrich and used as received. Deionized (DI) water with a resistivity of 18MΩ·cm was obtained with a Milli-Q unit (Millipore, USA). Thin film composite (TFC) forward osmosis membrane was provided by Hydration Technologies Inc. (HTI Albany, OR).
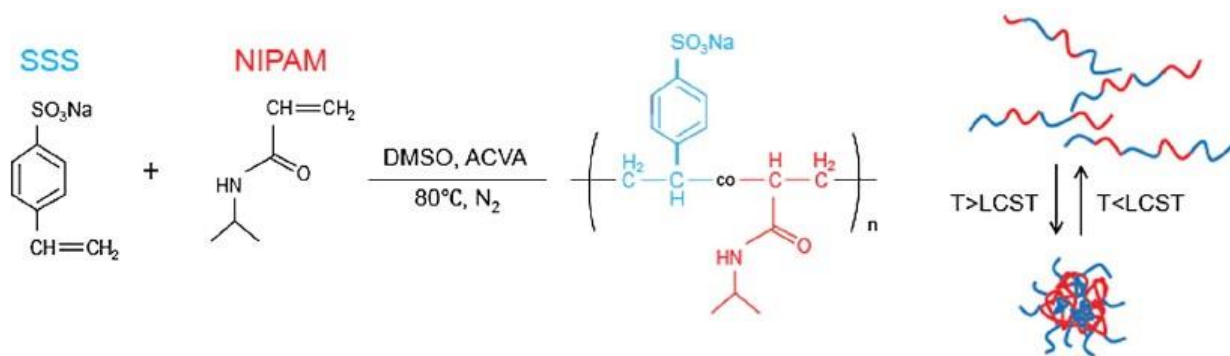
Figure 5.1 Synthesis of thermoresponsive PSSS-PNIPAAM.

5.2.2 Preparation and Characterization of PSSS-PNIPAM

The copolymer PSSS-PNIPAM was synthesized based on an adaptation of the approach reported by Grebosz *et al.*[55] Briefly, SSS and NIPAM with designated feeding ratio (Table 5.1) were charged into a three-neck flask loaded with 120 mL of DMSO. The mixture was degassed for 20 min by bubbling N_2 to remove O_2. After degassing, it was heated up to 80°C, followed by the

injection of ACVA. The reaction was allowed to proceed at 80°C for 24 hr under the protection of N_2. After cooling down to room temperature, the copolymer was precipitated by adding acetone and washed with acetone for three times. The resulting product was dissolved in water and purified by dialysis membranes with a molecular weight cut-off of 3500 (slide-A-lyzer dialysis cassette G2, Thermo Fisher). Finally the copolymer was dried under vacuum. PSSS-PNIPAM copolymers with 5, 10, 15 and 20 wt% of SSS were prepared and denoted as 5SN, 10SN, 15SN, and 20SN, respectively. The relative viscosities (η_r, compared to DI water) of the copolymer solutions at different concentrations were calculated with the following equation:

$$\eta_r = \eta/\eta_0 = (t\,\rho)/(t_0\,\rho_0)$$

where t and t_0 (s) are the respective elution times of 15SN solution and DI water measured by an AVS 360 inherent viscosity meter; ρ and ρ_0 (g mL^{-1}) are the densities of 15SN solution and DI water, respectively.

Fourier transform infrared (FTIR) spectra were recorded on a BIO-RAD spectrometer (Excalibur series, FTS3500). The molecular weight of the copolymer was measured by gel permeation chromatography (Waters GPC system) equipped with a Waters 1515 isocratic HPLC pump, a Waters 717 plus Autosampler injector, a Waters 2414 refractive index detector, and an Agilent PLgel 5 μm mixed-D column (Cat. No. 79911GP-MXD), using DMF as the eluent at 30 °C and at a flow rate of 1.0 mL min^{-1}.

Table 5.1 Amounts of chemicals used for the preparation of PSSS-PNIPAAM of different weight percentages of SSS.

	5 wt% (5SN)	10 wt% (10SN)	15 wt% (15SN)	20 wt% (20SN)
SSS (g)	1	2	3	4
NIPAM (g)	19	18	17	16
DMSO (mL)	120	120	120	120
ACVA (g)	0.96	0.94	0.92	0.90

5.2.3 Characterization of Thermoresponsive Property

The low critical solution temperatures (LCSTs) of the solutions containing 33.3 wt% of 5SN, 10SN, 15SN and 20SN, respectively, were measured by a UV-Vis spectrophotometer (SHIMADZU, UV-3600). Transmittance at a wavelength of 500 nm was measured as the temperature was increased and stabilized for 5 min for each data point. The LCST is defined as the temperature at which the transmittance is below 5%. Osmolality of the copolymer solution was measured with an osmometer (Wescor, VAPRO vapor pressure osmometer). Typically, 10 μl of the solution was dropped on a small piece of filter paper (6.5 mm in diameter). By measuring the vapor pressure at room temperature in natural equilibrium, the osmolality of the solution was determined.

The osmotic pressures of the copolymer solutions with respect to DI water and 0.6 M NaCl solution were determined by a lab-built direct membrane osmometer (DMO) adapted from the design reported by Chahin *et al*. (Figure 5.2).[56] During the measurement, 1 mL of the polymer solution was injected slowly into the fluid chamber using a syringe to avoid the formation of bubbles. The solution was sealed inside the chamber with an O-ring, a dialysis membrane (50 KDa, Shanghai Yuanye Biology Technology), and an FO membrane (Hydration Technologies

Inc.) in tandem. A stainless steel wire mesh was then put on top of the membranes to prevent deformation. The assembled osmometer connected with a pressure transducer (Omega, model number: MMA1.0KUSBP6A0T8A9CE, pressure range: 0-1000 psia) was placed in DI water or 0.6 M NaCl solution right before the measurement. The pressure readings were taken with a computer connected to the transducer *via* USB connection. The osmotic pressures below and above the LCST were tested at 23°C and 45°C, respectively.
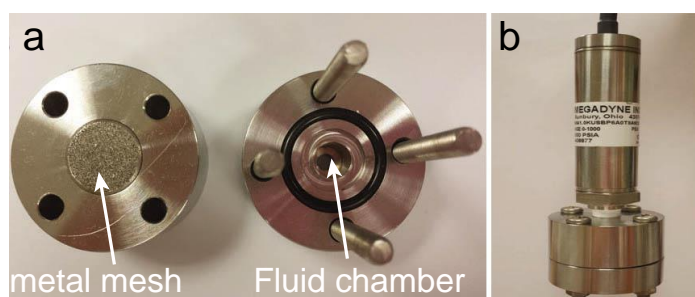
Figure 5.2 (a) Direct membrane osmometer (DMO) and (b) Assembled DMO connected with a pressure transducer for osmotic pressure measurement.

5.2.4 FO Desalination Process

FO tests were carried out through a lab-scale setup as shown in Figure 5.3 (the part on the left). FO membrane was a thin film composite (TFC) embedded support membrane (batch number: 842121) provided by Hydration Technologies Inc. (Albany, OR). The dimensions of the membrane were 1cm×2cm. The feed solutions were simulated seawater (0.60 M NaCl aqueous solution) and DI water, respectively. The draw solution was 33.3 wt% 15SN solution (100 ml) with a measured osmolality of 2137 mOsm kg^{-1}. The feed solution and draw solution flowed concurrently through the two sides of the cell channel at a flow velocity of 25 cm s^{-1}. Water fluxes were measured with the selective layer of the membrane in contact with the draw solution

at room temperature (25 °C). The following formula was used to calculate the water fluxes (J_v, L $m^{-2} h^{-1}$, abbreviated as LMH) from the weight decrement (Δm, g) of the feed solution:

$$J_v = \Delta m/(A_m \cdot \Delta t \times 1000)$$

where Δm (g) is the mass of water permeated across the effective FO membrane surface area A_m (m^2) over a time period of Δt (h), assuming the density of water is 1000 g L^{-1}. The reverse flux of the draw solute was tested using DI water as the feed solution based on the change in conductivity.
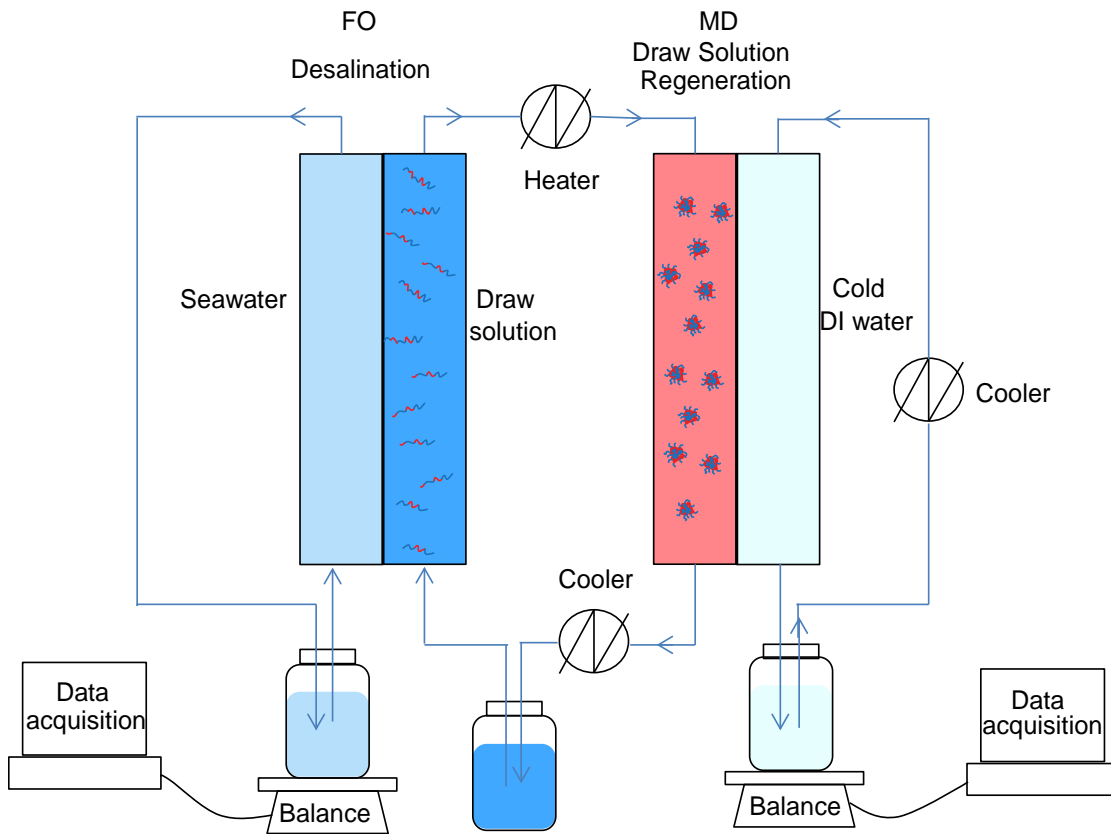
Figure 5.3 Laboratory-scale FO-MD process.

92

5.2.5 Regeneration of Draw Solution *via* Membrane Distillation

MD processes were carried out through a lab-scale setup as depicted in Figure 5.3 (the part on the right) to recover the draw solution. A multi-bore PVDF hollow fiber (MBF) membrane with lotus root-like geometry was used. The spinning conditions (Table 5.2) and the characterizations of the MBF were reported by Wang *et al.*[57] The effective MD membrane surface area was 22.4 cm^2. The diluted draw solution after the FO process with an osmolality of about 2000 mOsm kg^{-1} was circulated through the shell-side of the MD module after being heated up to 50 °C. DI water as the permeate solution was concurrently circulated through the lumen side of the MD module after being cooled to 10 °C. The flow velocity of the two solutions was 20 cm s^{-1}. The water fluxes in MD processes were calculated by the same method as that of FO process.

Table 5.2 Spinning conditions for the MD MBF membrane.

Dope composition (wt%)	PVDF HSV#900/NMP/EG:15/77/8
Dope flow rate (ml min^{-1})	14
Bore fluid composition (wt%)	NMP/water: 70/30
Bore flow rate (ml min^{-1})	11
Take up speed ($mmin^{-1}$)	Free fall
External coagulant (wt%)	IPA/water: 50/50
Air gap (cm)	3
Temperature (ºC)	25-29
Humidity	65%-75%
Post treatment	Soak in water & Freeze Dry

5.3 Results and Discussion

5.3.1 Characterization of the Copolymer

The success in synthesizing the PSSS-PNIPAM copolymer was confirmed by FTIR spectroscopy (Figure 5.4).[51] Commercial PSSS displays characteristic peaks at 1176 and 1003 cm^{-1}, corresponding to S=O asymmetric stretching and S-O stretching, respectively. In PNIPAM, characteristic peaks at 1654 and 1542 cm^{-1} are due to C=O stretching and N-H bending, respectively. The existence of the above four characteristic peaks in the synthesized 5SN, 10SN, and 15SN indicates the presence of both PSSS and PNIPAM in the copolymers. GPC results show that the average molecular weights of 5SN, 10SN, 15SN and 20SN were 34560, 44820, 16270, and 11073, respectively. The SSS contents of 5SN, 10SN, 15SN and 20SN were 6.0, 13.9, 14.6, 18.9 wt%, determined by UV-Vis.
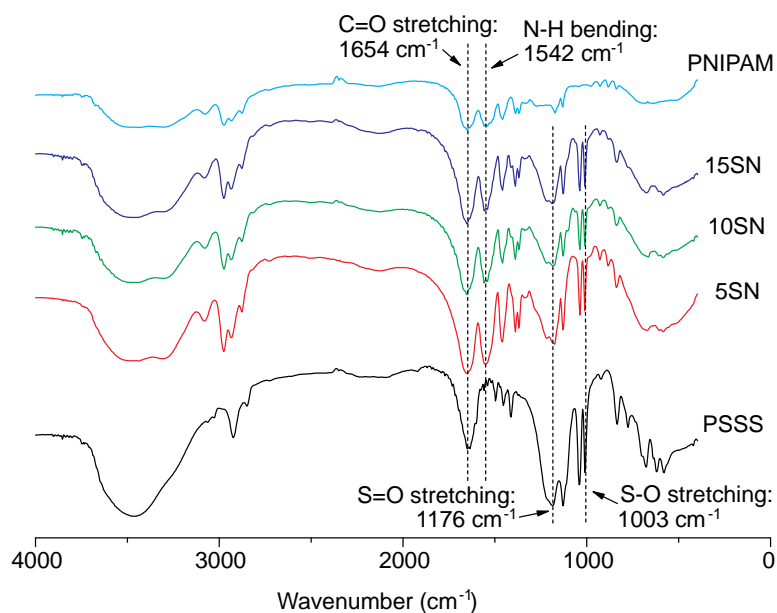
Figure 5.4 FTIR spectra of commercial PSSS, commercial PNIPAM, and synthesized 5SN, 10SN and 15SN.

94

Figure 5.5a shows the change in transmittance of 5SN, 10SN, 15SN and 20SN at 500 nm with the increase of temperature. At LCST, the transmittance of the thermoresponsive copolymer dropped abruptly. For 5SN, 10SN and 15SN, the measured LCSTs were 32.0, 33.5 and 34.0 °C, respectively. The LCST increases with the SSS content in the copolymer. However, when the SSS content reaches 20 wt%, the LCST does not exist within the selected temperature range. Clearly, PSSS-PNIPAM copolymer with SSS content higher than 20 wt% cannot be used as thermoresponsive draw solute.
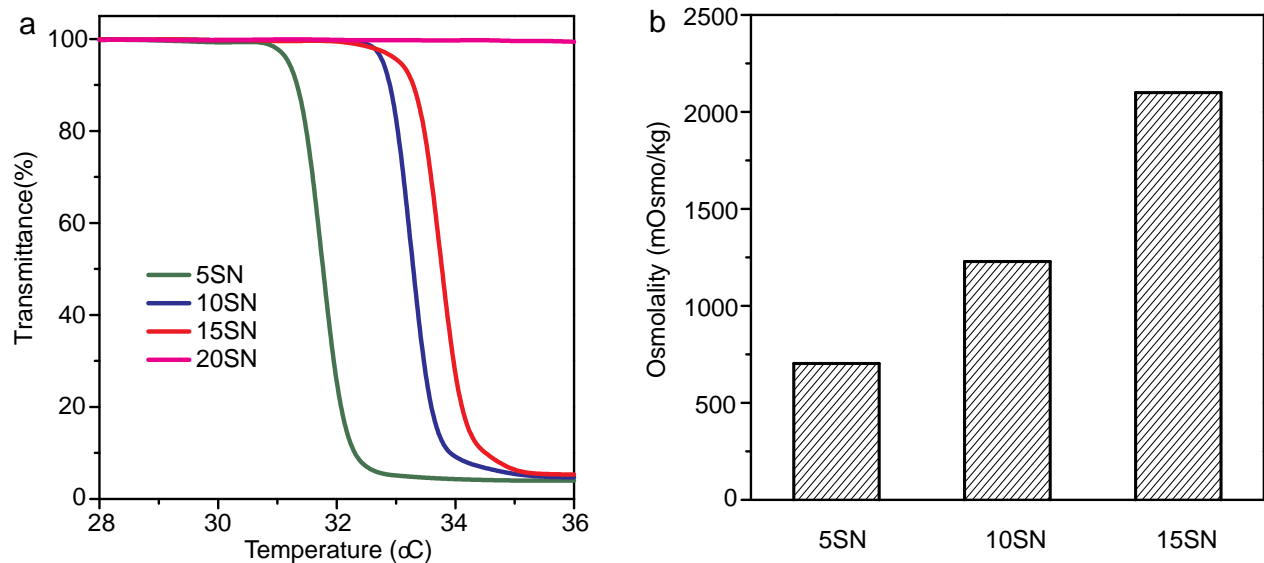
Figure 5.5 (a) Transmittance at 500 nm of the copolymers with different weight percentages of SSS; (b) Osmolalities of PSSS-PNIPAM copolymers with different weight percentages of SSS (5%, 10%, and 15% for 5SN, 10SN, and 15SN, respectively) in solutions with a concentration of 33.3 wt%.

Figure 5.5b presents the measured osmolalities of 5SN, 10SN and 15SN solutions with a concentration of 33.3 wt%. The osmolalities of 5SN, 10SN and 15SN were 715, 1250, 2137 mOsm kg^{-1}, respectively. As expected, copolymers with higher SSS content yield higher

osmolality because the dissociation of SSS provides most of the ions in solution. To desalinate seawater, the draw solution must have an osmolality higher than that of seawater (~1200 mOsm kg^{-1}). Although the osmolality of 10SN is higher than that of seawater, the difference is too small to allow any substantial water flux. Therefore, 15SN was chosen as the draw solute for FO tests.

The osmotic pressures of 33.3 wt% 15SN solution at temperatures below and above its LCST were measured using our direct membrane osmometer. The osmotic pressures of the copolymer at room temperatures and 45 °C, respectively, were monitored once the osmometer loaded with 15SN solution was put into DI water. The pressure in the fluid chamber increased gradually as water flowed into the chamber due to the osmotic pressure difference. Finally, the pressure stabilized when the system reached equilibrium. The maximum pressures attained were 28.3 atm at room temperature and 7.7 atm at 45 °C, respectively (Figure 5.6a, b). As expected, a notable drop in osmotic pressure of the 15SN solution was observed when it was heated above the LCST due to the shrunk polymer chains. This drop in osmotic pressure would facilitate the regeneration of the draw solution in MD process. It should be noted that due to the higher diffusivity at higher temperature, the time to reach equilibrium at 45 °C was much shorter than that at room temperature. In addition, the measured osmotic pressure at room temperature is much lower than that calculated based on the osmolality of the solution using van't Hoff's equation $\pi = cRT$ (at c = 2137 mOsm kg^{-1}, π =52 atm) by assuming ideal solution. This difference can be attributed to the concentration polarization at the interface between the membrane and the polymer solution and the non-ideality of the polymer solution due to its high concentration. To further confirm the high osmotic pressure of the polymer solution, the differential osmotic pressure between the 15SN solution and seawater was also measured. When 33.3 wt% 15SN solution was loaded in the fluid chamber and 0.6 M NaCl was used as the buffer solution, an osmotic pressure of 9.0

atm was observed (Figure 5.6c), indicating that the polymer solution has an osmotic pressure that is much higher than seawater. This is critical for the draw solution to extract water from seawater.
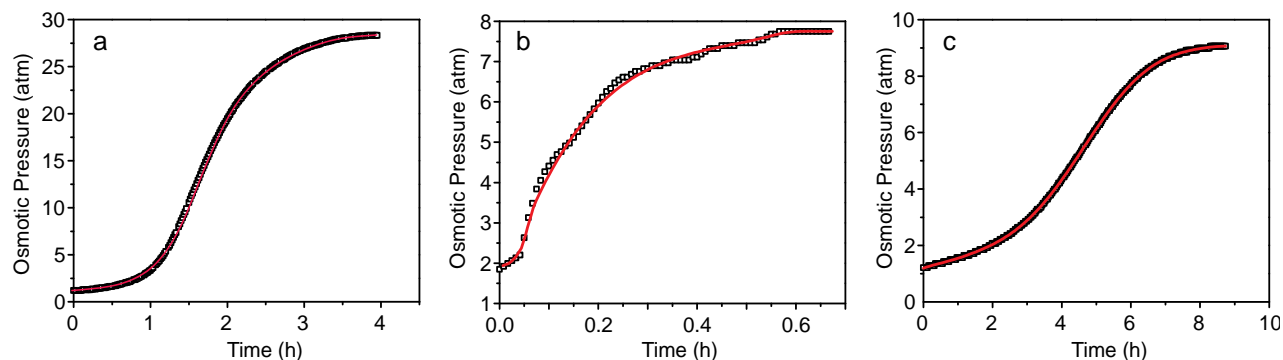
Figure 5.6 (a, b) The osmotic pressures of 15SN solution (33.3 wt%) using DI water as the buffer solution at room temperature and 45 °C, respectively. (c) The osmotic pressure of 15SN solution (33.3 wt%) using 0.6M NaCl solution as the buffer solution at room temperature.

It should be noted although the high concentration of the copolymer solution might lead to relatively high viscosity, we found that the solution can be continuously pumped to the FO module without interruption or substantial temperature increase. The relative viscosity (η_r) of 15SN solutions (10, 20 and 33.3 wt%) is shown in Figure 5.7a. As expected, the relative viscosity increases with concentration. For 33.3 wt% 15SN solution, the relative viscosity η_r is 68. This viscosity is lower than sodium polyacrylate solution (0.72 g mL^{-1}) which has been successfully employed as FO draw solution by Ge *et al.*[43] To confirm that the heat generated from pumping the solution would not cause much temperature increase, the temperature of the draw solution was monitored during circulation. As shown in Figure 5.7b, the temperature increased only from 23.5 °C to 24.5 °C and stabilized after continuous circulation for 8 hours.
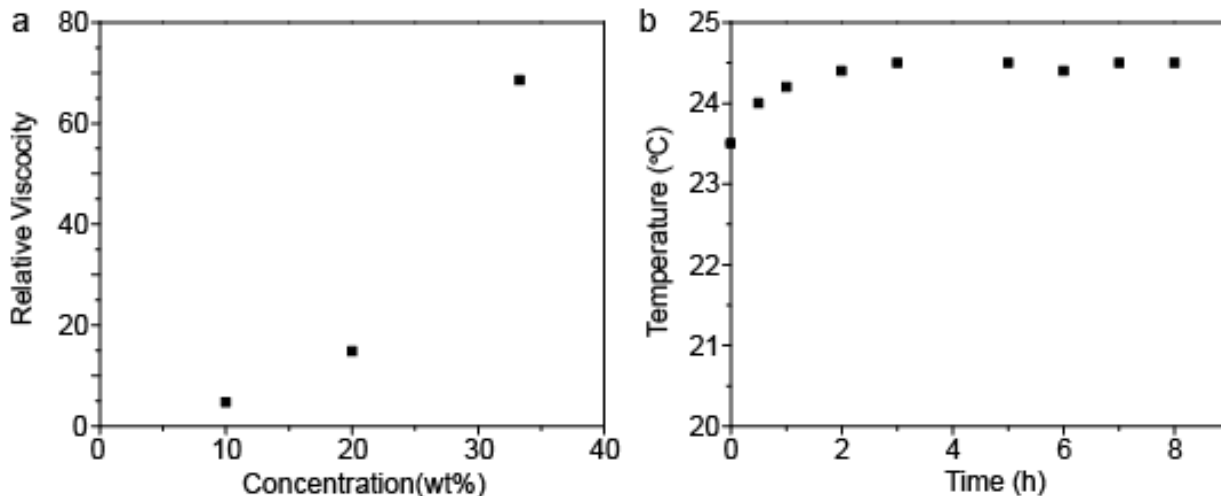
Figure 5.7 (a) Relative viscosities of 15SN solutions (10, 20 and 33.3 wt%); (b) Temperature change of the draw solution (15SN, 33.3 wt%) during pumping.

5.3.2 FO Performance and Regeneration of Draw Solution

In this work, alternating FO and MD processes were performed for three cycles to evaluate the 15SN copolymer as draw solute for seawater desalination. After the FO test, the osmolality of the draw solution dropped from 2137 to 2000 mOsm kg^{-1} due to dilution. MD was then applied to re-concentrate the draw solution to the original concentration. A commercial HTI thin film composite (TFC) embedded support membrane was chosen for FO due to its high permeability (~20 LMH in FO mode with 1 M NaCl as draw solution and DI water as feed solution), high salt rejection (> 99.3%) and wide pH tolerance (about 2.0 to 12.0). A multi-bore PVDF hollow fiber (MBF) membrane was used for MD in view of its high mechanical strength, suitable pore size, good stability in vapor permeation flux, and high salt rejection. Figure 5.8 summarizes the FO and MD water fluxes for three cycles. For the first cycle, FO and MD water fluxed of 4.0 and 2.7 LMH were attained, respectively. Afterwards, the water fluxes for both FO and MD processes dropped slightly. After three cycles, the average FO water flux was 3.5 LMH; and the average

MD flux was 2.5 LMH. It should be noted that when the desalination and regeneration are coupled as shown in Figure 5.3, the following equation should be satisfied for continuous and stable performance of the whole system:

$$J_{v,FO} \times A_{FO} \approx J_{v,MD} \times A_{MD}$$

where $J_{v,FO}$ and $J_{v,MD}$ are FO and MD water fluxes, and A_{FO} and A_{MD} are FO and MO membrane areas, respectively. The required balance can be achieved by adjusting the area of the FO (A_{FO}) or MD membrane (A_{MD}), or changing the temperature for MD.
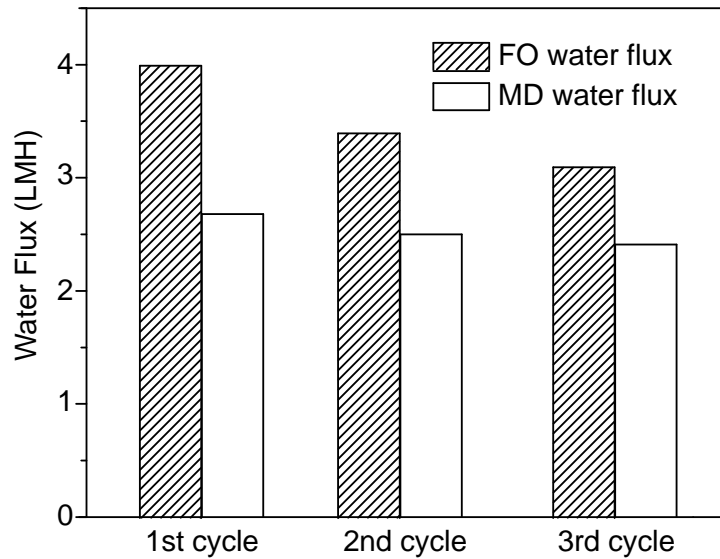
Figure 5.8 FO water fluxes with 15SN solution (33.3 wt%) as the draw solution and simulated seawater (0.6 M NaCl solution) as the feed solution; and MD water fluxes at 50 ^{o}C with the diluted 15SN solution as the feed solution.

The use of thermoresponsive polymers as FO draw solute that can be regenerated via MD offers a few advantages. First, the molecular structure of 15SN minimizes the reverse flux in both FO and MD processes. According to previous reports,[43] polyelectrolytes have significantly lower salt

leakage than conventional draw solutions like NaCl, $MgCl_2$ and $MgSO_4$ in membrane processes since the former have much larger sizes and an expanded structure. In this work, the measured reverse flux of 15SN in FO tests was 2 gMH, much lower than 90 gMH obtained with the same membrane when salt water was used as the draw solution. In the MD process, the measured conductivities of the DI water before and after the test were both 0.7 μS cm^{-1}, indicating that there was negligible leakage of 15SN. This is because although the structure of the copolymer shrinks at temperatures above its LCST, the polymer chains would agglomerate to form particles with size larger than the membrane pore size. Such low leakage in FO and MD makes the copolymer 15SN a promising candidate as draw solute with low replenishment cost and high quality of product water. Furthermore, the use of 15SN may also prolong the operation time of MD membranes. MD membranes usually exhibit pore wetting after a certain time of operation when using seawater as the feed solution. Although MD membrane materials are hydrophobic, water and salt may still go through the membrane pores after a long operation time. As a result, the water quality on the permeate side will decrease dramatically due to salt leakage. However, agglomerated 15SN could hardly pass through the pore channels even when pore wetting happens. In addition, for MD process, as the osmolality of the 15SN solution decreases when heated above its LCST, the water activity and the effective vapor pressure increase, therefore an enhanced water flux can be expected compared to conventional draw solutions without thermoresponsive property. It is worth noting that although generally the solution salinity in MD does not have significant effect on the separation efficiency, at high concentrations and temperatures, the change in concentration of the feed solution may cause significant difference in MD water flux.[54]

5.3.3 Energy Consumption of the FO-MD Process

RO is an energy intensive process because a high hydraulic pressure is necessary to overcome the osmotic pressure generated by seawater. Based on thermodynamic analysis, assuming 3.5% salinity and 50% recovery of water, the practical minimum energy of RO process is approximately 1.5 kWh/m^3;[2] while in general it can be in the range of 3–7 kWh/m^3. The overall energy requirement of an FO process including the recovery system should be less than 4 kWh/m^3 to be competitive with existing RO technology.[58] It has been reported that the electrical power requirement of FO process alone in seawater desalination would be about 0.25 kWh/m^3,mainly for fluid pumping.[59] As the MD setup is similar to FO, the energy consumption for fluid pumping is approximately the same as FO process, namely, 0.25 kWh/m^3. Therefore, in the FO-MD hybrid system, the main energy consumption would be caused by heating the feed solution in MD. For 1m^3 water to increase 1 °C, the required energy is 1.16 kWh. The energy for heating water from room temperature to the MD operating temperature of 50 °C would be 29 kWh/m^3. Apparently, the total energy needed for the FO-MD hybrid process will be larger than that of RO process. However, one should note that due to the low temperature required for MD, the heating can be provided by low-grade waste heat to significantly reduce the energy cost. Similar process utilizing waste heat has been reported by Elimelech *et al.*[59] in their NH_4HCO_3-promoted FO seawater desalination process, which saves up to 85% of energy compared with other desalination technologies. Therefore, by using low-grade waste heat to minimalize cost, we could expect the FO-MD hybrid system might offer similarly improved energy efficiency.

5.4 Conclusions

PSSS-PNIPAM copolymers with different SSS contents were synthesized. Considering the osmotic pressure and LCST, PSSS-PNIPAM with 15 wt% of SSS was chosen as the draw solute in FO to desalinate seawater. With simulated seawater (0.6 M NaCl solution) as the feed solution, FO water fluxes larger than 3.5 LMH were attained. It was also found that the osmotic pressure of PSSS-PNIPAM solution drops at temperatures above its LCST. This thermoresponsive property improves the regeneration of the draw solution *via* MD because the decreased osmotic pressure allows higher water vapor pressure and favors the separation of water from the solution. In addition, the use of PSSS-PNIPAM may reduce salt leakage in MD and produce high-quality water. It is believed that with further improvement to increase the osmotic pressure and reduce the viscosity of thermoresponsive copolymers, they can be promising draw solutes for FO desalination.

5.5 References

1. Cath, T. Y.; Childress, A. E.; Elimelech, M. Forward osmosis: principles, applications, and recent developments. *J. Membr. Sci*. **2006**, 281, 70–87.

2. Elimelech, M.; Phillip, W. A. The future of seawater desalination: energy, technology, and the environment. *Science* **2011**, 333, 712–717.

3. Ghaffour, N.; Missimer, T. M.; Amy, G. L. Technical review and evaluation of the economics of water desalination: current and future challenges for better water supply sustainability. *Desalination* **2013**, 309, 197–207.

4. Greenlee, L. F.; Lawler, D. F.; Freeman, B. D.; Marrot, B.; Moulin, P. Reverse osmosis desalination: water sources, technology, and today's challenges. *Water Res.* **2009**, 43, 2317–2348.

5. Likhachev, D. S.; Li, F. C. Large-scale water desalination methods: a review and new perspectives. *Desali. Water Treat*. **2013**, 51, 2836–2849.

6. Shannon, M. A.; Bohn, P. W.; Elimelech, M.; Georgiadis, J. G.; Mariñas, B. J.; Mayes, A. M. Science and technology for water purification in the coming decades. *Nature* **2008**, 452, 301–310.

7. Wilf, M. Future of the osmotic processes. *Desali. Water Treat*. **2010**, 15, 292–298.

8. Choi, Y. J.; Choi, J. S.; Oh, H.J.; Lee, S.; Yang, D. R.; Kim, J. H. Toward a combined system of forward osmosis and reverse osmosis for seawater desalination, *Desalination* **2009**, 247, 239–246.

9. Chung, T.-S.; Zhang, S.; Wang, K. Y.; Su, J.; Ling, M. M. Forward osmosis processes: yesterday, today and tomorrow. *Desalination* **2012**, 287, 78–81.

10. Zhao, S.; Zou, L.; Tang, C. Y.; Mulcahy, D. Recent developments in forward osmosis: opportunities and challenges. *J. Membr. Sci.* **2012**, 396, 1–21.

11. Ge, Q.; Wang, P.; Wan, C.; Chung, T.-S. Polyelectrolyte-promoted forward osmosis–membrane distillation (FO–MD) hybrid process for dye wastewater treatment. *Environ. Sci. Technol*. **2012**, 46, 6236–6243.

12. Ling, M. M.; Wang, K. Y.; Chung, T.-S. Highly water-soluble magnetic nanoparticles as

novel draw solutes in forward osmosis for water reuse, *Ind. Eng. Chem. Res*. **2010**, 49, 5869–5876.

13. Bai, H.; Liu, Z.; Sun, D. D. Highly water soluble and recovered dextran coated Fe_3O_4 magnetic nanoparticles for brackish water desalination. *Sep. Purif. Technol.* **2011**, 81, 392–399.

14. Li, D.; Zhang, X.; Simon, G. P.; Wang, H. Forward osmosis desalination using polymer hydrogels as a draw agent: influence of draw agent, feed solution and membrane on process performance. *Water Res.* **2013**, 47, 209–215.

15. Li, D.; Zhang, X.; Yao, J.; Simon, G. P.; Wang, H. Stimuli-responsive polymer hydrogels as a new class of draw agent for forward osmosis desalination. *Chem. Commun*. **2011**, 47, 1710-1712.

16. Ling, M. M.; Chung, T.-S. Desalination process using super hydrophilic nanoparticles via forward osmosis integrated with ultrafiltration regeneration. *Desalination* **2011**, 278, 194–202.

17. McCutcheon, J. R.; McGinnis, R. L.; Elimelech, M. A novel ammonia—carbon dioxide forward (direct) osmosis desalination process, *Desalination* 2**005**, 174, 1–11.

18. Phuntsho, S.; Hong, S.; Elimelech, M.; Shon, H. K. Forward osmosis desalination of brackish groundwater: meeting water quality requirements for fertigation by integrating nanofiltration. *J. Membr. Sci.* **2013**, 436, 1–15.

19. Ling, M. M.; Chung, T.-S. Novel dual-stage FO system for sustainable protein enrichment

using nanoparticles as intermediate draw solutes. *J. Membr. Sci*. **2011**, 372, 201–209.

20. Wang, K. Y.; Teoh, M. M.; Nugroho, A.; Chung, T.-S. Integrated forward osmosis–membrane distillation (FO–MD) hybrid system for the concentration of protein solutions. *Chem. Eng. Sci*. **2011**, 66, 2421–2430.

21. Yang, Q.; Wang, K. Y.; Chung, T.-S. A novel dual-layer forward osmosis membrane for protein enrichment and concentration. *Sep. Purif. Technol*. **2009**, 69, 269–274.

22. Achilli, A.; Cath, T. Y.; Childress, A. E. Power generation with pressure retarded osmosis: an experimental and theoretical investigation. *J. Membr. Sci*. **2009**, 343, 42–52.

23. Lee, K. L.; Baker, R. W.; Lonsdale, H. K. Membranes for power generation by pressure-retarded osmosis, *J. Membr. Sci*. **1981**, 8, 141–171.

24. Yip, N. Y.; Tiraferri, A.; Phillip, W. A.; Schiffman, J. D.; Hoover, L. A.; Kim, Y. C.; Elimelech, M. Thin-film composite pressure retarded osmosis membranes for sustainable power generation from salinity gradients. *Environ. Sci. Technol*. **2011**, 45, 4360–4369.

25. Nguyen, N. C.; Chen, S. S.; Yang, H. Y.; Hau, N. T. Application of forward osmosis on dewatering of high nutrient sludge. *Bioresour. Technol*. **2013**, 132, 224–229.

26. Phuntsho, S.; Shon, H. K.; Hong, S.; Lee, S.; Vigneswaran, S. A novel low energy fertilizer driven forward osmosis desalination for direct fertigation: evaluating the performance of fertilizer draw solutions. *J. Membr. Sci*. **2011**, 375, 172–181.

27. Phuntsho, S.; Shon, H. K.; Hong, S.; Lee, S.; Vigneswaran, S.; Kandasamy, J. Fertiliser drawn forward osmosis desalination: the concept, performance and limitations for fertigation.

Rev. Environ. Sci. Biotechnol. **2011**, 11, 147-168.

28. Zhu, H.; Zhang, L.; Wen, X.; Huang, X. Feasibility of applying forward osmosis to the simultaneous thickening, digestion, and direct dewatering of waste activated sludge. *Bioresour. Technol*. **2012**, 113, 207–213.

29. Butler, E.; Silva, A.; Horton, K.; Rom, Z.; Chwatko, M.; Havasov, A.; McCutcheon, J. R. Point of use water treatment with forward osmosis for emergency relief, *Desalination* **2013**, 312, 23–30.

30. Yip, N. Y.; Tiraferri, A.; Phillip, W. A.; Schiffman, J. D.; Elimelech, M. High performance thin-film composite forward osmosis membrane. *Environ. Sci. Technol*. **2010**, 44, 3812–3818.

31. Flanagan, M. F.; Escobar, I. C. Novel charged and hydrophilized polybenzimidazole (PBI) membranes for forward osmosis. *J. Membr. Sci*. **2013**, 434, 85–92.

32. Han, G.; Chung, T.-S.; Toriida, M.; Tamai, S. Thin-film composite forward osmosis membranes with novel hydrophilic supports for desalination. *J. Membr. Sci*. **2012**, 423-424, 543–555.

33. Han, G.; Zhang, S.; Li, X.; Widjojo, N.; Chung, T.-S. Thin film composite forward osmosis membranes based on polydopamine modified polysulfone substrates with enhancements in both water flux and salt rejection. *Chem. Eng. Sci*. **2012**, 80, 219–231.

34. Su, J.; Yang, Q.; Teo, J. F.; Chung, T.-S. Cellulose acetate nanofiltration hollow fiber membranes for forward osmosis processes. *J. Membr. Sci*. **2010**, 355, 36–44.

35. Wang, K. Y.; Ong, R. C.; Chung, T.-S. Double-skinned forward osmosis membranes for reducing internal concentration polarization within the porous sublayer. *Ind. Eng. Chem. Res.* **2010**, 49, 4824–4831.

36. Zhang, S.; Wang, K. Y.; Chung, T.-S.; Chen, H.; Jean, Y. C.; Amy, G. Well-constructed cellulose acetate membranes for forward osmosis: minimized internal concentration polarization with an ultra-thin selective layer. *J. Membr. Sci*. **2010**, 360, 522–535.

37. Zhang, S.; Wang, K. Y.; Chung, T.-S.; Jean, Y. C.; Chen, H. Molecular design of the cellulose ester-based forward osmosis membranes for desalination. *Chem. Eng. Sci*. **2011**, 66, 2008–2018.

38. Hu, M.; Mi, B. Enabling graphene oxide nanosheets as water separation membranes. *Environ. Sci. Technol.* **2013**, 47, 3715–3723.

39. Huang, L;. Bui, N. N.; Meyering, M. T.; Hamlin, T. J.; McCutcheon, J. R. Novel hydrophilic nylon 6,6 microfiltration membrane supported thin film composite membranes for engineered osmosis. *J. Membr. Sci.* **2013**, 437, 141–149.

40. Chekli, L.; Phuntsho, S.; Shon, H. K.; Vigneswaran, S.; Kandasamy, J.; Chanan, A. A review of draw solutes in forward osmosis process and their use in modern applications. *Desali. Water Treat*. **2012**, 43, 167–184.

41. Ge, Q.; Ling, M. M.; Chung, T.-S. Draw solutions for forward osmosis processes: developments, challenges, and prospects for the future. *J. Membr. Sci*. **2013**, 442, 225–237.

42. Achilli, A.; Cath, T. Y.; Childress, A. E. Selection of inorganic-based draw solutions for

forward osmosis applications. *J. Membr. Sci*. **2010**, 364, 233–241.

43. Ge, Q.; Su, J.; Amy, G. L.; Chung, T.-S. Exploration of polyelectrolytes as draw solutes in forward osmosis processes. *Water Res*. **2012**, 46, 1318–1326.

44. Ge, Q.; Su, J.; Chung, T.-S.; Amy, G. Hydrophilic superparamagnetic nanoparticles: synthesis, characterization, and performance in forward osmosis processes. *Ind. Eng. Chem. Res*. **2011**, 50, 382–388.

45. Ling, M. M.; Chung, T.-S.; Lu, X. Facile synthesis of thermosensitive magnetic nanoparticles as "smart" draw solutes in forward osmosis. *Chem. Commun.* **2011**, 47, 10788–10790.

46. Noh, M.; Mok, Y.; Lee, S.; Kim, H.; Lee, S. H.; Jin, G. W.; Seo, J. H.; Koo, H.; Park, T. H.; Lee, Y. Novel lower critical solution temperature phase transition materials effectively control osmosis by mild temperature changes. *Chem. Commun*. **2012**, 48, 3845-3847.

47. Ou, R.; Wang, Y.; Wang, H.; Xu, T. Thermo-sensitive polyelectrolytes as draw solutions in forward osmosis process. *Desalination* **2013**, 318, 48–55.

48. Stone, M. L.; Rae, C.; Stewart, F. F.; Wilson, A. D. Switchable polarity solvents as draw solutes for forward osmosis. *Desalination* **2013**, 312, 124–129.

49. Stone, M. L.; Wilson, A. D.; Harrup, M. K.; Stewart, F. F. An initial study of hexavalent phosphazene salts as draw solutes in forward osmosis. *Desalination* **2013**, 312, 130–136.

50. Yen, S. K.; Mehnas Haja N, F.; Su, M.; Wang, K. Y.; Chung, T.-S. Study of draw solutes using 2-methylimidazole-based compounds in forward osmosis. *J. Membr. Sci*. **2010**, 364,

242–252.

51. Zhao, Q.; Chen, N.; Zhao, D.; Lu, X. Thermoresponsive magnetic nanoparticles for seawater desalination. *ACS Appl. Mater. Interfaces* **2013**, 5, 11453-11461.

52. Han, H.; Lee, J. Y.; Lu, X. Thermoresponsive nanoparticles + plasmonic nanoparticles = photoresponsive heterodimers: facile synthesis and sunlight-induced reversible clustering. *Chem. Commun*. **2013**, 49, 6122-6124.

53. Razmjou, A.; Simon, G. P.; Wang, H. Effect of particle size on the performance of forward osmosis desalination by stimuli-responsive polymer hydrogels as a draw agent. *Chem. Eng. J.* **2013**, 215-216, 913–920.

54. Schofield, R. W.; Fane, A. G.; Fell, C. J. D.; Macoun, R. Factors affecting flux in membrane distillation. *Desalination* **1990**, 77, 279-294.

55. Nowakowska, M.; Szczubiałka, K.; Grębosz, M. Modifying the thermosensitivity of copolymers of sodium styrene sulfonate and N-isopropylacrylamide with dodecyltrimethylammonium chloride. *Colloid Polym Sci*. **2004**, 283, 291–298.

56. Chahine, N. O.; Chen, F. H.; Hung, C. T.; Ateshian, G. A. Direct measurement of osmotic pressure of glycosaminoglycan solutions by membrane osmometry at room temperature, *Biophys. J*. **2005**, 89, 1543–1550.

57. Wang, P.; Chung, T.-S. Design and fabrication of lotus-root-like multi-bore hollow fiber membrane for direct contact membrane distillation. *J. Membr. Sci*. **2012**, 421-422, 361-374.

58. Qin, J. J. Recent developments and future challenges of forward osmosis for desalination: a

review. *Desalination* **2012**, 39, 123-136.

59. McGinnis, R. L.; Elimelech, M. Energy requirements of ammonia-carbon dioxide forward osmosis desalination. *Desalination* **2007**, 207, 370-382.

CHAPTER 6

THERMORESPONSIVE IONIC LIQUID AS FORWARD OSMOSIS DRAW SOLUTE FOR BRACKISH WATER AND SEAWATER DESALINATION

6.1 Introduction

Clean water scarcity has been a worldwide crisis of our time and the near future. Improving the use of existing water resources is not enough to address this issue. Only searching for other water supply can alleviate the stress of water shortage.[1, 2] Seawater desalination has been proposed as a probable solution since seawater offers unlimited and constant water supply. Desalination of brackish groundwater is also a choice for inland districts. Widely employed desalination technologies include multi-effect distillation (MED), multi-stage flash (MSF), and reverse osmosis (RO). However, high temperature is needed for MED and MSF; while RO requires high hydraulic pressure with high electrical energy cost.[3-5] Therefore, despite the recent advances, reducing the energy cost of desalination remains a great challenge.

In recent years, forward osmosis (FO) has attracted extensive attention.[6-8] In a typical FO process, water molecules in a solution of low osmotic pressure (feed solution) can spontaneously pass across a semi-permeable membrane to solution of high osmotic pressure (draw solution). Contrary to RO, FO is a spontaneous process driven by the osmotic pressure difference between the feed solution and draw solution. However, after the draw solution extracts clean water from

the feed solution, it needs to undergo a regeneration process to separate water from the draw solution and be reused in the next FO process. The regeneration method substantially determines the energy input of a closed-loop FO process (including FO and draw solution regeneration). In the last few years, a variety of novel draw solutions have been developed.[9-18] Among them, draw solutes which are temperature sensitive and can be regenerated upon thermal stimuli have attracted increasing attention, because the regeneration of such draw solutions may take the advantage of low grade heat which is an abundant and less expensive energy resource. Recently, various novel thermoresponsive draw solutions have been investigated. MsCutcheon, Elimelech and co-workers employed NH_4HCO_3 in FO seawater desalination process.[19, 20] NH_4HCO_3 solution was used as draw solution in FO, after which it was decomposed to NH_3 and CO_2 gases around 60 °C and separated from water. By re-dissolving CO_2 and NH_3, the draw solution could be recycled. Zhao *et al*. presented a study on a thermoresponsive copolymer, poly(sodium styrene-4-sulfonate-*co*-n-isopropylacrylamide) (PSSS-PNIPAM) as FO draw solute for seawater desalination in a process combined with forward osmosis and membrane distillation (FO-MD).[21] Magnetic nanoparticles could be successfully modified with this thermoresponsive copolymer.[22] These modified magnetic nanoparticles would agglomerate spontaneously to lager particles when heated above the low critical solution temperature (LCST). This thermoresponsive behavior enables these large particles to be easily captured by either a low-strength magnetic field or UF membrane. Poly(*N*-isopropylacrylamine) (PNIPAM) hydrogel was also investigated as FO draw agent.[23] It would absorb water at the volume phase transition temperature (VPTT, ~32 °C) and expel water in its network when the temperature is above the VPTT. However, the driving force provided by this hydrogel was poor. In 2014, Nakayama *et al.* demonstrated the temperature-controlled osmotic change of di(ethylene glycol) n-hexyl ether (DEH) solution.[24] However, while 12 mol L^{-1} DEH solution has an osmolality higher than 3000 mOsm kg^{-1}, it could only generate a water

flux of 1.4LMH with DI water as the feed solution, which might be only one-tenth of the expected water flux.[24]

Ionic liquids (ILs) are organic salts which have melting points below 100 °C. Unlike conventional ILs which either dissolve in water or repel water, thermoresponsive ILs exhibit subtle balance between hydrophilicity and hydrophobicity. Most thermoresponsive ILs undergo lower critical solution temperature (LCST)-type phase change,[25] in which the compatibility of ILs and water decreases upon heating. Therefore, when homogeneous thermoresponsive ILs are used as FO draw solution, they can draw water from saline water at a temperature below its LCST. After the FO process, the diluted draw solution is heated above its LCST and forms liquid-liquid separated phases (Figure 6.1). The water-rich phase with low IL content can be further purified by energy-efficient nanofiltration (NF) to produce high quality or drinkable water. Both the rententate in NF and the IL-rich phase with high IL content are reused in the next FO process. The inherent ionic nature, low viscosity even at high concentration, and ease of separation from water make thermoresponsive ILs promising FO draw solutes. Very recently, Cai *et al.* employed thermoresponsive ionic liquids (ILs), tetrabutylphosphonium 2,4-dimethylbenzenesulfonate ($P_{4444}DMBS$) and tetrabutylphosphonium mesitylenesulfonate ($P_{4444}TMBS$), as draw solutes for FO seawater desalination.[26] However, similarly to the case of DEH solution, 60 wt% $P_{4444}DMBS$ solution with an osmolality of 4000 mOsm kg^{-1} gave only 2.7 LMH for seawater desalination.[26] These water fluxes are much lower than other draw solutions that have similar osmolality. However, detailed study has not been carried out to explore the reasons for such low FO water flux.
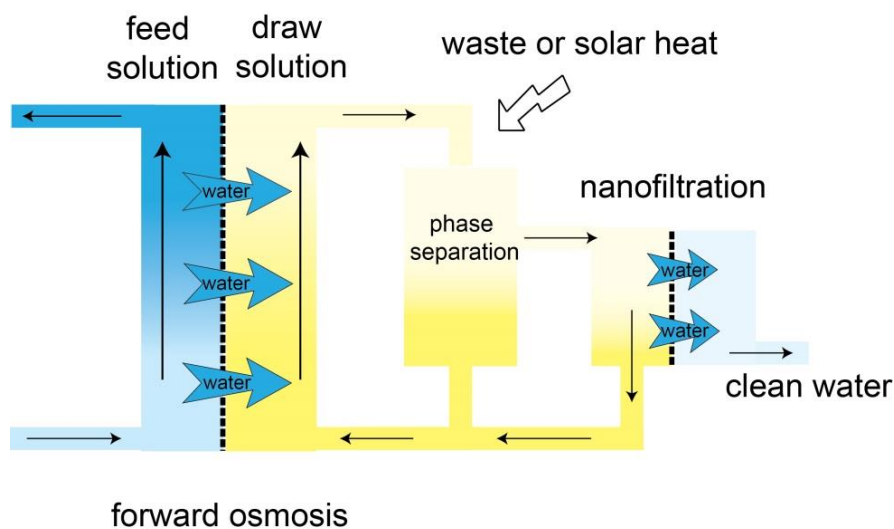
Figure 6.1 Schematic illustration of the FO process with thermoresponsive ionic liquids as draw solutes.

In this study we explored another thermoresponsive IL, tetrabutylphosphonium trifluoroacetate (abbreviated as $P_{4444}[CF_3COO]$), as the FO draw solute. Similar to other thermoresponsive ILs, the water flux generated by $P_{4444}[CF_3COO]$ solution was lower than many other conventional draw solutions with similar osmolalities. Even when the osmolality of the draw solution reached 4500 mOsm kg^{-1}, it could not generate water flux for seawater (1200 mOsm kg^{-1}) desalination at room temperature. Thin-film theory analysis was conducted to understand the mechanism of the unusual low water flux of $P_{4444}[CF_3COO]$ solution. Moreover, the FO performance of $P_{4444}[CF_3COO]$ solution, at higher temperature but below the LCST, was also investigated. We found that at higher FO operational temperature, the FO water flux could be increased.

6.2 Experimental Section

6.2.1 Materials and Instruments

114

Tetrabutylphosphonium hydroxide solution ($P_{4444}OH$, 40 wt% in H_2O), trifluoroacetic acid (CF_3COOH, 99%) and sodium chloride (NaCl, >99.5 %) were purchased from Sigma-Aldrich and used as received. Deionized (DI) water in all experiments was obtained from a Milli-Q unit (Millipore, USA). Seawater (840 mOsm kg^{-1}), which was employed as one of the feed solutions in the FO tests, was collected from Sentosa coast, Singapore. FO membrane was provided by Hydration Technologies Inc. (HTI, Albany, OR). The osmolality of solutions was measured by an osmometer (Wescor, Vapro vapor pressure osmometer). The content of $P_{4444}[CF_3COO]$ in aqueous solution was determined by thermogravimetric analysis (TGA, Shimazu DTG-60AH) under N_2 from room temperature to 120 °C. Relative viscosity of draw solution was calculated by the following equation:

$$\eta_r = \eta/\eta_0 = (t\,\rho)/(t_0\,\rho_0) \qquad (1)$$

where t and t_0 (s) are the respective elution time of the draw solution and DI water measured by AVS 360 inherent viscosity meter; ρ and ρ_0 (g mL^{-1}) are the density of the draw solution and DI water, respectively.

The shear viscosity of $P_{4444}[CF_3COO]$ solution with different concentrations and at different temperatures was measured at shear rate from 100 to 600 s^{-1} by a rotational cone and plate rheometer (AR-G2 rheometer, TA instruments, USA). A steady-state mode with a 60 mm, 1° cone geometry was employed. The hydrodynamic size of the molecules was measured by a ZetaSizer Nano system (Nano ZS, Zen3600). The osmotic pressure of $P_{4444}[CF_3COO]$ solution with different concentrations and at different temperatures was tested according to the method reported in a previous paper.[21]

6.2.2 Synthesis of P$_{4444}$[CF$_3$COO]

To prepare P$_{4444}$[CF$_3$COO], aqueous solution of P$_{4444}$OH was directly neutralized by a slightly excess of trifluoroacetic acid.[27] The product was evaporated under reduced pressure at 40 °C. At room temperature, pure P$_{4444}$[CF$_3$COO] is in wax form.

6.2.3 FO Tests

FO water flux was measured with a lab-scale cross-flow cell. In all FO tests, the selective layer of the FO membrane was oriented to the draw solution (PRO mode). The effective membrane area was 1cm×2 cm. Draw solutions were 73 wt% and 82 wt% of P$_{4444}$[CF$_3$COO] aqueous solution (osmolality 1500 mOsm kg^{-1} and 4500 mOsm kg^{-1}, respectively). The feed solutions were DI water (0 mOsm kg^{-1}), simulated brackish water (2g L^{-1} MgSO4 solution, 30 mOsm kg^{-1}), seawater from Singapore coast (840 mOsm kg^{-1}), and simulated seawater (3.5 wt% NaCl solution, 1200 mOsm kg^{-1}). During the FO process, the feed solution and the draw solution flowed concurrently through two sides of the cell which was separated by a piece of FO membrane. The flow rate was 12.5 cm s^{-1} and 6 cm s^{-1} for the draw solution the feed solution, respectively. Each process was run for 30 mins to determine the FO water flux by calculating the weight increment of the draw solution during certain time using Equation (2):

$$J_v = \Delta m/(A_m \cdot \Delta t \times 1000) \qquad (2)$$

where Δm (g) is the mass of water permeated across the effective FO membrane area A_m (m^2) over a time period of Δt (h), assuming the density of water is 1000 g L^{-1}.

6.3 Results and Discussion

6.3.1 Osmolality and Phase Separation

Figure 6.2 presents the osmolalities of $P_{4444}[CF_3COO]$ solution at different concentrations. The osmolalities of 10, 20, 30, 40, 50, 60, 70 and 80 wt% solutions were 403, 595, 621, 633, 682, 812, 1294 and 4056 mOsm/kg, respectively. As shown in Figure 6.1, when the concentration increased, the osmolality did not increase linearly as conventional draw solutes such as simple salts and polyelectrolytes.[28, 29] This is due to the hydrophobic association of the ionic liquid molecules.[30] Above 70 wt%, the osmolality of $P_{4444}[CF_3COO]$ solution was higher than that of simulated seawater (3.5 wt%, 1200 mOsm/kg).
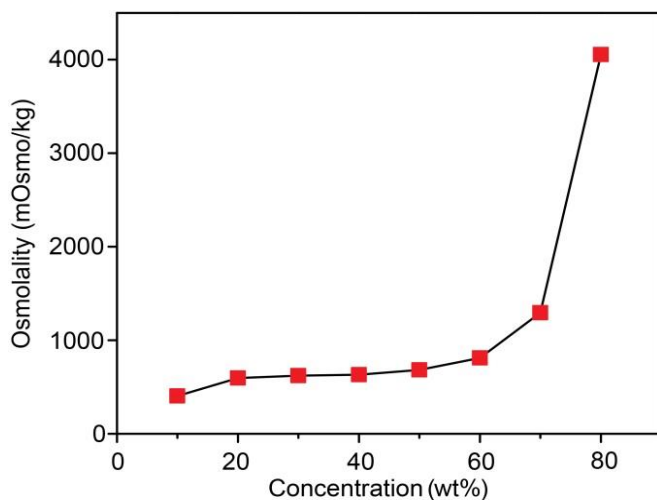
Figure 6.2 Osmolality of $P_{4444}[CF_3COO]$ solution with different concentrations.

117
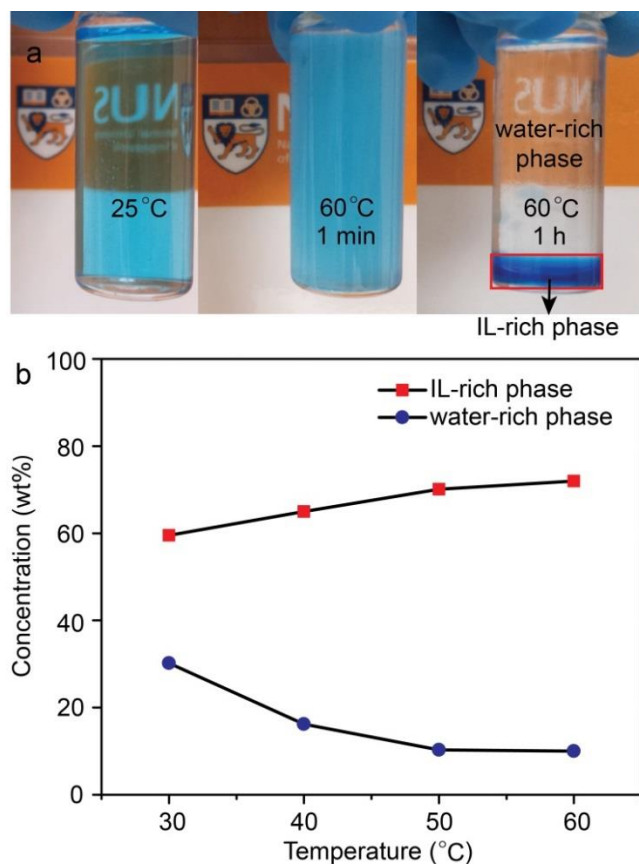
Figure 6.3 (a) LCST-type phase transition of 20 wt% P$_{4444}$[CF$_3$COO] solution; (b) concentration of P$_{4444}$[CF$_3$COO] in the water-rich supernatants and IL-rich sediments at different phase transition temperatures.

Figure 6.3a shows an example of the LCST-type phase transition. An aqueous solution containing 20 wt% P$_{4444}$[CF$_3$COO] was homogeneous at room temperature. The solution was clearly phase-separated at 60 °C after 1 hour. The IL phase was colored with Coomassie Brilliant Blue, which is not soluble in the aqueous phase but the IL phase. It has been found that after the solution is stabilized at a temperature above its LCST, the concentrations of the IL-rich phase and the water-rich phase are constant regardless of the initial concentration of the solution,[25, 27] but they change with the temperature. We studied the temperature dependence of the P$_{4444}$[CF$_3$COO] concentration in both phases after the phase separation. The initial concentration

of the $P_{4444}[CF_3COO]$ solution was 50 wt%. The homogeneous solution was then heated to induce phase separation and stored stably at certain temperature for 2 hours. Afterwards, the concentration of $P_{4444}[CF_3COO]$ in the IL-rich phase and the water-rich phase was analyzed as shown in Figure 6.3b. It was found that when the temperature increased, the content of $P_{4444}[CF_3COO]$ in the IL-rich phase would increase. At 30 °C, it was 59.5 wt%, and it increased to 73 wt% at 60 °C. On the contrary, the content of $P_{4444}[CF_3COO]$ in the water-rich phase dropped from 30.2 wt% to 10.0 wt% as the temperature increased from 30 °C to 60 °C. This occurred due to the fact that the compatibility of $P_{4444}[CF_3COO]$ molecules and water decreases upon heating. Consequently, the number of water molecules attached to each P_{4444}^+ and $[CF_3COO]^-$ pair in the IL-rich phase drops, thus the content of $P_{4444}[CF_3COO]$ in the IL-rich phase increases.[27] The IL-rich phase separated at 60 °C, which contains 73 wt% of $P_{4444}[CF_3COO]$, was employed as the FO draw solution in the following tests.

6.3.2 FO Performance

The IL-rich sediment at 60 °C, namely 73 wt% $P_{4444}[CF_3COO]$ solution, was employed as the draw solution in FO. After being diluted after the FO process, it was reconcentrated by phase separation at 60 °C again and reused directly in the next FO process without any further treatment. The feed solution was DI water and brackish water. It should be noted that 73 wt% solution could not be used for seawater desalination as the osmotic pressure difference between the draw solution and feed solution was insignificant. As shown in Figure 6.4a, using DI water as the feed solution, the water flux was 4.3, 4.7 and 5.6 LMH when the operational temperature was set as 25, 35 and 50 °C, respectively. When the feed solution was brackish water (2g L^{-1} MgSO4

solution, 30 mOsm kg^{-1}), the water flux reduced a little bit to 4.2, 4.6 and 4.9 LMH as the driving force between the two sides of the FO membrane dropped.
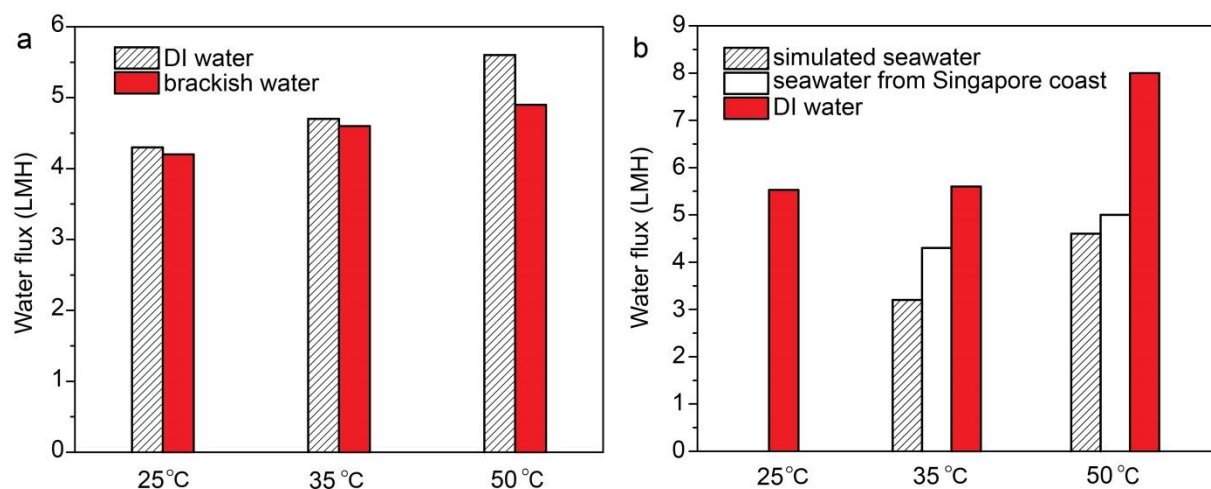
Figure 6.4 (a) FO water flux of 73 wt% $P_{4444}[CF_3COO]$ solution using DI water and brackish water as the feed solution; (b) FO water flux of 82 wt% $P_{4444}[CF_3COO]$ solution using DI water, seawater from Singapore coast and simulated seawater as the feed solution.

For seawater desalination, $P_{4444}[CF_3COO]$ solution with higher concentration (82 wt%, 4500 mOsm kg^{-1}) was employed as the draw solution in FO. Figure 6.4b summarizes the FO water flux with 82 wt% $P_{4444}[CF_3COO]$ solution as the draw solution and DI water, seawater from Singapore coast (840 mOsm kg^{-1}) and simulated seawater (3.5 wt% NaCl solution, 1200 mOsm kg^{-1}) as the feed solutions. At the room temperature (25 °C) and with DI water as the feed solution, 82 wt% solution exhibited a higher water flux than 73 wt% solution (5.5 LMH and 4.3 LMH, respectively). And similar to 73 wt% solution, the water flux increased when the operational temperature was increased. At 50 °C, the water flux could reach 8 LMH with DI water as the feed solution. At room temperature (25 °C), there was also no water flux across the membrane using the seawater from Singapore coast and simulated seawater as the feed solution.

However, when the solution was heated to a higher temperature, such as 35 °C and 50 °C, water

fluxes between 3~5 LMH were attained and an increasing trend according to temperature was

observed.
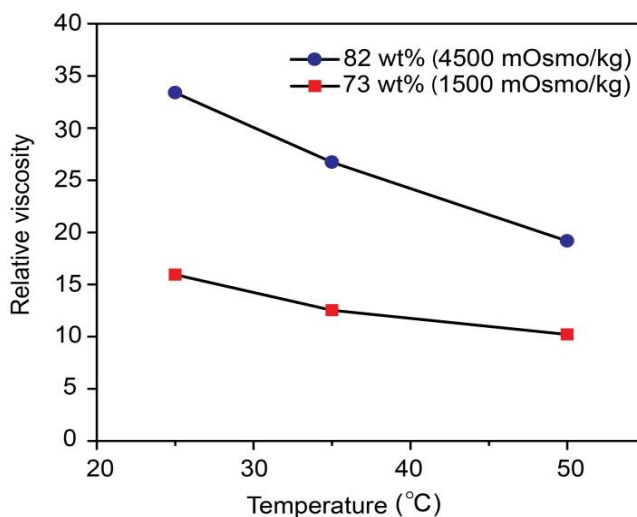
Figure 6.5 Relative viscosity of P$_{4444}$[CF$_3$COO] solution (73 and 82 wt%) at different temperatures (25, 35 and 50°C).

The relative viscosity of 73 and 82 wt% P$_{4444}$[CF$_3$COO] solution at different temperatures is

shown in Figure 6.5. As expected, the relative viscosity of 82 wt% solution is higher than that of

73 wt% solution. In addition, the relative viscosity decreased as the temperature of the solution

increased. The relative viscosity of 82 wt% solution dropped from 33.4 to 19.18 when the

solution was heated from 25 °C to 50 °C. The shear viscosity listed in Table 6.1 also followed

the same trend. The molecular weight of P$_{4444}$[CF$_3$COO] is much smaller than that of

polyelectrolytes, which leads to a much lower viscosity of P$_{4444}$[CF$_3$COO] solution even with a

much higher concentration. For instance, the relative viscosity of sodium polyacrylate (molecular

weight: 1200, 0.72 g mL^{-1}) reported by Ge *et al.* was about 70,[29] similar as the thermoresponsive

copolymer PSSS-PNIPAM (33.3 wt%) reported by Zhao *et al.*[21] The low viscosity of the draw solution can not only lead to a lower energy consumption for fluid pumping, but also less severe internal concentration polarization in FO mode (support layer of FO membrane towards the draw solution).

6.3.3 Mechanism Study

The FO results reveal that the water flux generated by $P_{4444}[CF_3COO]$ solution was lower than many other conventional draw solutions with similar osmolalities. Even when the osmolality of the draw solution reached 4500 mOsm kg^{-1}, it could not generate water flux for seawater (1200 mOsm kg^{-1}) desalination at room temperature. In addition, the FO water flux of $P_{4444}[CF_3COO]$ solution, at higher temperature but below the LCST, was increased. In FO processes, water flux is mainly affected by the osmotic pressure difference across the membrane, the severity of external and internal concentration polarization (ECP and ICP), and the performance of FO membrane as well.[31] We looked into these three factors for the reasons of 1) the relatively lower FO water flux than our expectation and 2) the temperature-sensitive FO water flux.

The permeation driving force across the FO membrane is the gradient in chemical potential of water. When using DI water as the feed solution and under PRO mode, there is no internal concentration polarization. To predict the water flux in the presence of ECP, we need to determine the effective osmotic pressure difference by using film theory. The generalized water flux is defined as

$$J_w = A(\Delta P - \Delta \pi) \qquad (3)$$

where A is the solvent permeability through the membrane, ΔP is the transmembrane pressure, and $\Delta\pi$ is the osmotic pressure difference between the draw solution and feed solution near the membrane surface.[32] ΔP is zero when there is no hydraulic pressure difference across the membrane, and $\Delta\pi$ is the osmotic pressure of the draw solution side when using the DI water as the feed solution (Figure 6.6).
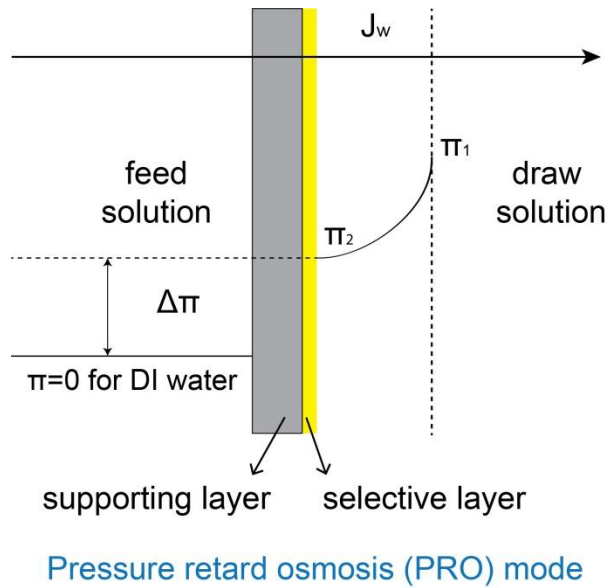
Figure 6.6 Schematic illustration of external concentration polarization (ECP) under PRO mode.

The effect of ECP is expressed as Equation 4.[33]

$$\frac{\pi_2}{\pi_1} = \exp\left[-\frac{J_w}{k}\right] \qquad (4)$$

where π_2 is the osmotic pressure of draw solution near the membrane surface, π_1 is the osmotic pressure of the bulk draw solution, and k is the mass transfer coefficient of the draw solution which is defined as

$$k = \frac{Sh D_s}{d_h} \qquad (5)$$

where *Sh* is the Sherwood number defined as Equation 6, *Ds* is the solute diffusion coefficient defined as Equation 7, and d_h is the hydraulic diameter (0.33 cm for the FO cell we used).[33]

$$Sh = 1.62[Re\ Sc\ \frac{d_h}{L}]^{0.33} \qquad (6) \qquad \text{for laminar flow}$$

where Re is the Reynolds number (= Vd_h/μ, with *V* being the bulk crossflow velocity and μ the solution shear viscosity as listed in Table 6.1), Sc is the Schmidt number (= μ/Ds), and *L* is the channel length (2cm for the FO cell we used).[34]

$$D_s = \frac{k_0 T}{6\pi\mu r} \qquad (7)$$

where k_0 is the Boltzman constant (the molar gas constant divided by the Avogadro number, = 1.38×10^{-23} m^2 kg s^{-2} K^{-1}), T is the absolute temperature, and r is the hydrodynamic radius of the particle/molecule (Table 6.1).[34]

By integrating the Equation 4-7, we can obtain Equation 8 for the calculation of k.

$$k = \frac{Sh D_s}{d_h} = \frac{1.62\left[\frac{Vd_h\rho}{\mu} \times \frac{\mu}{\rho D_s} \times \frac{d_h}{L}\right]^{0.33} D_s}{d_h} = \frac{1.62\left[\frac{Vd_h^2}{D_s L}\right]^{0.33} D_S}{d_h} \qquad (8)$$

The theoretical osmotic pressure of draw solution near the FO membrane, π_2, could be calculated by integrating Equation 3 with 4 to obtain Equation 9. For the commercial HTI FO membrane we used in the experiments, A was 0.84, 1.69 and 2.57 LMH atm^{-1} for 25 °C, 35 °C and 50 °C, respectively. Then the calculated FO water flux J_w can be determined by Equation 4 (Table 6.1).

$$\frac{\pi_2}{\pi_1} = \exp\left[-\frac{A(\pi_2 - 0)}{k}\right] \qquad (9)$$

Table 6.1 Shear viscosity, μ, hydrodynamic radius of the particle/molecule, r, mass transfer coefficient, k, osmotic pressure of draw solution near the membrane surface, π_2, and calculated FO water flux for 73 wt% and 82 wt% $P_{4444}[CF_3COO]$ solution under different temperatures.

	T (°C)	μ (mPa·s)	r (nm)	k (m s^{-1})	π_2 (atm)	Jw (LMH)
	25	15.2	4.12	4.34×10^{-7}	4.0	3.37
73 wt%	35	10.5	4.53	5.33×10^{-7}	2.8	4.72
	50	7.0	4.63	7.10×10^{-7}	2.6	6.55
82 wt%	25	22.7	2.37	4.81×10^{-7}	5.8	4.90

As seen in Table 6.1, the mass transfer coefficient of this highly concentrated $P_{4444}[CF_3COO]$ solution, k was much lower compared to other draw solution reported.[35] This may arise from the large hydraulic diameter of the draw solute. Although the molecular size of a single $P_{4444}[CF_3COO]$ molecule should be less than 1 nm according to its molecular weight, the hydraulic diameter measured by the zeta-sizer was higher than 4 nm. This indicates the hydrophobic association of several $P_{4444}[CF_3COO]$ molecules in the aqueous solution,[30] which could not only result in a low osmolality of the solution but also slower mass transfer of the solute. The slower mass transfer of the draw solute could further lead to more serious ECP on the side of selective layer. As a result, the effective osmotic pressure of the draw solution π_2 was much lower than the bulk draw solution π_1. This might be the reason for the relatively lower FO water flux of $P_{4444}[CF_3COO]$ solution compared with other draw solutions reported that have similar osmolality.[31] When the osmolality was increased to 4500 mOsm kg^{-1} (82 wt%), the water flux was higher than that of 1500 mOsm kg^{-1} (73 wt%), but less than expected, since the ECP

was still dominating. Although the osmotic pressure of bulk solution for 82 wt% $P_{4444}[CF_3COO]$ was three times that of 73 wt%, the effective osmotic pressure π_2 of 82 wt% solution was only a little higher than that of 73 wt% solution.
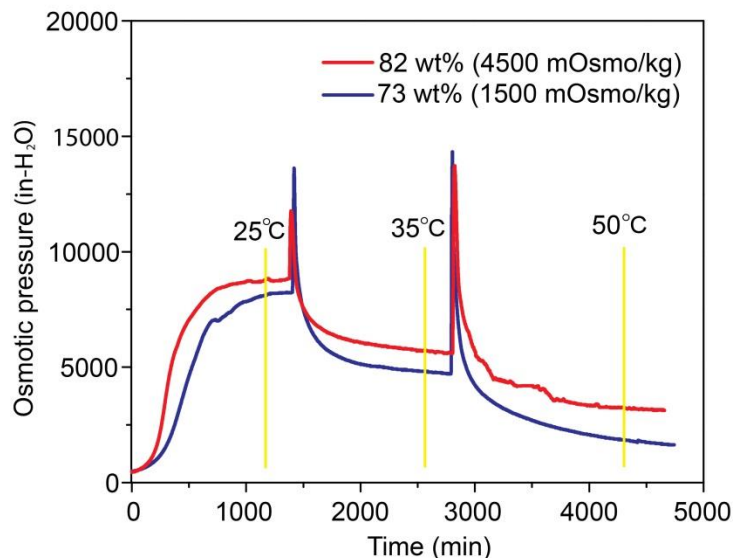
Figure 6.7 Osmotic pressure of $P_{4444}[CF_3COO]$ solution (73 and 82 wt%) under different temperature (25, 35 and 50 °C).

When the solution was heated to a higher temperature, the osmotic pressure did not increase as we expected (Figure 6.7). However, it declined as a result of its thermoresponsive property. The hydrodynamic size of the solutes became larger, which means the $P_{4444}[CF_3COO]$ molecules became more hydrophobic and aggregated together to form a larger cluster in response to the heat. k increased upon heating as summarized in Table 6.1. This indicates that at a higher temperature, the mass transfer of draw solute is faster, which would lead to less severity of ECP, and thus a higher π_2. However, the higher FO water flux could dilute the draw solution, and thus resulting in a lower π_2. By taking these two factors into the considerations, π_2 in fact declined

according to the calculation. However, A, which is the water permeability through the FO membrane, was enhanced when the temperature was higher. For the FO membrane employed, A is 0.84, 1.69 and 2.57 LMH atm^{-1} at 25 °C, 35 °C and 50 °C, respectively. This much enhanced water permeability of FO membrane is beneficial for water molecules in the feed solution to pass through the membrane pores to the draw solution side. Ultimately, FO water flux increases at higher operational temperature.

6.4 Conclusions

In this work, a thermoresponsive ionic liquid, P$_{4444}$[CF$_3$COO] was evaluated as an draw solute for FO desalination. With simulated brackish water as the feed solution and IL-rich sediments of P$_{4444}$[CF$_3$COO] solution at 60 °C (73 wt%) as the draw solution, FO water flux 4.2 LMH and 4.9 LMH was obtained under 25 °C and 50 °C, respectively. With higher concentrated P$_{4444}$[CF$_3$COO] solution (82 wt%), it was able to generate water flux in seawater desalination both with simulated seawater and seawater from Singapore coast at high operational temperature. At 50 °C, the FO water flux was about 5 LMH with seawater from Singapore coast as the feed solution. Regeneration was achieved by liquid-liquid phase separation at 60 °C. The IL-rich phase could be recycled directly as the draw solution or further concentrated by NF to obtain a draw solution with higher concentration. The heat, which is the major energy input of the whole process can be provided by less expensive and clean energy sources such as geothermal or solar thermal energy, and low grade industrial waste heat. The water-rich phase which has low osmotic pressure can be purified though a low-pressure NF. Through theoretical calculation, ECP was believed to be the main reason for the relatively low FO water flux of P$_{4444}$[CF$_3$COO]

solution. And the increased k and A both contributed to the increment of FO water flux when the operational temperature of FO process increased.

6.5 References

1. Elimelech, M.; Phillip, W. A. The future of seawater desalination: Energy, technology, and the environment. *Science* **2011**, 333, 712-717.

2. Likhachev, D. S.; Li, F. C. Large-scale water desalination methods: A review and new perspectives. *Desalin. Water Treat*. **2013**, 51, 2836-2849.

3. Shannon, M. A.; Bohn, P. W.; Elimelech, M.; Georgiadis, J. G.; Marinas, B. J.; Mayes, A. M. Science and technology for water purification in the coming decades. *Nature* **2008**, 452, 301-310.

4. Greenlee, L. F.; Lawler, D. F.; Freeman, B. D.; Marrot, B.; Moulin, P. Reverse osmosis desalination: Water sources, technology, and today's challenges. *Water Res.* **2009**, 43, 2317-2348.

5. Ghaffour, N.; Missimer, T. M.; Amy, G. L. Technical review and evaluation of the economics of water desalination: Current and future challenges for better water supply sustainability. *Desalination* **2013**, 309, 197-207.

6. Cath, T. Y.; Childress, A. E.; Elimelech, M. Forward osmosis: Principles, applications, and recent developments. *J. Membr. Sci*. **2006**, 281, 70-87.

7. Chung, T.-S.; Zhang, S.; Wang, K. Y.; Su, J. C.; Ling, M. M. Forward osmosis processes: Yesterday, today and tomorrow. *Desalination* **2012**, 287, 78-81.

8. Zhao, S. F.; Zou, L.; Tang, C. Y. Y.; Mulcahy, D. Recent developments in forward osmosis: Opportunities and challenges. *J. Membr. Sci.* **2012**, 396, 1-21.

9. Cai, Y. F.; Shen, W. M.; Wang, R.; Krantz, W. B.; Faneb, A. G.; Hu, X. CO2 switchable dual responsive polymers as draw solutes for forward osmosis desalination. *Chem. Commun.* **2013**, 49, 8377-8379.

10. Duan, J.; Litwiller, E.; Choi, S. H.; Pinnau, I. Evaluation of sodium lignin sulfonate as draw solute in forward osmosis for desert restoration. *J Membr. Sci.* **2014**, 453, 463-470.

11. Ge, Q.; Fu, F. J.; Chung, T.-S. Ferric and cobaltous hydroacid complexes for forward osmosis (FO) processes. *Water Res.* **2014**, 58, 230-238.

12. Guo, C. X.; Huang, S. H.; Lu, X. A solventless thermolysis route to large-scale production of ultra-small hydrophilic and biocompatible magnetic ferrite nanocrystals and their application for efficient protein enrichment. *Green Chem.* **2014**, 16, 2571-2579.

13. Guo, C. X.; Zhao, D.; Zhao, Q.; Wang, P.; Lu, X. Na+-functionalized carbon quantum dots: A new draw solute in forward osmosis for seawater desalination. *Chem. Commun.* **2014**, 50, 7318-7321.

14. Hau, N. T.; Chen, S. S.; Nguyen, N. C.; Huang, K. Z.; Ngo, H. H.; Guo, W. S. Exploration of edta sodium salt as novel draw solution in forward osmosis process for dewatering of high nutrient sludge. *J. Membr. Sci.* **2014**, 455, 305-311.

15. Lutchmiah, K.; Lauber, L.; Roest, K.; Harmsen, D. J. H.; Post, J. W.; Rietveld, L. C.; van Lier, J. B.; Cornelissen, E. R. Zwitterions as alternative draw solutions in forward osmosis for application in wastewater reclamation. *J Membr. Sci.* **2014**, 460, 82-90.

16. Zhao, D.; Chen, S.; Wang, P.; Zhao, Q.; Lu, X. A dendrimer-based forward osmosis draw solute for seawater desalination. *Ind. Eng. Chem. Res.* **2014**, 53, 16170-16175.

17. Ge, Q.; Chung, T.-S. Oxalic acid complexes: Promising draw solutes for forward osmosis (fo) in protein enrichment. *Chem. Commun*. **2015**, 51, 4854-4857.

18. Zhou, A. J.; Luo, H. Y.; Wang, Q.; Chen, L.; Zhang, T. C.; Tao, T. Magnetic thermoresponsive ionic nanogels as novel draw agents in forward osmosis. *Rsc. Adv*. **2015**, 5, 15359-15365.

19. McCutcheon, J. R.; McGinnis, R. L.; Elimelech, M. A novel ammonia-carbon dioxide forward (direct) osmosis desalination process. *Desalination* **2005**, 174, 1-11.

20. McGinnis, R. L.; Elimelech, M. Energy requirements of ammonia-carbon dioxide forward osmosis desalination. *Desalination* **2007**, 207, 370-382.

21. Zhao, D.; Wang, P.; Zhao, Q.; Chen, N.; Lu, X. Thermoresponsive copolymer-based draw solution for seawater desalination in a combined process of forward osmosis and membrane distillation. *Desalination* **2014**, 348, 26-32.

22. Zhao, Q.; Chen, N.; Zhao, D.; Lu, X. Thermoresponsive magnetic nanoparticles for seawater desalination. *ACS Appl. Mater. Inter*. **2013**, 5, 11453-11461.

23. Fei, R. C.; George, J. T.; Park, J.; Means, A. K.; Grunlan, M. A. Ultra-strong thermoresponsive double network hydrogels. *Soft Matter.* **2013**, 9, 2912-2919.

24. Nakayama, D.; Mok, Y.; Noh, M.; Park, J.; Kang, S.; Lee, Y. Lower critical solution temperature (lcst) phase separation of glycol ethers for forward osmotic control. *Phys. Chem. Chem. Phys.* **2014**, 16, 5319-5325.

25. Kohno, Y.; Ohno, H. Temperature-responsive ionic liquid/water interfaces: Relation between hydrophilicity of ions and dynamic phase change. *Phys. Chem. Chem. Phys.* **2012**, 14, 5063-5070.

26. Cai, Y.; Shen, W. Energy-efficient desalination by forward osmosis using responsive ionic liquid draw solutes. *Environ. Sci.: Water Res. Technol.* **2015**, 1, 341-347.

27. Kohno, Y.; Arai, H.; Saita, S.; Ohno, H. Material design of ionic liquids to show temperature-sensitive lcst-type phase transition after mixing with water. *Aust. J. Chem.* **2011**, 64, 1560-1567.

28. Achilli, A.; Cath, T. Y.; Childress, A. E. Selection of inorganic-based draw solutions for forward osmosis applications. *J. Membr. Sci.* **2010**, 364, 233-241.

29. Ge, Q.; Su, J.; Amy, G. L.; Chung, T.-S. Exploration of polyelectrolytes as draw solutes in forward osmosis processes. *Water Res.* **2012**, 46, 1318-1326.

30. Spickermann, C.; Thar, J.; Lehmann, S. B. C.; Zahn, S.; Hunger, J.; Buchner, R.; Hunt, P. A.; Welton, T.; Kirchner, B. Why are ionic liquid ions mainly associated in water? A car-

parrinello study of 1-ethyl-3-methyl-imidazolium chloride water mixture. *J. Chem. Phys.* **2008**, 129, 104505-104517.

31. Ge, Q.; Ling, M. M.; Chung, T.-S. Draw solutions for forward osmosis processes: Developments, challenges, and prospects for the future. *J. Membr. Sci.* **2013**, 442, 225-237.

32. Gao, Y. B.; Wang, Y. N.; Li, W. Y.; Tang, C. Y. Y. Characterization of internal and external concentration polarizations during forward osmosis processes. *Desalination* **2014**, 338, 65-73.

33. Qin, J. J.; Chen, S. J.; Oo, M. H.; Kekre, K. A. Cornelissen, E. R.; Ruiken, C. J. Experimental studies and modeling on concentration polarization in forward osmosis. *Water Sci. Technol.* **2010**, 61, 2897-2904.

34. Porter, M. C. Concentration polarization with membrane ultrafiltration. *Ind. Eng. Chem. Prod. Res. Dev.* **1972**, 11, 234-248.

35. Yong, J. S.; Phillip, W. A.; Elimelech, M. Coupled reverse draw solute permeation and water flux in forward osmosis with neutral draw solutes. *J. Membr. Sci.* **2012**, 392, 9-17.

CHAPTER 7

CONCLUSIONS AND RECOMMENDATIONS

7.1 Conclusions

In conclusion, we have successfully designed and synthesized four kinds of novel FO draw solutions and applied them in seawater desalination. Firstly, a dendrimer-based draw solution was employed due to its multiple and dissociable terminal groups. We further demonstrate that Na^+-functionalized carbon quantum dots have high potential in the application of FO seawater desalination process. Next, we found that the thermoresponsive copolymer-based draw solution can facilitate the regeneration due to its thermoresponsive property. Finally, another thermoresponsive material, a thermoresponsive ionic liquid, was investigated. Its ionic nature, low molecular weight and viscosity, and phase separation at a mild temperature make it promising as a draw solution. The core findings of this project are summarized as follows:

- 1.5G, 2.5G, 3.5G and 4.5G PAMAM-COONa were synthesized and evaluated as FO draw solutes. For the same solution concentration, a higher generation of PAMAM-COONa would lead to a lower osmolality and FO water flux with a smaller reverse flux. By taking the synthesis cost into further consideration, 2.5G PAMAM-COONa was found to be a better candidate as the FO draw solute since it could give a comparably high water fluxes as well as low reverse fluxes with DI water, seawater from Singapore and simulated seawater as the feed solutions. After FO tests, the diluted draw solution could be successfully re-concentrated *via* MD at a mild temperature. It is believed this

133

dendrimer-based draw solute is promising for seawater desalination by the FO-MD combined process.

- Na$^+$- functionalized carbon quantum dots (Na_CQDs) were reported as a new class of draw solute in forward osmosis for seawater desalination. The unique characteristics of Na_CQDs, including an ultra–small size of 3.5 nm, abundant carboxyl groups, and rich ionic species, favor high osmotic pressure and thus FO water flux. At concentrations of 0.4 and 0.5 g mL^{-1}, the Na_CQDs provide respective osmotic pressures of 30.9 and 53.6 atm, much higher than that of seawater (~26 atm). In FO tests with DI water as the model feed solution, the Na_CQDs (0.4 g mL^{-1}) showed a water flux of 29.8 LMH, exceeding that of 2.0 M NaCl draw solution by 55%. This FO water flux is among the highest reported. When seawater was used as feed solution, the Na_CQDs provide an FO water flux of 10.4 LMH with only a slight drop after 5 cycles. In addition, the Na_CQDs showed negligible reverse draw solute permeation. It is worth noting that for practical applications, further investigation is necessary to understand the energy consumption in the FO desalination process using Na_CQDs as draw solutes.

- A thermoresponsive copolymer, poly(sodium styrene-4-sulfonate-*co-n*-isopropylacrylamide) (PSSS-PNIPAM) with different SSS contents has been successfully synthesized and applied to draw water from simulated seawater. Considering the osmotic pressure and LCST, PSSS-PNIPAM with 15 wt% of SSS was chosen as the draw solute in FO to desalinate seawater. With simulated seawater (0.6 M NaCl solution) as the feed solution, FO water fluxes larger than 3.5 LMH were attained. It was also found that the osmotic pressure of PSSS-PNIPAM solution dropped at temperatures above its LCST. This thermoresponsive property improves the

134

regeneration of the draw solution *via* MD because the decreased osmotic pressure allows higher water vapor pressure and favors the separation of water from the solution. In addition, the use of PSSS-PNIPAM may reduce salt leakage in MD and produce high-quality water. It is believed that with further improvement to increase the osmotic pressure and reduce the viscosity, thermoresponsive copolymers can be promising draw solutes for FO desalination.

- A thermoresponsive ionic liquid, $P_{4444}[CF_3COO]$ was evaluated as a draw solute for FO desalination. With simulated brackish water as the feed solution and IL-rich sediments of $P_{4444}[CF_3COO]$ solution (73 wt%) as the draw solution, FO water flux 4.2 LMH and 4.9 LMH was obtained under 25 °C and 50 °C, respectively. $P_{4444}[CF_3COO]$ solution with higher concentration (82 wt%) was able to generate water flux with simulated seawater and seawater from Singapore coast as feed solutions at high operational temperature. At 50 °C, the FO water flux was about 5 LMH with seawater from Singapore coast as the feed solution. Regeneration was achieved by liquid-liquid phase separation at 60 °C. The IL-rich phase could be recycled directly as the draw solution or further concentrated by NF to obtain a draw solution with higher concentration. The heat, which is the major energy input of the whole process can be provided by less expensive and clean energy sources such as geothermal or solar thermal energy, and low grade industrial waste heat. The water-rich phase which has low osmotic pressure can be purified though a low-pressure NF. Through theoretical calculation, ECP was believed to be the main reason for the relatively low FO water flux of $P_{4444}[CF_3COO]$ solution.

Among these four kinds of newly developed draw solutions, non-thermoresponsive dendrimer-based and Na_CQDs draw solutions showed higher FO water flux than thermoresponsive copolymer and ionic liquid. However, the thermoresponsive property of the copolymer can enhance the performance of regeneration process, namely MD process. It also facilitates the regeneration of ionic liquid by simple phase separation. The results of this study may show significance in 1) improving the performance of FO draw solutes in seawater desalination; 2) contributing to a better understanding of how draw solutes behave in FO and regeneration processes; and 3) inspiring the exploration of new materials as FO draw solutes.

7.2 Recommendations

Based on the findings of this thesis work, the following future work is recommended:

- investigating the draw solutions developed in this work for other FO applications, such as wastewater treatment, protein enrichment or power regeneration;
- analyzing energy and economical cost and comparing with other desalination technologies, such as RO;
- developing other novel multifunctional compounds that can be easily separated from water in response to cheap or renewable stimuli such as mild heating.

List of Publication

1. **Zhao, D.;** Chen, S.; Wang, P.; Zhao, Q.; Lu, X. A dendrimer-based forward osmosis draw solute for seawater desalination. *Ind. Eng. Chem. Res*. **2014**, 53, 16170-16175.

2. Guo, C. X.*; **Zhao, D.*;** Zhao, Q.; Wang, P.; Lu, X. A new draw solute in forward osmosis for seawater desalination. *Chem. Commun*. **2014**, 50, 7318-7321 (*equal contribution).

3. **Zhao D.;** Wang, P.; Zhao, Q.; Chen, N. P.; Lu, X. M. Thermoresponsive copolymer-based draw solution for seawater desalination in a combined process of forward osmosis and membrane distillation. *Desalination* **2014**, 348, 26-32.

4. **Zhao, D.;** Chen, S.; Guo, C.; Zhao, Q.; Lu, X. Multi-functional forward osmosis draw solutes for seawater desalination. *Chinese J. Chem. Eng*. **2015**, Accepted.

5. **Zhao, D.;** Zhao, Q.; Lu, X. Thermoresponsive ionic liquid as forward osmosis (FO) draw solute for brackish water and seawater desalination. In preparation.

6. Zhao, Q.; Chen, N.; **Zhao, D.;** Lu, X. Thermoresponsive magnetic nanoparticles for seawater desalination. *ACS Appl. Mater*. *Interfaces* **2013**, 5, 11453-11461.

7. Zhao, Q.; **Zhao, D.;** Lu, X. Synthesis and temperature switchable magnetic separation. Under review.